IMMUNOPATHOLOGICAL RESPONSE TO PORCINE-DERIVED SCAFFOLDS FOR REGENERATIVE MEDICAL APPLICATIONS

JASEER MUHAMED CJ

Ph.D. THESIS
2014

SREE CHITRA TIRUNAL INSTITUTE
FOR
MEDICAL SCIENCES AND TECHNOLOGY,
THIRUVANANTHAPURAM

IMMUNOPATHOLOGICAL RESPONSE TO PORCINE-DERIVED SCAFFOLDS FOR REGENERATIVE MEDICAL APPLICATIONS

A THESIS PRESENTED BY

JASEER MUHAMED CJ

TO

SREE CHITRA TIRUNAL INSTITUTE FOR MEDICAL
SCIENCES AND TECHNOLOGY
THIRUVANANTHAPURAM
INDIA

IN PARTIAL FULFILMENT OF THE REQUIREMENTS
FOR THE AWARD OF
DOCTOR OF PHILOSOPHY

2014

DECLARATION

I, Jaseer Muhamed CJ, hereby certify that I had personally carried out the work depicted in the thesis entitled, ***"Immunopathological Response to Porcine-Derived Scaffolds for Regenerative Medical Applications",*** except where due acknowledgment has been made in the text. No part of the thesis has been submitted for the award of any other degree or diploma prior to this date.

Thiruvananthapuram

Jaseer Muhamed CJ
Reg No: PhD/2010/04
Roll No: 6083

SREE CHITRA TIRUNAL INSTITUTE FOR MEDICAL SCIENCES & TECHNOLOGY, TRIVANDRUM

Thiruvananthapuram – 695011, INDIA
(An Institute of National Importance under Govt. of India)
Phone-(91)0471-2520282 Fax-(91)0471-2341814
Email: tvanilkumar@sctimst.ac.in Web site – www.sctimst.ac.in

CERTIFICATE

This is to certify that **Mr. Jaseer Muhamed CJ**, in the Division of Experimental Pathology of this institute has fulfilled the requirements prescribed for the Ph. D. degree of the Sree Chitra Tirunal Institute for Medical Sciences and Technology, Thiruvananthapuram. The thesis entitled, ***"Immunopathological Response to Porcine-Derived Scaffolds for Regenerative Medical Applications"*** was carried out under my direct supervision. No part of the thesis was submitted for the award of any degree or diploma prior to this date.

* Clearance was obtained from the Institutional Ethics Committee/ Institutional Animal Ethics Committee for carrying out the study.

Thiruvananthapuram

Dr. TV Anilkumar PhD
(Research Supervisor)

Scientist F & Head
Division of Experimental- Pathology
BMT wing, SCTIMST
Thiruvananthapuram

The thesis entitled

Immunopathological Response to Porcine-Derived Scaffolds for Regenerative Medical Applications

Submitted by

Jaseer Muhamed CJ

for the degree of

Doctor of Philosophy

of

SREE CHITRA TIRUNAL INSTITUTE FOR MEDICAL SCIENCES AND TECHNOLOGY, THIRUVANANTHAPURAM

is evaluated and approved by

…….	……..
Dr. T.V. Anilkumar	Examiner
(Research Supervisor)	

ACKNOWLEDGMENT

I am grateful to the following for their help, support and contribution throughout these years.

I would like to express my sincere gratitude and respect to my supervisor Dr. TV Anilkumar, Scientist F and Head, Division of Experimental Pathology-BMT wing, SCTIMST. His supervision, advice, critical evaluations and encouragement helped me throughout the course of study. I thank him for the entire support offered during my Ph.D programme.

I am grateful to the former and present Director of SCTIMST and the present Head and the previous Heads, BMT Wing for all support provided during the course of my work.

I thank members of the doctoral advisory committee, Dr. Lissy K Krishnan, (Scientist G, Thrombosis Research Unit) and Dr. Annie John, (Scientist F, Transmission Electron Microscopy) for their timely suggestions, critical comments and encouragements.

I am thankful to Dr. Sundar Jayasingh, Deputy Registrar, Dr. Prabha D. Nair, Associate Dean for PhD affairs, Dean, and all members of academic division and Director's office for their administrative support.

I am grateful to Indian Council for Medical Research for providing me the research fellowship and international travel grant. I thank Department of Biotechnology for financial support. I also thank Council of scientific and Industrial Research for the international Travel grant.

I thank Dr Abdul Jaleel and Mr Arun Surendran of Rajive Gandhi Center for Biotechnology for their support for doing mass-spectroscopy and protein identification.

I thank Dr Harikrishnan, Mr Pradeep, Mr Manoj and all members of the Department of Laboratory Animal Science of SCTIMST for their help and support during the animal experiments.

I'm extremely thankful to the members of Division of experimental pathology, Mr. Thulaseedharan NK, Ms. Vineetha VP, Ms. Deepa Revi, Dr. Akhila Rajan, Ms. Geetha Surendran, Ms. Reshma and Ms. Reshmi for their support and help.

I am thankful to Dr CP Sharma, Dr. Mira Mohanty, Dr. Sabareeswaran, Dr Roy Joseph, Dr. Anwar Azad, Dr. Unnikrshnan S, Dr. Renjith P Nair, Dr. Josna, Dr. Anugya, Mr. Renjith S Kartha, Ms Priyanka, Mr Rajesh P, Mr Ansar, Mr Al Ameen, Dr. Aravind, Mr. Nishad K V, Ms Remya NS, Ms Serine Hilary and Ms Tara for their valuable support and help.

Thanks to the staff of various administrative departments and library of the Institute, other research scholars of the institute for their help and friendship.

I am thankful to my parents, siblings, friends and teachers for their, blessings, prayers, support and constant encouragements.

I further thank many who directly or indirectly helped me to prepare this thesis.

My immense gratitude to the most merciful God... for showering immeasurable blessings with ever loving family, caring supervisor, supporting friends, and so on for the completion of this endeavour.

Jaseer Muhamed CJ

TABLE OF CONTENTS

LIST OF FIGURES

LIST OF TABLES

ABBREVIATIONS

C3a	Complement component-3a
CDE	Cholecyst derived extracellular matrix
CDS	Cholecyst derived scaffold
DAB	Diaminobenzidine
DMEM	Dulbecco's modified minimum essential medium
DTT	Dithiothreitol
ECM	Extracellular matrix
EDC	Carbodiimide
ELISA	Enzyme-linked immunosorbent assay
ESI	Electrospray ionization
ETO	Ethylene oxide
FBGC	Foreign body giant cell
GAGs	Glycosaminoglycans
Gal epitope	α-Gal (Galα1,3-Galβ1–4GlcNAc-R)
GAPDH	Glyceraldehyde 3-phosphate dehydrogenase
GLP	Good laboratory practice
HAP	Hydroxyapatite
HEPES	4-(2-Hydroxyethyl)piperazine-1-ethanesulfonic acid
HRP	Horseradish peroxidase
IEF	Isolelectric focusing
IgG	Immunoglobulin-G
INF-γ	Interferon-gamma
iNOS	Inducible nitric oxide synthase
IPG	Immobilized pH gradient
JDE	Jejunum derived extracellular matrix
JDS	Jejunum derived scaffold
LAL	Limulus ameobocyte lysate
LC-MS	Liquid chromatography-mass spectroscopy
LPS	Lipopolysaccharide
MAC	membrane attack complex
MHC	Major histocompatibility complex
MS	Mass spectra

MS^E	Mass spectra at elevated collision energy
NBF	10% Neutral buffered formalin
NCBI	National Center for Biotechnology Information
NDSB-256	134mM 3-(benzyldimethylammonio) propanesulphonate
OECD	Organisation for economic co-operation and development
PBS	Phosphate buffered saline
PBST	Phosphate buffered saline with 0.1% Tween 20
PGA	Polyglycolic acid
PLA	Polylactic acid
PLGA	Poly lactic-co-glycolic acid
PLGS	ProteinLynx Global SERVER
PMA	Phorbol 12-myristate 13-acetate
Q-TOF	Quadrupole-time of flight
RNS	Reactive nitrogen species
ROS	Reactive oxygen species
RT-PCR	Reverse transcriptase-polymerase chain reaction
SDS-PAGE	Sodium dodecyl sulfate polyacrylamide gel electrophoresis
SIS	Small intestinal submucosa
SLA	Swine leukocyte antigen
TBST	Tris Buffer Saline with 1% Tween20
TCP	β-tricalcium phosphate
TGFBIp/βig-h3	Transforming growth factor-induced protein
TGF-β	Transforming growth factor-β
TNF-α	Tumor necrosis factor-alpha
UDE	Urinary bladder derived extracellular matrix
UDS	Urinary bladder derived scaffold
UPLC	Ultra-performance liquid chromatography
US-FDA	United states-Federal drug administration
VEGF,	Vascular endothelial growth factor
β-FGF	β-Fibroblast growth factor

SYNOPSIS

Extracellular matrix scaffolds prepared from mammalian organs and tissues are proven biomaterials used for regenerative medical applications, usually as xenografts. Porcine small intestinal submucosa is probably the most favourite scaffold of mammalian origin. It has been used for clinical applications in at least a million human patients worldwide. However, there are several reports of clinical complications like severe pain, local inflammation, graft versus host disease following the use of animal-derived biomaterials as xenografts. Most of these reported complications are due to the immunogenicity of the xenograft. Hence, there is a current research interest for identifying extracellular matrices, with minimal immunogenicity, from porcine hollow organs like small intestine. This study hypothesises that, when prepared by a non-detergent/enzymatic method cholecyst derived scaffold (CDS) elicits lesser immunogenicity compared to scaffolds prepared from jejunum (small intestine) and urinary bladder. In order to test the hypothesis, the nature of immune response induced by CDS was compared with jejunum-derived scaffold (JDS) and urinary bladder-derived scaffold (UDS) in a rat subcutaneous graft model. The data were supplemented with a study for identifying potential immunogenic proteins in CDS.

The thesis contains 7 chapters. Chapter 1 gives an introduction to the topic focusing on the use of extracellular matrix derived scaffolds in regenerative medicine, problems associated with residual immunogenicity and the need for identification of novel scaffolds with minimal immunogenicity. The chapter ends

with a clear statement on hypothesis and a short list of major objectives. The objectives of the study include:

1. Characterization of scaffolds for immunogenic potential

2. An assessment of local tissue response *in vivo* and biocompatibility

3. An assessment of distribution/function of immunocompetent cells around the grafts implanted in rat subcutaneous tissue

4. Comparison of the nature of immunogenicity elicited by CDS with that of a commercially available reference material in rat subcutaneous model

Chapter 2 includes a detailed review of literature related to the topics related to the thesis. This includes review on preparation, composition, degradation properties and regenerative medical applications of extracellular matrix scaffolds. A literature survey on the host response to biomaterials in general and immune response to biological scaffolds are also included in this chapter.

Chapter 3 is about the 'characterization of scaffolds for immunogenic potential'. The characterization methods used were Limulus amoebocyte lysate assay for determination of endotoxin content, quantification of cellularity of scaffolds, estimation of growth factor content in scaffolds and identification of extractable proteins in the scaffolds by electrophoresis, mass spectroscopy followed by database search. The ability of scaffolds to raise delayed type hypersensitivity was also tested by guinea pig maximization testing. Ability of scaffolds to induce innate immune response was tested with *in vitro* methods. The IgG antibody response induced by scaffolds when grafted in rat subcutaneous tissue was studied. Further, the immunogenic proteins of cholecyst derived scaffold were characterized by 2D

electrophoresis, mass spectroscopy and database search. The results largely indicated that the CDS did contain lot of immunogenic proteins.

Chapter 4 describes a study on the nature of 'local tissue response *in vivo* and biocompatibility'. The data were derived after subcutaneous implantation of the scaffolds in rat, appropriate histotechnology and biocompatibility assessment according to ISO 10993 part-6 guidelines. The results clearly indicated that the CDS is biocompatible with UDS and JDS.

The data on biocompatibility warranted a detailed study on the nature of local immunogenicity and the data are presented in Chapter 5. The 'distribution/function of immunocompetent cells around the grafts implanted in rat subcutaneous tissue' was studied in detail. The focus of this chapter is on the distribution and/or function of immunocompetent cells like mast cells, M1 and M2 macrophages and TH1 and TH2 lymphocytes around the graft. The study extensively used immunohistochemistry, histomorphometry image analysis, and real-time RT-PCR. The results revealed that despite the similarity in biocompatibility, the CDS induced a differential immunogenic reaction. The pro-inflammatory reaction was less but had a preferential remodelling or graft acceptance reaction around CDS-graft compared to the reaction around JDS- or UDS graft.

The observations presented in Chapter 5 prompted a comparative study on the nature of immunogenic reaction caused by CDS with a commercial product. Chapter 6 is thus a 'comparative study of distribution/function of immunocompetent cells around cholecyst derived scaffold and commercially available reference material implanted in rat subcutaneous tissue'. The results largely suggested the differential ability of

xenogeneic grafts to induce local immunopathologic reaction, despite similarities in the nature of histomorphological reaction induced *in vivo*.

Chapter 7 describes the summary of the major findings already presented in Chapter 3 to 6 and a discussion about the overall contemporary significance of the study in the field of biomaterials and regenerative medicine. The conclusion was that, the porcine cholecyst derived scaffold is a relatively less immunogenic xenograft when compared to jejunum and urinary bladder derived scaffolds. It may be a preferred scaffold for fabricating clinical products useful for regenerative medical applications. The chapter also includes limitations of the study and the future research perspectives based on the conclusions derived from the study.

In short, this thesis describes the immunogenic potential of extracellular matrix scaffolds prepared from porcine cholecyst, small intestine and urinary bladder using a non-detergent/enzymatic method.

CHAPTER-1

1. INTRODUCTION

Extracellular matrices (ECM) isolated from several mammalian organs and tissues are proven biomaterials used as scaffolds in regenerative medical applications, usually as xenografts (Badylak, 2007, Badylak *et al.*, 2009). These xenografts are generally fabricated out of ECM of variable purity, isolated from various organs/tissues such as liver, lung, tendon, cartilage and muscle by optimized decellularization techniques (Badylak, 2007, Deeken *et al.*, 2011, Kheir *et al.*, 2011, Zhang *et al.*, 2012, Nonaka *et al.*, 2014, Wang *et al.*, 2014). The isolates also called as scaffolds because of their ability to act as substrate for three dimensional growth of cells. The biomaterial-quality of these scaffolds largely depends on the donor species, source organ, processing or decellularization method used for the recovery of the scaffold, fabrication strategies adopted for developing the xenograft, the methods employed for long-term storage and the nature of end use (Badylak, 2007, Badylak *et al.*, 2009). ECM scaffolds derived from small intestinal submucosa (SIS) and decellularized human-dermis have been used to treat more than a million human patients worldwide (Badylak, 2007, LifeCell, 2014). There are several other scaffold materials derived from ECM of mammalian organs that are being used in a wide variety of regenerative medical applications (Crapo *et al.*, 2011). However, being xenogeneic in origin these materials may contain several xenogeneic molecules that are potentially immunogenic to human causing undesirable

host reactions. By selecting appropriate processing methods the immunogenicity can be reduced considerably (Schmidt and Baier, 2000, Badylak and Gilbert, 2008).

The components of ECM are evolutionarily conserved molecules and hence less likely to be antigenic across species barrier (Boot-Handford and Tuckwell, 2003, Hynes, 2012). On the other hand cellular components may be antigenic and if present they can cause inadvertent immune response *in vivo*. Decellularization is a major step in ECM scaffold preparation that reduces the immunogenicity. So the aim of any decellularization protocol is removal of cellular components as far as possible while retaining the ECM components intact. Decellularization involves chemical methods, physical methods or combination of both chemical/physical methods (Gilbert *et al.*, 2006). Though optimized decellularization protocols are available for a variety of tissues/organs none of them can assure absolute removal of cellular components and cellular residue remains even after the most efficient decellularization protocol (Zheng *et al.*, 2005, Badylak and Gilbert, 2008). These residual cellular components can be immunogenic and can cause adverse reactions like severe pain, inflammation, graft versus host disease etc (Ho *et al.*, 2004, Kalota, 2004, Petter-Puchner *et al.*, 2006, Petter-Puchner, 2007, Wang *et al.*, 2009). Moreover, from the database of 'MAUDE-manufacturer and user facility device experience' (US-FDA, 2014) it appears that several of the reported complications associated with the use of xenogeneic graft materials are related to immune function. Hence, there is a current research interest for identifying ECM scaffolds with minimal immunogenicity.

Cholecyst derived scaffold (CDS) is a relatively novel biomaterial of mammalian origin (Burugapalli *et al.*, 2007), which has potential clinical use as buttressing material for reinforcement of staple lines in intestinal surgery (Burugapalli *et al.*, 2008), skin graft (Revi *et al.*, 2013) and bladder repair graft (Kajbafzadeh *et al.*, 2014). It has been reported that compared to scaffolds isolated from small intestine and urinary bladder, CDS prepared by a non-detergent/enzymatic method contains relatively less residual cellular components (Anilkumar *et al.*, 2014). However, when used as xenograft/implant, the ability of this less cellular biomaterial to prevent adverse immunogenic reaction has not been studied.

With this background it was hypothesized that, 'when prepared by a non-detergent/enzymatic method porcine cholecyst derived scaffold is less immunogenic compared to those scaffolds prepared from jejunum and urinary bladder'. The results may have serious implications on the potential of CDS for regenerative medical applications.

In order to test the hypothesis the following objectives have been proposed.

1.1. *Objectives of the study*

1. Characterization of scaffolds prepared from porcine cholecyst, jejunum and urinary bladder for their immunogenic potential
2. An assessment of local tissue response *in vivo* and biocompatibility

3. An assessment of distribution/function of immunocompetent cells around the grafts implanted in rat subcutaneous tissue

4. Comparison of the nature of immunogenicity elicited by CDS with that of a commercially available reference material in rat subcutaneous model

CHAPTER-2

2. LITERATURE REVIEW

2.1. Regenerative Medicine

Regenerative medicine is an interdisciplinary field of research with an objective to repair damaged tissues or organs. It makes use of developments in the field of basic biology, stem cell biology, organ transplantation, materials and engineering (Greenwood *et al.*, 2006). A regenerative medical approach may involve the replacement of damaged tissue/organ with engineered tissue/organ or it may stimulate the natural healing ability of the body by means of targeted delivery of drugs/genes, recruitment of patients own stem cells (Feinberg, 2012, Christ *et al.*, 2013). All these strategies are designed according to the extent of damage, tissue/organ affected and the conditions of the particular patient.

The tissue engineering strategy of regenerative medicine involves the applications of engineered materials or scaffolds along with cells and suitable stimuli to regenerate or replace damaged tissue or organ. The scaffold should act as template for tissue formation and ideally mimic the ECM of the tissue to be engineered. The desirable properties the scaffold should have includes biocompatibility, adequate mechanical strength, and degradation properties (O'Brien, 2011). To date different types of scaffolds have been used for regenerative medical applications with variable results. This include scaffolds made out of natural polymers like collagen, elastin, fibrin, silk proteins, chitin, dextran or glycosaminoglycans and synthetic polymers like polylactic acid (PLA),

polyglycolic acid (PGA) or poly lactic-co-glycolic acid (PLGA). Ceramic materials used as scaffolds includes hydroxyapatite (HAP), β-tricalcium phosphate (TCP), certain compositions of silicate and phosphate glasses (bioactive glass) (Dhandayuthapani *et al.*, 2011).

However, the ideal scaffold for the growth of a tissue will be its own ECM (Chan and Leong, 2008). ECM is biocompatible, supports adhesion, migration, proliferation and proliferation of cells, biodegradable and have optimum mechanical properties as needed for an ideal scaffold material (Badylak, 2007). The matrix aids the development and repair of tissue by supporting cell adhesion, migration, proliferation and differentiation of cells. Therefore extracellular matrices obtained from various sources have been used for regeneration of various organs and tissues.

2.2. Extracellular matrices as scaffolds

Animal tissues are not made up solely of cells. The non cellular extracellular space is filled by an intricate network of fibrous proteins and proteoglycans which constitutes the extracellular matrix (Alberts *et al.*, 2002). In a solid tissue ECM is the collection of proteins and sugars surrounding the cells. The ECM is composed of an intricate mesh work of fibrillar collagens (collagen I, II, III, IV, XI), non-fibrillar collagens, elastic fibers and glycosaminoglycans containing non-collagenous glycoproteins (hyaluronan and proteoglycans) (Cox and Erler, 2011). Rather than fulfilling the biomechanical role and as a scaffold to stabilize the physical structure of organ/tissue ECM influences the

survival, development, migration, proliferation, shape, and function of cells (Alberts *et al.*, 2002).

The major components of the ECM such as collagen, glycosaminoglycans, laminin, fibronectin and hyaluronic acid, either individually or in combination have been used for tissue engineering scaffold fabrication (Rho *et al.*, 2006, Tate *et al.*, 2009, Wang and Spector, 2009, Caliari *et al.*, 2011). However these scaffolds lack the native microarchitecture and molecular composition of natural ECM. But, intact extracellular matrices isolated from mammalian organs and tissues that maintain the exact microarchitecture and molecular composition of natural ECM can be used as scaffolds (Badylak, 2007). Such scaffolds are preferable over synthetic scaffolds for a variety of tissue engineering and regenerative medical applications

2.2.1. Preparation of ECM scaffolds

The ECM from various tissues/organs can be isolated by various technologies. There are several protocols available for preparation of tissue engineering scaffolds from mammalian tissues/organs. However the major steps involved are collection and transport of the source organ in to the laboratory, decellularization, stabilization of the scaffold and terminal sterilization (Gilbert *et al.*, 2006).

2.2.1.1. Collection of source organ

The collection and transport are usually carried out in a media that preserve viability, matrix architecture and prevent overgrowth of microorganisms. Different source organ collection procedures have been used for the preparation of biological scaffold from

different mammalian organs. Usually the source organs are collected in culture media/phosphate buffered saline/normal saline with or without antimicrobial agents. The organs are then transported to the laboratory within hours (usually within 4h) in ice (Kasimir *et al.*, 2006, Burugapalli *et al.*, 2007, Zhou *et al.*, 2010).

2.2.1.2. Decellularization

Decellularization is the most important step in ECM scaffold preparation. This involves removal of all cellular components while retaining the intact ECM components. The components of ECM are evolutionarily conserved molecules and hence less likely to be antigenic across species barrier (Boot-Handford and Tuckwell, 2003, Hynes, 2012, Hynes and Naba, 2012). The cellular components may be antigenic and if present they can cause inadvertent immune response *in vivo*. So the aim of the decellularization protocol is the removal of cellular components as far as possible while retaining the ECM components intact. Decellularization involves chemical methods, physical methods, or combination of both chemical/physical methods (Gilbert *et al.*, 2006). Though optimized decellularization protocols are available for a variety of tissues/organs none of them can assure absolute removal of cellular components. Some amount of cellular residue remains even after the most efficient decellularization protocol (Zheng *et al.*, 2005, Badylak and Gilbert, 2008). These residual cellular components can be immunogenic and can cause adverse reactions like severe inflammation, pain, graft versus host disease etc (Ho *et al.*, 2004, Kalota, 2004, Petter-Puchner *et al.*, 2006, Petter-Puchner, 2007, Wang *et al.*, 2009, John *et al.*, 2008). The possibility of such complications is kept to the least feasible extent by deploying

efficient decellularization protocols that remove maximum cellular components. A criteria for evaluating efficiency of decellularization has been put forwarded so that the resultant scaffold is minimally immunogenic (Crapo *et al.*, 2011). The decellularized scaffold should have desirable features, viz., dsDNA content <50 ng/mg dry weight of the scaffold, residual DNA with fragment length <200bp, and the lack of visible nuclear material in tissue sections stained with 4',6-diamidino-2-phenylindole or haematoxylin and eosin.

2.2.1.3. Stabilization

Stabilization of biomolecules is then obtained by treatment of the scaffold with glutaraldehyde/protease inhibitors. The material is then either used as lyophilized dried material or as hydrated sheet (Gilbert *et al.*, 2006).

2.2.1.4. Sterilization

Terminal sterilization of the scaffold is important before use of material for various applications and this is generally by gamma irradiation/ETO gas sterilization (Gilbert *et al.*, 2006).

2.2.2. Regenerative medical applications of extracellular matrix scaffolds

Extracellular matrices from different mammalian organs/tissue have been used for regenerative medical applications. Biological scaffold isolated from porcine small intestine (SIS) have been used for manufacturing several U.S. Food and Drug Administration (US FDA) approved biomedical products. More than a million human patients have been benefitted with SIS alone (Badylak, 2007). The different regenerative

medical applications of SIS have been reviewed elsewhere (Andree *et al.*, 2013). To date small intestinal submucosa has been used as nerve guidance conduits, nerve protectant wraps (Kehoe *et al.*, 2012), hernia repair graft (Petter-Puchner and Fortelny, 2010), dural repair graft (Bejjani and Zabramski, 2007), wound matrix (Mostow *et al.*, 2005), pubovaginal sling (Siracusano *et al.*, 2011), cervicovaginal reconstruction (Ding *et al.*, 2014), fistula plug (Cintron *et al.*, 2013), repair of esophagus, (Badylak *et al.*, 2011), repair of tendon (Iannotti *et al.*, 2006) etc. Similarly human decellularized dermis alloderm also have been applied in more than a million patients worldwide (LifeCell, 2014). Biological scaffolds isolated from other organs like urinary bladder (Song *et al.*, 2014), cholecyst (Anilkumar *et al.*, 2014), bovine pericardium (Yang *et al.*, 2012), tendon (Deeken *et al.*, 2011), liver (Wang *et al.*, 2014), lung (Nonaka *et al.*, 2014), dermis (Reing *et al.*, 2010), cartilage (Kheir *et al.*, 2011), meniscus (Azhim *et al.*, 2013), and bone (Grayson *et al.*, 2010) have also been isolated and used for various regenerative medical applications. Several of them are also available commercially.

The biomaterial-quality of these scaffolds largely depends on the source organ, donor species, processing or decellularization method used for the recovery of the scaffold, fabrication strategies adopted for developing the xenograft, the methods employed for long-term storage and the nature of end use (Gilbert *et al.*, 2006).

2.2.3. The composition of ECM scaffold

The composition of ECM of each tissue/organ suits to the optimal functioning of the organ. Since the ECM of tissue/organs has been secreted by the cells of the tissue, the

specific composition and distribution of the ECM constituents will vary depending on the tissue source (Alberts *et al.*, 2002). Small intestinal submucosa (SIS) isolated from porcine small intestine is the most widely studied and characterized ECM scaffold material. It has been found that 90% of SIS is composed of collagen with majority of type-I collagen. Other collagen types such as collagen types III, IV, V and VI are also detected. It consist of a variety of glycosaminoglycans (GAGs), such as heparin, heparin sulfate, chondroitin sulfate and hyaluronic acid. SIS also contains fibronectin, laminin, glycoproteins like decorin, glycoproteins biglycan and entactin. Various growth factors like VEGF, β-FGF and TGF-β have also been reported to be present in porcine SIS. The activity of growth factors have been studied both *in vitro* and *in vivo*, and is found to retain the activity even after terminal sterilization (Badylak *et al.*, 2009, Yang *et al.*, 2010).

ECM scaffold isolated from urinary bladder also have a composition similar to that of SIS, type-III collagen being the major component (Badylak *et al.*, 2009). The protein composition of ECM scaffold isolated from urinary bladder was studied using mass spectroscopy followed by database search. The scaffold was isolated by a well standardized decellularization protocol. About 129 proteins were identified. Majority of them (73%) were cellular proteins whereas only 14% were ECM proteins. So it may be assumed that the so called decellularized materials, actually contains cellular components or in other word the decellularization protocols are not making absolutely acellular biomaterials. But the proteins identified included several proteins associated

with regulation of angiogenesis, remodeling response and wound healing (Marçal *et al.*, 2012).

The composition of ECM scaffolds also depends on the decellularization protocol used for the preparation of scaffold. The use of alkalies/acids and ionic detergents removes glycosaminoglycans. Tri(n-butyl)phosphate may remove collagen from the scaffold. Use of trypsin affects the laminin, fibronectin, elastin, and glycosaminoglycans content of the scaffold. Dispase enzyme treatment removes ECM components such as fibronectin and collagen IV. Alcohols or acetone can precipitate proteins including collagen. Accordingly the composition of ECM scaffolds may vary depending on the chemicals used in the preparation of scaffold (Crapo *et al.*, 2011, Gilbert *et al.*, 2006).

2.2.4. Degradation of ECM scaffold

Degradation of biological scaffold is important parameter that determines the remodeling response *in vivo* and the host immune response. The effect of scaffold degradation on host immune response has not been investigated so far (Badylak and Gilbert, 2008). The degradation of matrix proteins release several biologically active molecules that affect the downstream remodeling of the material when implanted *in vivo* and is referred to as the bio-inductive properties of the ECM scaffold. During scaffold degradation *in vivo* growth factors like β-FGF, TGF-β and VEGF are released from their binding proteins and can exert their biological function. These growth factors retain their biological activity even after terminal sterilization (Badylak, 2007, Badylak *et al.*, 2009). The biological activity of such growth factors has been demonstrated using cell culture

methods *in vitro* (Yang *et al.*, 2010). The degradation of scaffold is a gradual dynamic process that occurs by cellular and enzymatic action. This process causes continuous slow release growth factors and other biomolecules that regulate downstream remodeling. The degradation of scaffold release several cryptic peptides. Endostatin a cryptic peptide released from collagen XVIII, angiostatin released of the plasminogen molecule and anastellin fragment III1C originated from fibronectin are potent inhibitors of angiogenesis. Canstatin released from Type IV collagen can induce apoptosis and inhibit migration and proliferation of endothelial cells. 4 kDa fragment released from α1-antitrypsin is chemoattractant for neutrophils. Restin released from collagen XV can inhibit endothelial cell-migration. Tumstatin released from collagen IV has got anti-angiogenic and anti-tumor activity. ABT-510 released from thrombospondin-1 is an anti-angiogenic molecule (Badylak, 2007).

Degradation products of biological scaffolds can recruit stem cells to the site of injury. It has been demonstrated that a short oligopeptide released from the collagen IIIα molecule which is highly conserved across mammals can recruit progenitor cells and differentiated cells both *in vitro* and *in vivo*. When the oligopeptide is used to treat the mouse model of digit amputation endogenous Sox2+ and Sca1+, Lin− progenitor cells were recruited to the site of injury (Agrawal *et al.*, 2011). Bone marrow derived stem cells are also observed at sites implanted with small intestinal submucosa and urinary bladder derived biological scaffolds (Badylak *et al.*, 2001).

Optimum degradation rate of the biomaterial is essential for a particular clinical application. The degradation of scaffold can be delayed by treatment of the scaffold by cross linking with glutaraldehyde. Compared to native non-cross-linked cholecyst derived ECM which undergo complete degradation, the cross linked ECM undergo minimal degradation *in vivo* after subcutaneous implantation in rats up to 63 days (Burugapalli and Pandit, 2007). Burugapalli et al has shown that by controlling the extent of cross linking with carbodiimide (EDC), scaffolds of optimum degradation properties for a particular clinical application can be designed (Burugapalli *et al.*, 2014). Gilbert et al 2007 studied the fate of scaffold degradation products in dogs implanted with radioactive ^{14}C labeled porcine SIS. Radioactive ^{14}C labeled porcine SIS was isolated from pigs injected with ^{14}C labeled proline. It was found that about 40–60% of the scaffold is removed from the site of remodeling within 4 weeks of implantation. ^{14}C was undetectable after 60 days at implant site and after 90 days in the urine. So Approximately 60% of the scaffold mass was degraded within 4 weeks of implantation and complete resorption occurs by 3 months. The degradation products were eliminated almost completely via urine (Gilbert *et al.*, 2007).

2.2.5. ECM scaffold derived from porcine cholecyst

An intact ECM with a mesh-like architecture was prepared from porcine cholecyst. Peri-muscular subserosal connective tissue layer of cholecyst wall was isolated by mechanical delamination of other layers and decellularization with peracetic acid and ethanol solution in water. The scaffold obtained had collagen as the primary structural component. Ultra-structural studies revealed the three-dimensional fibrous mesh-like

network structure of the scaffold. *In vitro* cell culture studies showed that the scaffold supports attachment and proliferation of cells like 3T3 fibroblasts, human umbilical vein endothelial cells and rat adrenal PC12 pheochromocytoma cells (Burugapalli *et al.*, 2007). Burugapalli and Pandit 2007 evaluated *in vivo* degradation and tissue response of cholecyst-derived ECM after subcutaneous implantation in rats. Native non cross-linked scaffold was completely infiltrated with host tissue at 21 days and resorbed by 63 days. The glutaraldehyde cross-linked scaffold underwent no degradation until 63 days and had higher giant cell reaction and chronic inflammatory response (Burugapalli and Pandit, 2007).

The collagen fiber orientations and biaxial mechanical properties of cholecyst-derived ECM showed good strength and compliance in a physiologically relevant range of stresses and strains. Very weak anisotropic nature of the material allowed greater freedom with design parameters than a strongly anisotropic behavior. The consistent, wider range of collagen fiber orientations increased the suitability of cholecyst-derived ECM as a material for multi-axial loading applications (Coburn *et al.*, 2007).

Chan et al 2008 incorporated PAMAM dendrimer into CEM using the EDC/NHS cross-linking system resulting in covalent binding of PAMAM on CEM. Functionalization improved stability of CEM to enzymatic degradation, increased amine functional groups useful in tethering bioactive agents, maintenance of tensile strength but increased flexibility of scaffold, as well as preservation of the ability to support cells *in vitro*. The

method provided a strategy for designing degradable scaffold with predetermined biological functionality (Chan *et al.*, 2008).

To assess the potential of CEM for creating a tissue engineered heart valve, the proliferation of valvular endothelial cells (VECs) and valvular interstitial cells (VICs) on CEM was studied. CEM supported the growth of both VICs and VECs, and retained their phenotypic mRNA synthesis, protein expression and morphology similar to that in the native aortic heart valve (Brody *et al.*, 2007).

ECM derived from porcine cholecyst is a promising scaffold of animal origin that can be used as a xenograft. It has been used as a buttress material to reinforce staple lines in an ex vivo peristaltic inflation model (Burugapalli *et al.*, 2008), treatment of experimental full thickness wound (Revi *et al.*, 2013) and urinary bladder reconstruction (Kajbafzadeh *et al.*, 2014).

2.3. Biologic response to ECM based scaffolds

Generally biological response to implantation of any biomaterial passes through the sequence of events including injury, provisional matrix formation, acute inflammation, chronic inflammation, granulation tissue formation, foreign body reaction and fibrosis/fibrous encapsulation (Anderson, 2001).

2.3.1. Injury

Implantation of any biomaterial leads to injury to vascularized connective tissue. This follows vascular changes leading to increased vascular permeability and resultant

accumulation of exudates containing fluid, proteins, and blood cells. There will be activation of coagulation system and complement system with resultant generation of inflammatory mediators and thrombus formation (Anderson, 2001).

2.3.2. Provisional matrix formation

Because of the injury caused by the implantation process, blood material interaction occurs right away after the implantation leading to the development of provisional matrix. Major component provisional matrix is fibrin produced by activation of the coagulation system. The provisional matrix is also composed of fibronectin and thrombospondin bound to fibrin, and platelet granule release products including thrombospondin, TGF-α, TGF-β, PDGF, platelet factor 4 and platelet-derived endothelial cell growth factor. The provisional matrix once formed is stabilized by the cross-linking of fibrin by factor XIIIa. The provisional matrix act as a naturally derived biodegradable scaffold from which cytokines, growth factors, mitogens, chemoattractants, and other mediators are released to the site of injury and control the wound healing process (Anderson, 2001).

2.3.3. Inflammation

The injury to vascularized connective tissue follows vascular changes leading to increased vascular permeability and resultant accumulation of exudates containing fluid, proteins, and blood cells. The injury followed by blood material interaction generates several inflammatory mediators which act in the local implant tissue causing acute inflammation. Neutrophils are the major cells during the first several days of the injury

constituting the acute inflammatory response. The chemotactic factors for neutrophil migration are activated only in acute inflammation. Since neutrophils are short lived, they disintegrate and disappear after 1-2 days of implantation (Anderson, 2001). On the other hand the chemotactic factors for monocytes are activated over longer periods of time, monocytes emigration continue for several days to weeks of implantation. Monocytes differentiate to tissue macrophages which are having a very long life span, thus being major cell type at chronic inflammatory phase (Anderson, 2001).

2.3.4. Granulation tissue

Granulation tissue development is usually seen as a part of chronic inflammation. Within one day of implantation of biomaterial, the healing reaction is initiated by the action of monocytes and macrophages, followed by fibroblast proliferation and neo-vascularization leading to granulation tissue formation. Granulation tissue appears as pink, soft granular structure on the surface of healing wounds. Histologically granulation tissue is characterized by the proliferation of new small blood vessels and fibroblasts. New blood vessels are formed by proliferation, maturation, and organization of endothelial cells into capillary tubes known as neovascularization. At early phases fibroblasts in the granulation tissue predominantly produce proteoglycans and at later phases they secrete collagen type-1. Some of the fibroblasts of the granulation tissue have smooth muscle phenotype and is responsible for wound contraction (Anderson, 2001).

2.3.5. Foreign body reaction

Foreign body giant cells (FBGCs) and the granulation tissue components such as macrophages, fibroblasts and capillaries constitute the foreign body reaction. The extent of the foreign body reaction varies according to the properties of the biomaterial like surface properties, surface area to volume ratio etc. Foreign body reaction may persist at the tissue-material interface till the life time of the implant or until the material is completely degraded *in vivo*. Foreign body giant cells are the hallmark of foreign body reaction. Several tissue macrophages at the implant tissue coalesce to form multinucleated giant cells. FBGCs are associated with the degradation of biomaterials. Very large FBGCs with large number of nuclei may be present on the surface of the biomaterial (Anderson, 2001).

The persistence of foreign body giant cells at tissue-material interfaces is poorly understood. Reports suggest the presence of foreign body giant cells for several years. Ultra structural studies has been demonstrated apoptotic nuclei in FBGCs formed in collagen sponge implants and disappearance of FBGCs with the resorption of collagen sponge (Honma and Hamasaki, 1996).

2.3.6. Fibrosis and fibrous encapsulation

Healing response to biomaterial implant may be either by regeneration or fibrosis. Usually fibrous capsule development/fibrosis is the end-stage response to biomaterial implants. Regeneration involves healing of the implantation induced injury by the native paranchymal cells. Fibrosis involves healing by the development of connective tissue

leading to formation of fibrous capsule around the implant. The choice of healing reaction by fibrosis or regeneration generally depends on the proliferative potential of the cells of the implant tissue, the extent of injury, and extent of damage to the frame work of the tissue. Generally healing by regeneration occurs in tissues composed of cells with high proliferative potential and healing by fibrosis results in tissue composed of cells with low proliferative potential (Anderson, 2001).

Although general tissue response to the implant passes through the above mentioned sequence of events, duration and extent to which the events like inflammation, foreign body reaction and fibrosis induced by the biomaterial implants largely vary depending on the biomaterial properties like size, shape, chemical and physical properties (Anderson, 2001). Implantation of biological scaffold also induces a similar tissue response. Usually the biological scaffold materials induces constructive tissue remodeling response characterized by the cellular infiltration, deposition of new ECM in response to mechanical stimuli, self-assembly of various cell populations and re-establishment of an interface between remodeling tissue and adjacent normal tissue (Badylak, 2007).

Valentine et al, (2006) evaluated the host-tissue morphologic response to five commercially available ECM-derived biologic scaffolds, which differ at least in species of origin, processing methods or terminal sterilization. The scaffolds were used for abdominal wall repair in a rodent abdominal defect model. Each device elicited a distinct tissue morphologic response that differed with respect to cellular infiltration,

vascularity, the infiltration of multinucleated giant cells, and tissue remodeling at or after 7 days. Rapidly degrading materials and autologous tissue induced higher cellularity, especially at the early time-points. Materials that degraded slowly induced multinucleated giant cell formation, chronic inflammation, and/or remodeling with dense, poorly organized fibrous connective tissue. Study revealed remarkable differences in the acute and chronic host tissue response and in the downstream tissue remodeling outcomes induced by various biologic scaffolds that differ in species of origin, processing methods or terminal sterilization. Therefore the nature of tissue response induced by biological scaffold may vary according to the species of origin, source organ, processing methods, terminal sterilization and intended clinical application (Valentin *et al.,* 2006).

2.4. Immune response to biological scaffold materials

Since biological scaffolds derived from porcine tissues/organs are xenogeneic in nature it can be immunogenic to human. However, the use of these materials has been largely successful without causing any immunological rejection reactions. But there are some reports where the use of biological scaffolds led to severe pain, inflammation and graft versus host disease (Ho *et al.,* 2004, Zheng *et al.,* 2005, Petter-Puchner *et al.,* 2006, Catena *et al.,* 2007, Petter-Puchner, 2007, John *et al.,* 2008, Wang *et al.,* 2009). As documented in the US FDA database of 'manufacturer and user facility device experience' it appears that most of the reported complications associated with the use of xenogeneic graft materials related to immune response (US-FDA, 2014). However, only few studies have investigated the immune response biological scaffold materials.

Biological scaffolds consist of xenogeneic molecules, many of which are xenoantigens. Major xenoantigens present in the biologic scaffold materials are the Gal epitope and DNA (Badylak and Gilbert, 2008). The xenoantigens of ECM derived scaffolds that can cause immune response are Gal-epitope, DNA and xenogeneic collagen.

2.4.1. Gal epitope

The cell membrane oligosaccharide called as gal epitope i.e., α-Gal (Galα1,3-Galβ1–4GlcNAc-R) has been reported to be associated with hyperacute rejection following organ xenotransplantation. Gal epitope is present in all species except humans and old world monkeys. Since human and old world monkeys have mutations in the α1,3-galactosyl-transferase gene they do not have gal epitope. Instead they have anti-Gal antibodies of IgG, IgM or IgA type which is formed in response to intestinal bacteria with gal epitope. About 1% of human IgG is anti-Gal IgG. The Gal epitope may be present in cell associated glycoproteins and glycolipids, secreted glycoproteins such as thyroglobulin, fibrinogen, and immunoglobulin G (IgG). Laminin and other basement membrane proteins also contain gal epitope. (Badylak and Gilbert, 2008, Galili, 2005, Galili *et al.*, 1988). Konakci et al, 2005 studied the occurrence of gal epitope in glutaraldehyde treated porcine heart valves. There was enhanced anti-Gal IgM antibodies present in patients who received glutaraldehyde treated porcine heart valves. Study suggested potential association between anti-Gal antibodies and degeneration and calcification of bioprostheses particularly in younger individuals (Konakci *et al.*, 2005). Gal epitope has also been detected in porcine small intestinal submucosa (McPherson *et al.*, 2000), bioprostheses used in cardiac surgery (Konakci *et al.*, 2005), porcine anterior

cruciate ligament (Stone *et al.*, 2007) and porcine cartilage (Stone *et al.*, 1998). In order to overcome the problems associated with gal epitope during xenograft transplantation some methods have been used. This includes treatment of the xenograft with α-galactosidase enzyme and the use of gal negative knock out pigs as organ source. In a study conducted on α-galactosidase treated cartilage grafts there was significant reduction in the number of T lymphocyte infiltration in to the remodeling site when compared to non α-galactosidase treated cartilage grafts (Stone *et al.*, 1998). Raeder et al 2002 implanted porcine SIS in subcutaneous tissue of α-1,3 galactosyltransferase knock-out gal negative mice and wild type mice. Similar to response expected in human the α1,3 galactosyltransferase knock-out mice produced both IgG and IgM anti-Gal antibody. Histology showed that SIS implantation in wild type mice lead to complete remodeling of the SIS by 25 days. On the other hand α-1,3 galactosyltransferase knock-out mice showed persistence of inflammatory response and delayed remodeling of the implant site. When knock-out mice were immunized with sheep erythrocytes to enhance anti-Gal antibody response the SIS implantation led to an increased early inflammation. In all cases knock-out mice showed constructive tissue remodeling of the SIS implant. So the results of the study suggest that the presence of anti-Gal antibody do not prevent constructive remodeling response induced by SIS. However it may delay the constructive remodeling response (Raeder *et al.*, 2002). Daly *et al*, (2009) studied the effect of the Gal epitope on the host response to porcine small intestinal submucosa in a primate model of abdominal wall resection. Results suggested that porcine-small intestinal submucosa contains Gal epitope and stimulated an anti-Gal antibody response.

But the Gal epitope had no adverse effects on host remodeling response (Daly *et al.*, 2009).

2.4.2. Xenogeneic DNA

Presence of xenogeneic DNA in biological scaffolds may cause inadvertent inflammatory reactions following clinical applications *in vivo* (Badylak and Gilbert, 2008). Small amount of xenogeneic DNA is always expected in biologic scaffolds even after employing the most efficient decellularization protocols (Zheng *et al.*, 2005, Badylak and Gilbert, 2008). Gilbert et al, 2009 studied the presence and fragment length of remnant DNA present in several commercially available biological scaffold materials, namely Oasis™ (Cook Biotech, Inc.), derived from porcine SIS, Restore™ (DePuy Orthopedics Inc.), a 10-layer multilaminate porcine SIS, ACell Vet device (ACell, Inc.) derived from porcine urinary bladder matrix (UBM), Alloderm™ (LifeCell Corporation) made of human dermis, GraftJacket™ (Wright Medical Technology Inc.) made of human dermis, and the Zimmer collagen repair patch™ (Tissue Science Laboratories, UK) derived from porcine dermis. Most of the commercial scaffolds studied had measurable amount of remnant DNA. Alloderm™ and the Zimmer Collagen Patch™ did not contain residual DNA. Fragment length analysis of the residual DNA showed that the only material that had full DNA strands was GraftJacket™ originally derived from human dermis. The residual DNA detected in all other scaffolds was of less than 300 base pairs in length. Short DNA of this much length is very doubtful to be a matter of concern. More over critical amount of cellular remnants may be needed to elicit any adverse tissue response following the use of biological scaffolds (Gilbert *et al.*, 2009).

The processing methods used may modify the nature of cellular components, so that they no longer cause an adverse reaction (Gilbert *et al.*, 2006). In spite of the presence of trace amount of DNA and cellular components in commercially available biological scaffold materials, their clinical applications were enormously successful.

Zheng *et al,* (2005) investigated noninfectious edema and severe pain in human patients who have undergone tendon repair with a commercially available porcine SIS derived Restore™ biomaterial. Study revealed the presence of porcine cells and porcine DNA in Restore™. When implanted in mice and rabbits the material caused inflammatory reaction characterized by massive infiltration of lymphocytes. The result of the study established that Restore™ SIS is not an acellular biomaterial, and has the ability to cause inflammatory reaction after implantation (Zheng *et al.*, 2005).

2.4.3. Xenogeneic collagen

Major component of biological scaffold materials is collagen. Although animal derived collagen has been successfully used to fabricate a variety of biomedical devices there has been continuous concern over the immunogenicity of animal derived collagen in human. In spite of evidence that it can react with antibodies, collagen is still considered as a weak antigen. Major epitopes in collagen are of 3 types: Helical— formed by an intact triple helix, Central—present within the collagen triple helix, and terminal—located in the nonhelical terminal regions of the collagen molecule. Several studies have shown that the major antigenic determinants are that present in terminal part of the molecule. But antibodies that interact with central epitopes that are deep inside the helix

have also been identified. These epitopes may be important during degradation of the collagen *in vivo*. Immune response to collagen-containing implants is also complicated by other factors such as the presence of noncollagenous proteins, cellular components and modifications resulting from cross-linking/chemical treatments (Lynn *et al.*, 2004).

2.4.4. Mast cell response

Mast cells are the source of histamine and other inflammatory modulators responsible for acute/immediate hypersensitivity reactions (hypersensitivity type I) and they are implicated in acute inflammatory response to biomaterial implantation (Tang *et al.*, 1998). Mast cells have been shown to be associated with fibrotic encapsulation following implantation of biomaterials (Thevenot *et al.*, 2011). Mast cells in tissue sections can be detected by the presence of metachromatic granules which can be stained with toluidine blue (Bancroft and Gamble, 2008). To date no studies have examined the role of mast cells in response to biological scaffold implantation.

2.4.5. Granulocyte response

Neutrophils attach itself to biomaterial surface through binding of CD11b/CD18 (CR3) to iC3b deposited on to the biomaterial surface as a result of complement activation (Gemmell *et al.*, 1996). Reider *et al*, (2006) studied the *in vitro* human leukocyte migration towards protein extracts prepared form decellularized or glutaraldehyde cross-linked vascular tissue. There was reduced lymphocyte and monocyte migration towards extracts of glutaraldehyde cross linked tissue and decellularized vascular tissue. However the strong granulocyte migration was observed for both materials. The study

suggested that, though decellularization could effectively reduce lymphocyte and macrophage recruitment, the granulocyte response remain unaffected and may cause residual immune response (Rieder *et al.*, 2006). Bastian *et al*, (2008) has shown that upon contact with human blood plasma decellularized porcine pulmonary conduits get deposited with IgG and leads to activation of classical complement pathway. This results in subsequent neutrophil adhesion on to the acellular material. This inflammatory responses observed *in vitro* were strongly inhibited by protein extracts prepared from native tissue. So decellularization protocol effectively removes extracellular molecules that are essential for the inhibition of complement activation and/or granulocyte response (Bastian *et al.*, 2008).

2.4.6. Macrophage response

Macrophages are highly heterogeneous subset of the mononuclear cell population (Gordon and Taylor, 2005). Several studies have been described macrophage phenotype in response to biological scaffold remodeling. Valentine *et al*, (2009) studied the role of circulating macrophages in the degradation of native non-cross-linked small intestinal submucosa (noncrosslinked SIS), carbodiimide (CDI) crosslinked form of porcine-derived SIS and an autologous tissue graft using a rat body wall reconstruction model. The *in vivo* degradation of each scaffold was assessed with and without macrophage depletion by administration of clodronate-containing liposomes. Results showed that peripheral blood monocytes are essential for the early and rapid degradation of both SIS scaffolds and autologous graft. The CDI cross-linked SIS was resistant to macrophage-

mediated *in vivo* degradation. Therefore the macrophages have crucial role in biologic scaffold degradation and early remodeling events (Valentin *et al.*, 2009).

Similar to the TH1 and TH2 helper T-cell phenotypes macrophages can be classified in to M1 and M2 phenotypes. M1 and M2 phenotypes represent the two extremes in the spectrum of possible forms of macrophage activation. Macrophages with M1 phenotype being pro-inflammatory macrophages, participates in aggressive chronic inflammation but M2 phenotype being anti-inflammatory macrophages promotes constructive remodeling process (Mills *et al.*, 2000). The classical activation of macrophages by Interferon-γ alone or in concert with lipopolysaccharide and or tumor necrosis factor is characterized by high capacity for antigen presentation, high IL-12, IL-23 and low IL-10 production. Such macrophages are referred to as M1 macrophages. M1 macrophages produce high levels of inducible nitric oxide synthase and metabolize arginine to secrete toxic reactive oxygen species and nitrogen species. They also secrete inflammatory cytokines such as IL-1b, IL-6, and TNF and act as inducer and effector cells in TH1 type inflammatory responses. The M2 macrophages produce low level IL-2 and are involved in immunoregulation and tissue remodeling responses. The M2 macrophages can be again classified in to M2a, M2b and M2c. M2a which is also known as alternatively activated macrophages are induced by IL-4 or IL-13. M2b is induced by exposure to immune complexes and agonists of Toll-like receptors (TLRs) or IL-1 receptor (IL-1R). M2c is induced by IL-10 and glucocorticoid hormones. M2 macrophages produce wound healing cytokine TGF-β, high level of anti-inflammatory cytokine IL10, low levels of IL12 and express large quantity of arginase-I to produce ornithine and

polyamines from arginase (Mantovani *et al.*, 2004). So M2 macrophages can activate wound healing. In any tissue reaction, both M1 and M2 phenotypes can be expected but the predominance of either one of these macrophage phenotypes determines the outcome of the tissue reaction, largely by regulating the cytokine milieu of the microenvironment (Stout *et al.*, 2005).

Macrophage phenotypic polarization has been studied in the context biological scaffold implantation. Badylak *et al*, (2008) studied the M1/M2 macrophage polarization following the implantation of native non-cross-linked small intestinal submucosa (Restore SIS), carbodiimide crosslinked form of porcine-derived SIS (CDI-SIS) and an autologous tissue graft. SIS device predominantly induced constructive tissue remodeling response characterized by M2 macrophage predominance up to the 16 weeks. The CDI-SIS induced equal distribution of M1 and M2 macrophages at early time points and then showed M1 macrophage predominance at later time points. The tissue reaction was characteristic of persistent chronic inflammatory response. The autologous tissue graft induced M2 response at 1 week but equal distribution of both cells at 2 and 4 weeks and moderately well organized connective tissue by 16 weeks. Results of the study suggested that the processing methods used during the manufacturing of a biologic scaffold could have a profound influence upon the macrophage phenotype profile and downstream remodeling events (Badylak *et al.*, 2008).

Brown *et al*, (2009) studied the effects of cellular component within an implanted ECM scaffold upon macrophage phenotype, and the relationship between macrophage phenotype and tissue remodeling. They repaired partial-thickness defects in the abdominal wall musculature of Sprague–Dawley rats with autologous body wall tissue, acellular allogeneic rat body wall ECM, xenogeneic pig urinary bladder tissue, or acellular xenogeneic pig urinary bladder ECM. The acellular test articles induced M2 macrophage response and constructive tissue remodeling. The grafts with cellular component induced M1 macrophage response and resulted in deposition of dense connective tissue and/or scarring. The same results were obtained with graft containing autologous cellular component also. It was concluded that the phenotype of the macrophages participating in the host response is influenced by the presence of cellular material within an ECM scaffold. The final outcome of tissue remodeling following biological scaffold implantation is highly dependent on the phenotype of the macrophages in the tissue reaction (Brown *et al.*, 2009).

Keane et al 2012 used M1/M2 phenotypic polarization profile of macrophages to evaluate the consequences of ineffective decellularization on the host response. An aggressive decellularization was associated with a shift in macrophage phenotype predominance from M1 to M2 phenotype *in vitro*. But this shift was not quantitatively apparent in an *in vivo* rodent model of body wall repair model. Indeed there were notable differences in the distribution of M1 vs. M2 macrophages within the various scaffolds which differ according to their extent of decellularization. The results of the study showed that decellularization efficacy of biologic scaffold materials is also a

determinant of the macrophage phenotype response. But the study failed to demonstrate a cause-effect relationship between macrophage phenotype during remodeling response and the efficiency of decellularization (Keane *et al.*, 2012).

2.4.7. Lymphocyte response

In a study by Allman *et al*, (2001) mice were implanted subcutaneously with xenogeneic tissue, syngeneic tissue, or SIS, and the graft site analyzed histologically for rejection or acceptance and specific antibody response was studied. The antibody response to SIS was restricted to IgG1 isotype which had no complement activation potential. Similar results obtained after the secondary implantation of SIS. The cytokine expression in the implant tissue was limited to IL-4, TH2 cytokine with no detectable INF-γ the TH1 cytokine. In order to study the cell source of IL4, T-cell knock-out mouse was implanted with the material. These mice expressed neither interleukin-4 at the implant site nor anti-SIS-specific serum antibodies but they did accept the SIS graft. The results suggested that porcine ECM elicited an immune response that is predominately TH2-like, consistent with a remodeling reaction rather than rejection (Allman *et al.*, 2001).

2.4.8. Antibody response to biological scaffold materials

Several studies have been carried out to determine the antibody response to biological scaffold materials. Allman *et al*, (2001) studied the antibody response elicited against small intestinal submucosa implanted subcutaneously in mouse model. SIS specific antibodies were detected in mouse. Detailed study of the isotype of SIS specific antibody showed that the antibody response to SIS is limited to IgG1which is having

low complement activation potential. The results were indicative of Th2 helper T cell mediated response. The observation was same when the mice were re-implanted with SIS (Allman *et al.*, 2001). Konacki *et al,* (2005) studied the anti α-Gal IgM antibody response to porcine aortic valve prosthesis in human patients before and after 10 days of surgery. Compared to anti α-Gal IgM antibody level before surgery there was enhanced antibody response after surgery. The antibody formed after surgery was more cytotoxic to α-Gal bearing PK-15 cells *in vitro* (Konakci *et al.*, 2005). Ansaloni et al. 2007 evaluated the immune response to small intestinal submucosa in human patients who have undergone inguinal hernioplasty with Surgisis IHM xenograft. The SIS-specific antibodies, anti α-Gal antibodies and type I collagen specific antibodies were tested at 2 weeks, 6 weeks, and 6 months after the treatment. All patients were also clinically assessed up to 2 years for signs of clinical rejection, hernia recurrence, and other complications. All patients implanted with Surgisis IHM produced antibodies specific for SIS and α-Gal with a peak antibody response between 2 and 6 weeks after implantation. Type I collagen-specific antibodies was not detectable in any of the patients. By 6 months, all patients showed decreasing levels of anti-SIS antibodies. There was no sign of clinical graft rejection or any other complications up to 2 years after treatment. So the study observed significant immune response against small intestinal submucosa as evidenced by the production of anti-SIS specific and anti α-Gal antibodies, but the immune response did not lead to undesirable graft rejection or clinical complications (Ansaloni *et al.*, 2007).

Though antibody response to α-Gal epitope is described by several studies so far, no study has examined the antibody response to protein antigens in the biological scaffold materials. Griffiths *et al*, (2008) identified several immunogenic proteins in the bovine pericardium using an immunoproteomic approach. Most of the immunogenic proteins in bovine pericardium that were immunogenic to rabbit were of cellular in origin. Osteglycin molecule was found to be immunogenic protein of ECM (Griffiths *et al.*, 2008). The study warrants the importance of antigen removal rather than simple decellularization protocol during the preparation of biological scaffold materials.

CHAPTER-3

3. CHARACTERIZATION OF SCAFFOLDS FOR IMMUNOGENIC POTENTIAL

3.1. INTRODUCTION

This chapter is about the characterization of ECM scaffolds prepared by non-detergent/enzymatic method (Anilkumar *et al.*, 2014) for parameters related to immunogenic potential. As the endotoxin load may cause inadvertent inflammatory reactions (Gorbet and Sefton, 2005) the endotoxin level were also evaluated. As the immunogenic potential largely depends on the residual cellular components present in the scaffolds (Badylak and Gilbert, 2008) the number of residual cell nuclei retained in the scaffolds were characterized. Similarly the protein composition may have role in remodeling response and host response (Marçal *et al.*, 2012). Therefore extractable proteins in the extracellular matrices isolated from source organs used for scaffold preparation were studied. The potential of extracellular matrices to raise antibody response was evaluated after implantation of scaffolds in subcutaneous tissue of rats. Further the immunogenic proteins in cholecyst derived scaffold were identified by an immunoproteomic approach. The ability of scaffolds to induce delayed type hypersensitivity reaction was studied by guinea pig maximization test. Finally, the ability of scaffolds to activate innate immunity was characterized by *in vitro* methods.

3.2. MATERIALS AND METHODS

3.2.1. Preparation of scaffolds

3.2.1.1. Preparation of cholecyst derived scaffold (CDS)

3.2.1.1.1. Collection of cholecyst

Cholecyst (Gall bladder) was collected, under the supervision of a qualified/registered veterinarian, from market grade-pigs at slaughter in a modern slaughter house (Meat products of India, Government of Kerala undertaking, Edayar, Eranakulam, Kerala). The specimens without any gross lesion were transferred within five minutes of separation from the carcass to specimen bottles containing approximately 10 times volume of 10% neutral buffered formalin (NBF). The specimens were transferred to the laboratory at ambient temperature.

3.2.1.1.2. Isolation of extracellular matrix from cholecyst

Within 24-48h of collection the liver residue and any fat content were trimmed off from the outer part of serosal layer of the cholecyst. The bile was drained off by a single transverse incision or multiple incisions using a scalpel blade/scissors. The incisions may be at any part of the cholecyst to yield scaffolds of the desirable the shape and size. The neck and the fundus were trimmed-off to obtain a cylindrical hollow structure. A single longitudinal incision was made to get a flattened sheet and the sheet was thoroughly washed in running tap water for 5-10 minutes to remove the luminal contents. The inner mucosal layer was scraped off with the blunt end of the forceps. Serosal layer was peeled away as a single unit to isolate the greenish yellow translucent sheet of ECM.

3.2.1.2. Preparation of jejunum derived scaffold (JDS)

3.2.1.2.1. Collection of jejunum

The jejunum was collected from market grade-pigs from approved slaughter house (Meat products of India, Edayar, Eranakulam, Kerala) under the supervision of a qualified veterinarian. The specimens without any gross lesion were transferred within five minutes of separation from the carcass to specimen bottles containing approximately 10 times volume of NBF. The specimens were transferred to the laboratory at ambient temperature.

3.2.1.2.2. Isolation of extracellular matrix from jejunum

Within 24-48h of collection the specimens were cut to segments of 6cm in length for easy penetration of the cross-linking agent. A single longitudinal incision was made to get a flattened sheet using a scalpel blade/scissors and the sheet was thoroughly washed in running tap water for 5-10 minutes to remove the luminal contents. Residual tissue and any fat content were trimmed off from the outer part of serosal layer. The inner mucosal layer was scraped off with the blunt end of the forceps. Serosal and muscularis layer was peeled away to get sheets of submucosa. It was washed thoroughly to get, the ivory white colored ECM.

3.2.1.3. Preparation of urinary bladder derived scaffold (UDS)

3.2.1.3.1. Procedure for collection of urinary bladder

Urinary bladder was collected market grade-pigs from approved slaughter house (Meat products of India, Edayar, Ernakulam, Kerala) under the supervision of a qualified

veterinarian. The urine was drained off immediately by a single transverse incision on the neck part of the urinary bladder using a scalpel blade/scissors. The specimens without any gross lesion were transferred within five minutes of separation from the carcass to specimen bottles containing approximately 10 times volume of NBF. The specimens were transferred to the laboratory at ambient temperature.

3.2.1.3.2. Isolation of extracellular matrix from urinary bladder

Within 24h of collection the neck and the fundus were trimmed to obtain a cylindrical hollow structure. A single longitudinal incision was made to get a flattened sheet and the sheet was thoroughly washed in running tap water for 5-10 minutes to remove the luminal contents. Any fat content was trimmed off from the outer part of serosal layer. The inner mucosal layer was scraped off with the blunt end of the forceps. Serosal and muscularis layers were peeled away to get sheets of connective tissue beneath the mucosa. It was then washed thoroughly to get the creamish white translucent sheet of ECM.

3.2.1.4. Processing of extracellular matrix scaffolds

The isolated ECM sheets were thoroughly washed in running tap water for at least two hours to remove all the formalin residues. It was then stored at -80°C freezer. The materials were thawed at room temperature and spread on petri-plates, covered with aluminium foil and then kept for pre-freezing at -80°C for overnight. Lyophilisation was carried out in a freeze dryer (CHRIST–ALPHA 2-4LD plus^{TM}, Germany) for 16 h under vacuum condition. The lyophilized samples were then packed in Tyvek® packaging

material for Ethylene-trioxide (ETO) gas sterilization. After sterilisation the CDS, JDS and UDS were stored at room temperature for six months or until evaluation of scaffold properties or use in various experiments.

3.2.1.5. Reference scaffold

Wherever indicated, porcine small intestinal submucosa marketed by Cook® Medical, USA, in the form of 1-Layer Tissue graft Surgisis® Biodesign™ hereafter referred to as Cook-small intestinal submucosa (CSIS) was used as the reference scaffold.

3.2.2. Test for pyrogenicity

Physiological saline extract of the scaffolds were tested for endotoxin with limulus amoebocyte lysate (LAL) assay by a kinetic chromogenic method using Endosafe PTS endotoxin (Charle River Laboratories, India) as per USP 23/NF18<85> 21. The samples were extracted in physiological saline (6 cm^2 in 1 mL) at 37°C for 1 h. Then, they were mixed with LAL reagent and chromogenic substrate in an automated system with built-in standard. The color intensity was measured. Endotoxin level less than 0.5 EU/mL was considered non pyrogenic.

3.2.3. Histotechnology

The scaffolds were cut in to small pieces, hydrated, put in tissue cassettes and processed in Leica TP1020 automated tissue processor (Leica Biosystems, Germany). The processer treated the scaffolds in series of solutions starting from ascending grades of alcohols for dehydration. The alcohol was then cleared off by treatment with few changes in xylene. Finally the scaffolds underwent impregnation in two changes of

molten paraffin wax. The tissue cassettes were taken out of the tissue processor and the scaffolds were made in to paraffin blocks using a paraffin embedding center (SLEE, Germany). Four micron thick paraffin sections were cut with Leica RM2255 automated microtome (Leica Biosystems, Germany) and used for Harris's haematoxylin and eosin staining. The sections were de-paraffinized in xylene and brought to water through descending grades of alcohol. Tissue sections were treated in Harris's haematoxylin for 5 min, washed gently in water, differentiated in acid alcohol and blued in ammonia water. It was then treated in eosin stain for 2 min, washed gently in water, dehydrated through ascending grades of alcohol, cleared in xylene and mounted for microscopic evaluation (Bancroft and Gamble, 2008).

3.2.4. Quantification of cellularity in scaffolds

The scaffolds were cut in to small pieces, hydrated and processed for paraffin embedding as for routine histology. Four micron thick sections were made and stained with haematoxylin and eosin stains. The cellularity of CSIS, CDS, JDS and UDS was then assessed by counting the number of nuclei (identified as purple spots) in images captured from histology sections at 400x magnification using DP71 camera loaded on to Olympus BX51 microscope (Olympus Corporation, Japan). The total area of the scaffold under the scan was determined by using Image-Pro 3DS version 6.1 software (Media Cybernetics, Silver Spring, MD) and nuclei were counted by manual tag option of the software. The cellularity was then calculated and expressed as the number of nuclei in unit area of the scaffold.

3.2.5. Identification of extractable proteins of extracellular matrices prepared from cholecyst, jejunum and urinary bladder

3.2.5.1. Preparation of extracellular matrices for protein extraction

Porcine cholecyst (gall bladder), small intestine and urinary bladder were collected in phosphate buffered saline (PBS) supplemented with 0.1% (w/v) ethylenediamine tetraacetic acid and 100 KIU/mL aprotinin (protease inhibitor). This was the transported to the laboratory in ice (4°C). The extracellular matrices were then isolated by previously described procedure (Anilkumar *et al.*, 2014) as described in the section 3.2.1, but without any cross-linking of ECM proteins. Extracellular matrices isolated were designated as cholecyst-derived-ECM (CDE), jejunum-derived-ECM (JDE) and urinary bladder-derived-ECM (UDE) respectively. The isolated ECM were than stored at -80°C in Dulbecco's modified minimum essential medium (DMEM) containing 15% dimethyl sulphoxide.

3.2.5.2. Protein extraction

The ECM stored in -80°C freezer were taken out and thawed in ice. The matrices were minced into small pieces of approximately 0.5–1 mm on a petri dish using sterile surgical blades. Using a tissue homogenizer under ice, minced ECM were homogenized in extraction buffer containing 10mM Tris–HCl (pH 8.0), 2mM $MgCl_2$, 10mM KCl, 100KIU/mL aprotinin, 0.5mM Pefabloc, 1mM dithiothreitol and 134mM 3-(benzyldimethylammonio) propanesulphonate (NDSB-256). The homogenate was centrifuged for 25 min at 17,000g and 4°C in refrigerated centrifuge 5430 R (Eppendorf, Germany). The supernatant collected were designated as the protein extract of CDE,

JDE or UDE. The protein extracts were then concentrated by centrifugal filtration using Amicon® Ultra-4 centrifugal filter device with nominal molecular weight limit of 3kDa (Millipore, Carrigtwohill, Ireland). The protein content in the extract was estimated by Peterson's modified Micro-Lowry method (Total Protein kit, Sigma).

3.2.5.3. Sodium dodecyl sulfate polyacrylamide gel electrophoresis (SDS-PAGE)

10% poly acrylamide gel was used for electrophoresis. The stacking gel used was 2.5%. 30μg of CDE, JDE or UDE protein extract was added into the corresponding wells. Precision plus protein dual colour standard (Cat. Number 161-0374, Biorad, USA) was used as molecular weight standard. The electrophoresis run was started at 15mA. After the dye front has moved in to the separating gel, current was increased to 20mA. When the dye front reached the bottom of the gel, the power pack was turned off. Gel plates were removed and separated apart gently without disturbing the gel. A corner of the bottom of the gel that was closer to the well number 1 was cut. The gel was then stained in PhastGel™ Blue R (GE Healthcare, Sweden) overnight. Destaining was carried out with solution of methanol, acetic acid and water in the ratio of 1:3:6. After destaining the gel was scanned and photographed (Canon 4200F scanner, China).

3.2.5.4. Nanoflow Liquid Chromatography- tandem mass spectrometry

Nanoflow ultra-performance liquid chromatography (nanoACQUITY UPLC® System, Waters) coupled to a Quadrupole-Time of Flight (Q-TOF) mass spectrometer (SYNAPT-G2, Waters Corporation, Milford, MA, USA) was used for the proteome analyses.

The SDS-PAGE gel with protein bands were cut linearly so that the all the proteins in the sample are present in the thin linear piece of gel. The gel piece was cut into ~1mm square pieces and treated with 50 mM ammonium bicarbonate/acetonitrile (1:1 vol/vol) for 1h with shaking. The supernatant was discarded and complete destaining was ensured by washing in acetonitrile until the gel pieces became white and shrink. The gel pieces were saturated with sequencing grade trypsin (Sigma, USA) modified in 50 mM ammonium bicarbonate and was left in an ice bucket for 45 min. Enzymatic digestion was performed by incubating the samples overnight at 37 °C.

The digested peptides were extracted into 1:2 (vol/vol) 5% formic acid/acetonitrile at 37 °C for 20 min in a shaker. The supernatant was collected into a PCR tube and freeze-dried in a vacuum lyophilizer. To the freeze-dried product in the tube, 20 µL of 0.1% formic acid/acetonitrile (97:3 vol/vol) was added and was centrifuged at 14,000 rpm for 12 min. The supernatant was collected and were transferred to autosampler vials (Total Recovery Vial, Waters Corporation, Milford, MA, USA) for peptide analysis via LC-MS^E (MS at elevated energy) method.

3.2.5.4.1. Nanoflow Liquid Chromatography

The tryptic peptides were separated using a nanoACQUITY UPLC® chromatographic system (Waters, Manchester, UK). Instrument control and data processing was done with MassLynx4.1 SCN781 software. In the nanoACQUITY UPLC®, the peptides were separated by reversed-phase chromatography technology. The peptide sample was injected in partial loop mode in 5 µL loop (injection volume 4.0 µL). Water was used as mobile phase-A and acetonitrile was used as mobile phase-B. All mobile phases for the

ultra-performance liquid chromatography (UPLC) system contained 0.1 % formic acid. The tryptic peptides were trapped and desalted on a trap column (Symmetry® 180µm x 20mm C18 5µm, Waters, Manchester, UK) for 1 minute at a flow rate of 15 µL/min. The trap column was placed in line with the reversed-phase analytical column, a 75 µm i.d. X 200 mm BEH C18 (Waters, Manchester, UK) with particle size of 1.7 µm. Peptides were eluted from the column with a linear gradient of 1 to 40% mobile phase B over 18.5 min at a flow rate of 300 nL/min followed by a 2.5 min rinse of 80 % mobile phase B. The column was immediately re-equilibrated at initial conditions (3% mobile phase B) for 6 min. The column temperature was maintained at 40^{O} C. The *lock mass*, [Glu^{1}]-Fibrinopeptide B human (Sigma) was delivered from the auxiliary pump of the UPLC system through the reference sprayer of the NanoLockSpray™ source (Waters Corporation, Milford, MA, USA) at a flow rate of 500 nL/min. Each sample was injected in duplicate with blank injections between each sample.

3.2.5.4.2. Mass Spectrometry analysis

Mass spectral analysis of eluting peptides from the nanoACQUITY UPLC® was carried out on a SYNAPT® G2 High Definition MS™ System ($HDMS^{E}$ System, Waters Corporation, Milford, MA, USA). It was a hybrid, quadrupole, time-of-flight mass spectrometer controlled by MassLynx4.1 SCN781 (Waters Corporation, Milford, MA, USA) software. The instrument settings were: nano-ESI capillary voltage – 2.5 KV, sample cone - 35 V, extraction cone - 4 V, source temperature - 80 °C.

All analyses were performed using positive mode electrospray ionization (ESI) using a NanoLockSpray™ source. The lock mass channel was sampled every 45s. The time of

flight analyzer (TOF) of the mass spectrometer was calibrated with a solution of 500 fmole/µL of [Glu^1]-Fibrinopeptide B human (Sigma, USA). This calibration set the analyzer to detect ions in the range of 50 - 2,000 *m/z*. The mass spectrometer was operated in resolution mode (V mode) with a resolving power of 18,000 FWHM and the data acquisition was done in *continuum* format. In MS^E mode, the data was acquired by rapidly alternating between two functions; Function-1 (low energy) and Function-2 (high energy). In Function-1, only low energy mass spectra (MS) and in Function-2 mass spectra at elevated collision energy ($MS^{E)}$ were acquired. In Function-1, collision energy was set to 1 eV in the Transfer region and 4 eV in the Trap region. In Function-2, collision energy was set to 1 eV in the Transfer region and was ramped from 14 eV to 38 eV in the Trap region to attain fragmentation in the MS^E mode. The *continuum* spectral acquisition time in each function was 0.9 seconds with an interscan delay of 0.024s.

3.2.5.4.3. Data analysis

The LC-MS^E data was analyzed by using ProteinLynx Global SERVER™ v2.5.3 (PLGS, Waters Corporation, Milford, MA, USA) for protein identification. Data processing includes *lock mass* correction post acquisition. Processing parameters for PLGS were set as follows: noise reduction thresholds for low energy scan ion–150 counts, high energy scan ion–50 counts and peptide intensity–500 counts (as per the suggestions of the manufacturer). The protein identifications were obtained by searching against the *Sus scrofa* database of national center for biotechnology information (NCBI, 2013). During database search, the protein false positive rate was set to 4 %. The parameters for protein identification was made in such a way that a peptide was required

to have at least 2 fragment ion matches, a protein was required to have at least 5 fragment ion matches and a protein was required to have at least 1 peptide match for identification. Mass tolerance was set to 10 ppm for precursor ions and 20 ppm for fragment ions. The subcellular localization, and function of proteins thus identified were then obtained by UniProt database search (The-UniProt-Consortium, 2014).

3.2.6. Assessment of IgG antibody response

3.2.6.1. Subcutaneous implantation of scaffolds in rats

With the approval of Institutional Animal Ethics Committee, the materials were implanted subcutaneously into Sprague-Dawley rats as suggested in ISO10993, Part-6 for evaluating local tissue response (ISO:10993-6, 2007) and detailed below. Out bred young adult Sprague-Dawley rats of either sex weighing not less than 200g, were used for the study. Experimental animals were housed in individually ventilated cages at 22°C with 12 h day/night cycle and provided with feed and water *ad libitum*. Fourty-eight rats were used for the study under the supervision of a veterinarian: 12 animals each for CSIS, CDS, JDS or UDS subcutaneous implantation. The rats were anaesthetized with intramuscular injection of Ketamin (70mg/Kg) and Xylazin (5mg/Kg). Hair of the supra spinal area was clipped off and swabbed with antiseptic lotion. Four subcutaneous pockets were made through skin incision (1cm long), the material ($1cm^2$) was folded and implanted in the pockets observing sterile precautions. The incision was then closed by suturing with 3/0 Mersilk (Ethicon Inc., UK). Animals were allowed to recover. The animals did not receive any antibiotic or analgesic at any stage of the experiment.

After 3 days, 7 days, 14 days, 28 days, 60 days and 90 days, blood samples were taken from two rats from each experimental group and the animals were killed in carbon dioxide chamber. Serum was separated and stored in -20°C freezer. The implant tissue was collected from each site. Samples from two sites were used for the study and other two were kept as back-up samples. Each sample was cut into two halves. Then, one of them was preserved in NBF for histomorphological evaluation. The other half of the tissue sample for gene expression analysis was put in RNAlater (Sigma) and stored in -20^0C freezer.

3.2.6.2. Antiserum Production

Anti ECM scaffold serum was prepared by immunization of Sprague-Dawley rats. Out bred young adult Sprague-Dawley rats of either sex weighing not less than 200g, were used for the study. Experimental animals were housed in individually ventilated cages at 22°C with 12 h day/night cycle and provided with feed and water *ad libitum*. ECM scaffolds for this purpose were prepared as described in Section 1.6.1. About 1g of scaffold was placed in 5mL of extraction buffer containing 10mM Tris–HCl (pH 8.0), 2mM MgCl2, 10mM KCl, 100KIU/mL aprotinin, 0.5mM Pefabloc, 1mM DTT and 134mM 3-(benzyldimethylammonio) propanesulphonate (NDSB-256) and mechanically homogenized with a porcelain pestle and mortar on ice to make fine suspension of scaffold. It was then homogenized with equal volume of complete Freund's adjuvant (Sigma, USA) using a tissue homogenizer (IKA, Germany) for 1-2 minute. About 400 µl of the homogenized suspension was injected subcutaneously into Sprague-Dawley rats. Similarly, after 14 days a booster dose of scaffold protein suspension homogenized with

incomplete Freund's adjuvant (Sigma, USA) was also given. Blood sample was taken at 0, 7, 21, 42, 56, and 72 days of immunization, serum was separated and stored in a -20°C freezer.

3.2.6.3. Test for the efficiency of immunization

3.2.6.3.1. Sodium dodecyl sulphate-polyacrylamide gel electrophoresis and Western blotting

Scaffolds were prepared as described in Section 3.2.5.1. The proteins extracted as described in Section 3.2.5.2. A preparatory comb having a standard well and large preparatory well was used for creating wells in the gel. Into the standard well colored protein marker (Rainbow marker, GE healthcare, Sweden) was loaded. About 300µg of protein extract was loaded into the large preparatory well. Electrophoresis was carried out as described in Section 3.2.5.3. When adequate separation of protein had obtained the electrophoresis run was stopped and the gel was equilibrated in Towbin buffer (3.0g Tris, 14.4g Glycine, 1g SDS dissolved in 600 mL water, 200 mL methanol, make up to 1000 mL with water) for 5 minutes. Proteins were then transferred to nitrocellulose paper (High bound, GE healthcare, Sweden) by semi-dry electro transfer using TE70 electro transfer unit (GE healthcare, Sweden). Briefly, the stacking gel was cut off and the length and breadth of the remaining gel was measured. Six blotting papers and nitrocellulose paper of same length and breadth as that of the gel were cut and immersed in Towbin buffer for few minutes. 3 blotting papers were placed one above the other and nitrocellulose paper was placed above on to the anode plate of the Western blot apparatus. The gel was then placed above the nitrocellulose paper and followed by 3

layers of blotting paper. Using a glass rod the gel, nitrocellulose paper and blotting paper assembly was pressed gently to remove any air bubble that may present between the layers. The cathode plate was placed over the paper-gel assembly and electrotransfer was started at 0.8mA per mm^2 for 1h. The complete transfer of proteins was ensured by confirming the transfer of entire protein bands of the colored protein marker.

After electro-transfer the nitrocellulose paper was washed in distilled water and blocked for 1h in 5% bovine serum albumin (BSA) in PBS. The paper was then cut in to several longitudinal strips of 0.5-1 cm width in the direction of electropheretic separation. The strips were then washed in TBST (Tris Buffer Saline containing 1% Tween 20) and treated overnight at 4°C with 10% immune sera (obtained from immunized rats at 0, 7, 21, 42, 56 and 72 days) in TBST. It was then washed 3 times in TBST and treated with 1 in 2500 dilution of anti-rat IgG-HRP conjugate (KPL laboratories, USA) for 30 minutes. The strips were washed again and the antigen antibody reaction was detected with DAB enhanced liquid substrate system (Sigma, USA) for 1-2 minutes or until the reactive protein bands were visible.

3.2.6.4. Quantification of IgG antibody response

Standard stripwell enzyme-linked immunosorbent assay plates with protein absorption capacity of 300ng/well were purchased from Corning Incorporated, Corning, NY. Proteins extracted as in Section 3.2.5.2 was diluted in PBS to 4000 ng/mL. 50 µl (200ng protein) of the diluted proteins were added into the 96 wells of microtiter plates and incubated overnight at 4°C. The plates were washed 3 times with PBS and blocked with

3% BSA in PBS for 2 h at RT. Plates were washed 3 times with PBST dried by tapping over the tissue paper and used for enzyme-linked immunosorbent assay. 90 µl of 3% BSA in PBS was added into all wells. 10µl of positive control sample obtained from immunized rats serum samples were added into control wells. 10µl of the test sera was added into the corresponding wells identified as test wells. Into the blank added 10µl distilled water. All the wells were mixed thoroughly by pipetting up and down. The plate was sealed with adhesive tape and incubated for 1h at room temperature. The plates were then washed 3 times in PBST and dried by tapping over the tissue paper. 100 µl of 1 in 4000 diluted anti-rat IgG HRP conjugate (KPL laboratories, USA) in 3% BSA was added in to all wells, sealed with adhesive tape and incubated for 45 minutes. The plate was again washed 3 times in PBST and dried by tapping over the tissue paper. Working solution of horseradish-peroxidase (HRP) substrate solution was prepared by mixing equal volume of solution-A and solution-B (Thermo Fisher Scientific Inc., USA) and 100µl working solution was added into all wells. The plate was sealed with adhesive tape and incubated for 15minutes in dark. By this time blue color developed as a result of HRP activity on chromogenic substrate. The reaction was then stopped by adding 1M H_2SO_4 and color turned yellow. The yellow color developed was measured at 450nm wavelength using Chameleon Multi Technology plate reader (Hidex, Finland). The optical density obtained was used as a measure of IgG antibody response against scaffold proteins.

3.2.7. Identification of Immunogenic proteins in CDS

3.2.7.1. 2D-Electrophoresis

Scaffolds were prepared as described in Section 3.2.5.1. The proteins extracted from CDS scaffold as described in Section 3.2.5.2 were used for 2D gel electrophoresis. 250mg of total protein isolated was cleaned and concentrated with 2D clean up kit (BioRad, USA). The cleaned protein was dissolved in 125 µl rehydration buffer and pipetted out into rehydration tray. Immobilized pH gradient (IPG) strips of pH 3 to 10 (GE healthcare, Sweden) was used for isoelectric focusing (IEF). The IPG strips were inserted with gel side facing down into the rehydration tray with protein dissolved in rehydration buffer and incubated for 1h at 20°C. A layer of mineral oil was added on to the top and incubated at 20°C overnight (Rehydration by passive method). The IPG strips were taken out of the rehydration tray and the mineral oil was drained off. The IPG strips were then placed into the focusing tray with 2 hydrated paper wicks attached to either side of the IPG strip to make contact with electrodes. Mineral oil was applied over the IPG strip and focusing was started with following settings. Rapid increase of voltage to 250V was applied for 30 minuntes. Then a linear increase of voltage to 4000V followed by 20000 Vh. After the separation the gel was hold at 500V until the strips were removed from the IEF unit. After IEF the IPG strips were removed, the mineral oil was drained off and stored in -80°C freezer until the second dimension separation was carried out.

For separation of proteins by second dimension 10% SDS PAGE resolving gel was prepared and filled between the glass plates leaving approximately 1cm space above.

Isopropyl alcohol was poured over the resolving gel and the gel was allowed to set. When the gel was set the alcohol was poured off and washed with distilled water. The semisolid agarose overlay stored at 4°C, was placed in a boiling water bath to dissolve completely. The agarose overlay solution was then kept at room temperature and allowed to cool. The IPG strip was taken out of the freezer and thawed for 10 minutes at room temperature. It was then treated with 1mL of equilibration buffer-I for 10 minutes and in equilibration buffer-II for another 10 minutes with continuous shaking. The strips were washed briefly in SDS-PAGE running buffer and placed above the resolving gel. Agarose overlay solution was poured over the gel and allowed to solidify. The electrophoresis and staining of the gel was performed as described in Section 3.2.5.3.

3.2.7.2. Two-dimensional Western blotting

Proteins were separated by 2D-gel electrophoresis as above. After electrophoresis the proteins of the gel was transferred into nitrocellulose paper by Western blotting as described in Section 3.2.6.3.1. The Western blot obtained was then treated with 56day and 72day immune serum obtained from rats immunized with CDS proteins. The immunostaining was also performed as described in Section 3.2.6.3.1.

3.2.7.3. Nanoflow Liquid Chromatography- tandem mass spectrometry

The 2 D gel electrophoretogram obtained was compared manually with 2D Western blot. Based on their position, those proteins spots in 2D Western blot were identified in the 2 D gel electrophoretogram. The protein spots identified were then picked with sterile pipette tip and put in 50% methanol solution taken in a labeled 200µl PCR tubes and

stored at -80°C freezer until it is used for mass spectroscopy. The protein spots were taken for Nanoflow Liquid Chromatography- tandem mass spectrometry as described in Section 3.2.5.4. The subcellular localization, and function of proteins thus identified were then obtained by UniProt database search.

3.2.8. Guinea pig maximization test

Guinea pig maximization test (GPMT) was conducted as recommended per ISO standards (ISO:10993-10., 2010(E)) in accordance with OECD (organization for economic co-operation and development) principles of GLP (good laboratory practice). In this study there were 45 Guinea pigs: 15 animals (10 for test and 5 for control) each for CDS, JDS and UDS extract. The body weight range of the animals was 300-500g. The physiological saline extract of the test materials and control (physiological saline alone) was intra-dermally injected and after seven days it was topically applied. Challenge test was carried out after fourteen days on all the animals. The appearance of the challenge skin sites of test and control animals were observed at 24h, 48h and 72h after removal of dressings and patches. The skin reactions for erythema and edema were scored and recorded the numerical grading as per ISO 10993-10: 2010(E).

3.2.9. Evaluation of innate immune response to scaffolds *in vitro*

3.2.9.1. Complement activation

Blood from human volunteer was collected into the anticoagulant citrate-dextrose solution. The test materials (2x2 cm) were placed in polystyrene culture plates and agitated with PBS before they were exposed to blood. To each plate 2mL blood was

added and 1mL sample was collected immediately for analysis. Remaining 1mL of blood was exposed to materials for 30 minutes under agitation at 70±5 rpm using an environ shaker at 35 ± 2^{0}C. Empty polystyrene dishes were exposed with blood as reference. Platelet poor plasma was prepared by centrifuging blood at 4000 rpm for 15 minutes. Complement activation was analyzed with commercially available enzyme-linked immunosorbent assay kit (Quidel, USA) as per manufacturer's instructions. Absorbance was read in Chameleon multi-technology plate reader (Hidex, Finland) and data was processed using Mikrowin 2000 software.

3.2.9.2. Macrophage response to extracellular matrix scaffolds in vitro

Phorbol 12-myristate 13-acetate (PMA) can differentiate THP-1 cells in to adherent macrophage phenotype. Here the response of PMA differentiated THP-1 macrophages towards ECM scaffolds were studied *in vitro*. The ability of macrophages to produce reactive oxygen species and reactive nitrogen species were studied.

3.2.9.2.1. Culture and maintenance of THP 1 cells

THP-1 cells were purchased from national centre for cell science, Pune, India. Cells were maintained in RPMI 1640 media with 10 mM HEPES buffer, 1 mM sodium pyruvate, 4.5 g/L glucose, 0.05 mM 2-mercaptoethanol, antibiotics, and 10% fetal bovine serum.

3.2.9.2.2. Estimation of macrophage production of reactive oxygen species

Macrophages produce reactive oxygen species (ROS) like H_2O_2, O_2^{-} and OH^{-} in response to lipopolysaccharides (LPS), certain cytokines or as part of innate immune

defense. The reactive oxygen species produced by THP-1 macrophage in response to LPS in the presence of ECM scaffolds were studied by method described by Smith *et al* (2009). Briefly, THP-1 cells were first differentiated to macrophages by culturing with 50nM PMA for 72 h. The cells ($2x10^6$ cells/mL) were then seeded on to 96 well plates with 3mm discs of CDS, JDS, UDS or CSIS scaffolds and cultured overnight in media containing 200μg/mL LPS. To this an equal volume of 1 in 1000 diluted luminol solution (0.556 g NaOH, 0.618 g boric acid, and 0.014 g luminol in 10 mL ultra pure water) was added. The plates were covered quickly with an adhesive film and luminescence was measured in Chameleon Multi Technology plate reader (Hidex, Finland). Results were expressed as luminescence counts per second.

3.2.9.2.3. Macrophage production of nitric oxide

Nitric oxide produced was measured indirectly by quantifying the total nitrite concentration subsequent to reduction of nitrate to nitrite. The nitric oxide (NO^{-}) produced by THP-1 macrophages in response to LPS in the presence of ECM scaffolds were estimated. Briefly, THP-1 cells were first differentiated to macrophages by culturing with 50nM PMA for 72 h. The cells ($2x10^6$ cells/mL) were then seeded on to 96 well plates with 3mm discs of CDS, JDS, UDS or CSIS scaffolds and cultured overnight in media containing 200μg/mL LPS. The total nitrite concentration in culture supernatants were estimated using Griess reagent (Sigma). Known concentration of sodium nitrite was used as standard and a standard curve was plotted. Optical density

was measured at 540nm sing Chameleon Multi Technology plate reader (Hidex, Finland).

3.2.10. Statistical analysis

The data were analyzed by one-way analysis of variance with Tukey-Kramer multiple comparisons test. Those differences with p value less than 0.05 was considered significant. All statistical analysis was performed using GraphPad InStat software version 3.10 (GraphPad Software, Inc. CA, USA).

3.3. RESULTS

3.3.1. Preparation of scaffolds

Fig.1 shows the scaffolds isolated from cholecyst, jejunum, and urinary bladder from their source organs by non-detergent/enzymatic method.

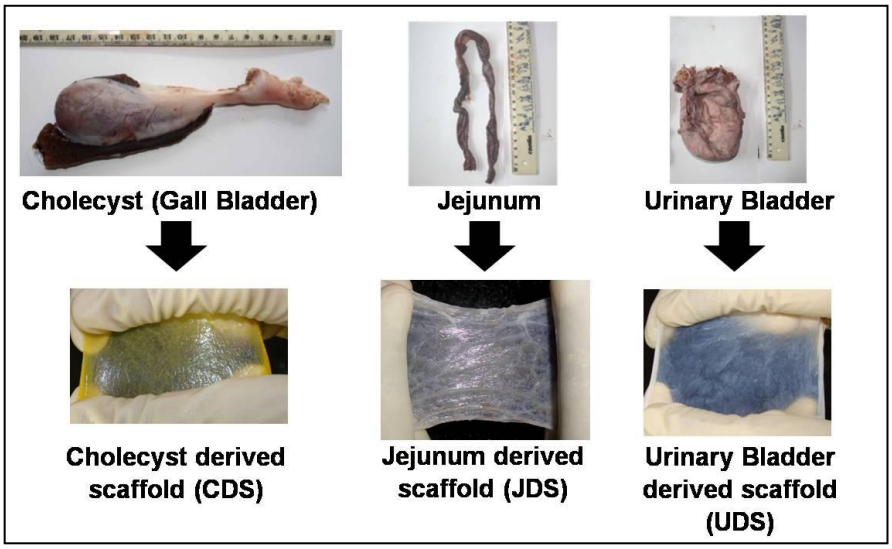

Figure 1: ECM scaffolds isolated from porcine cholecyst, jejunum, and urinary bladder.

3.3.2. Test for pyrogenicity

All the scaffolds had endotoxin level less than 0.5 EU/mL. Hence, as per USP 23/NF21<85>, the scaffolds studied were considered as non-pyrogenic.

3.3.3. Cellularity of scaffolds

Microscopically visible intact nuclei were present in all scaffolds but CDS had significantly less nuclei (Fig. 2). Quantitatively, there was less number of nuclei in CDS than other scaffolds (Fig. 3). The CSIS had less number of nuclei than JDS and UDS. Among the scaffolds studied UDS had highest quantity of cellular residue.

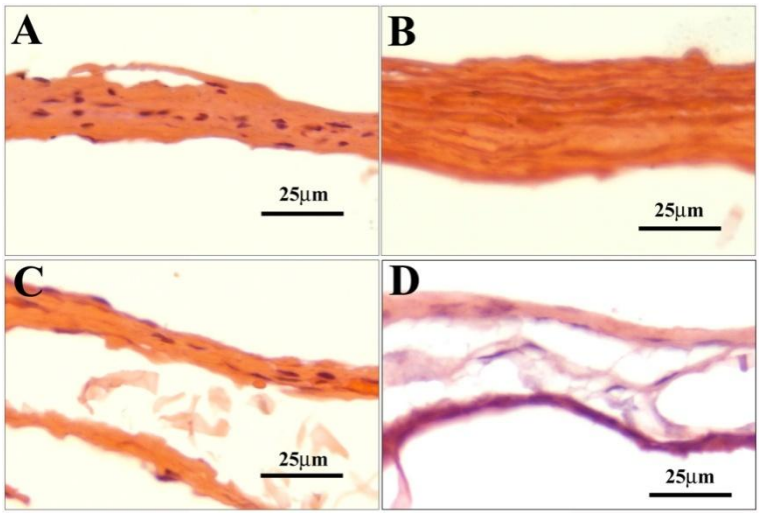

Figure 2: Histomorphology of the scaffolds, Haematoxylin and eosin staining CSIS (A), CDS (B), JDS (C) and UDS (D). Purple dots and pink background represent nuclei and ECM respectively. Scale bar indicates 25µm. See figure 3 for quantitative data.

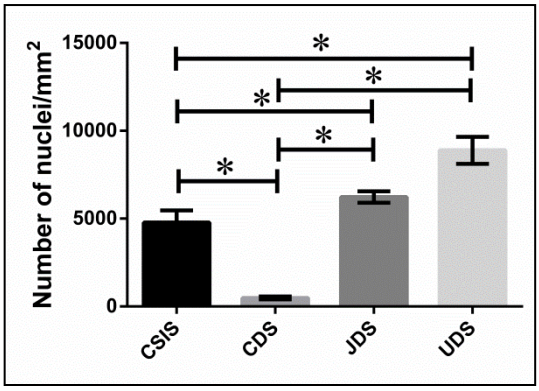

Figure 3: Bar diagram showing the number of nuclei per mm^2 of scaffolds quantified by histomorphometry using Image-Pro 3DS6.1 software (mean±1SD, n=6). * represents significant difference.

3.3.4. Identification of extractable proteins of the scaffolds

3.3.4.1. Protein isolation from scaffolds

The yield of protein extraction before concentration with centrifugal filtration was very less with concentration undetectable with Micro-Lowry method for protein estimation. About 4 mL of the tris extract was concentrated in to 400µl final concentrate, which yielded protein preparation of 3mg/mL, which was used for further experiments like electrophoresis.

3.3.4.2. Sodium dodecyl sulfate polyacrylamide gel electrophoresis (SDS-PAGE)

Fig. 4 shows the electrophoretogram obtained by 10% SDS PAGE electrophoresis of CDE, JDE and UDE protein extracts.

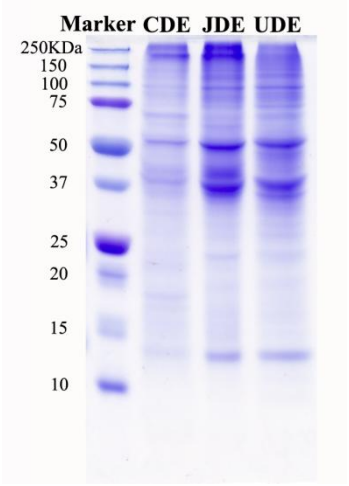

Figure 4: Electrophoretic separation of proteins (30µg) extracted from CDE, JDE and UDE.

3.3.4.3. Protein identification by Mass Spectroscopy

The number of proteins identified from CDE, JDE and UDE are given in Table 1. CDE had lowest percentage of cellular proteins (79.2%) and highest percentage of ECM

proteins (8.4%) compared to other scaffolds. 12.3% proteins of CDE protein extract was secreted proteins. The UDE had highest number of extractable proteins.

Table 1: The number of proteins identified in the CDE, JDE and UDE protein extracts

Extracellular matrices	Number of Proteins Identified	Cellular (%)	Secreted (%)	ECM (%)
CDE	154	79.2	12.3	8.4
JDE	186	90.3	6.4	3.2
UDE	253	89.2	6.2	4.4

Fig 5 represents the Venn diagram showing the sharing of protein between the CDE, JDE and UDE protein extracts. Forty-seven proteins were unique to CDE, 72 proteins were unique to JDE and 125 proteins were unique to UDE. There were 49 proteins common to CDE, JDE and UDE. Table 2 shows some of the important proteins common in CDE, JDE and UDE.

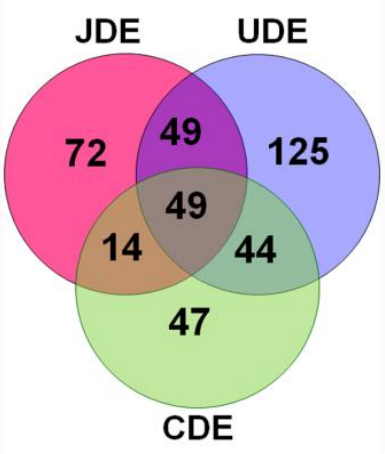

Figure 5: Venn diagram showing the sharing of proteins identified by mass spectroscopy between the CDE, JDE and UDE extracellular matrices.

Table 2: Important proteins common to CDE, JDE and UDE.

Uniprot Entry	Protein names	Function	Subcellular location
P00336	L lactate dehydrogenase B chain	Enzymatic	Cytoplasm
P02540	Desmin	Cross-linking	Cytoplasm
P08670	Vimentin	Structural	Cytoplasm
P12814	Alpha-actinin-1	Adhesion	Cytoplasm
P60709	Actin, cytoplasmic 1 (Beta-actin)	Motility	Cytoplasm
P62736	Actin, aortic smooth muscle	Motility	Cytoplasm
Q0R678	DJ-1 protein	Binding	Cytoplasm
Q6RVA9	Caveolin-1	Structural	Golgi apparatus
P00829	ATP synthase subunit beta	Transport	Mitochondrion
P62802	Histone H4	Structural	Nucleus
P02749	Beta-2-glycoprotein 1	Binding	Secreted
P19620	Annexin A2	Binding	Secreted, ECM
P20774	Mimecan (Osteoglycin)	Growth factor	Secreted, ECM
P51884	Lumican	Structural	Secreted, ECM
P01008	Antithrombin-III	Regulatory	Secreted, ECM

Proteins identified were also classified in to groups based on their function (Table 3). The enzymatic proteins were high in all extracellular matrices studied. However the percentage of enzymatic proteins was relatively less in CDE (21.3%) as compared to JDE (27.4%) and UDE (38%). Other proteins present were binding, structural, regulatory, transport, adhesion, etc were also present. All scaffolds had several proteins that had important role in wound healing reaction. A small fraction of proteins with immunological role were there in all matrices as described below.

Table 3: Classification of extractable proteins based on their function

Protein functions	Percentage of proteins in CDE	Percentage of proteins in SDE	Percentage of proteins in UDE
Adhesion	5.8	1.6	5.5
Anti-apoptosis	0.6	0.5	0.3
Antimicrobial	--	--	0.7
Apoptotic	--	--	0.3
B cell development	--	0.5	0.3
Binding	16.2	14.5	11.4
Blood coagulation	--	--	0.7
Chaperone	5.8	1.1	4.4
Contraction.	0.6	--	--
Cross-linking	3.2	1.6	2.5
Enzymatic	21.4	27.4	38.0
Growth factor	0.6	0.5	0.3
Immunity	1.9	3.8	0.7
Inhibitor	4.5	0.5	1.8
Mitosis	--	0.5	--
Motility	4.5	1.6	0.7
Regulatory	9.7	18.3	11.4
Stimulatory	--	0.5	--
Stress response	2.5	1.6	2.9
Structural	11.0	11.8	8.1
Transport	9.7	10.2	7.3
Wound healing	1.3	--	--
Other	--	3.2	1.8

Complement components factor B, C3 and prolargin were identified in CDE protein extract. Histocompatibility antigens like MHC class I antigen, H-2 class II histocompatibility antigen E-S beta chain, SLA class II histocompatibility antigen (DQ

haplotype C beta chain) and MHC class II antigen were present in JDE protein extract. Proinflammatory proteins like S100 A6 as well as antimicrobial peptides like Protegrin-1 and Protegrin-3 were identified in UDE protein extract. Table 4-6 shows the important proteins identified in CDE, JDE and UDE.

Table 4: Important proteins identified in CDE protein extract

Uniprot entry	**Protein name**	**Function**	**Subcellular location**
P16110	Galectin-3 (Gal-3)	Wound healing	Cytoplasm
P29700	Alpha-2-HS-glycoprotein (Fetuin-A)	Wound healing	Secreted
P51884	Lumican	Wound healing	ECM
Q9XSD9	Decorin	Wound healing	ECM
P20774	Mimecan	Wound healing	ECM
P02751	Fibronectin (FN)	Wound healing	ECM
P14543	Nidogen-1 (NID-1)	Wound healing	ECM
Q14112	Nidogen-2 (NID-2)	Wound healing	ECM
P02749	Beta-2-glycoprotein 1	Regulation of angiogenesis	Secreted
Q05707	Collagen alpha-1(XIV) chain (Undulin)	ECM assembly	ECM
P12110	Collagen alpha-2(VI) chain	ECM organization	ECM
Q15063	Periostin (PN)	Cell adhesion, matrix mineralization	Golgi apparatus
Q03710	Complement factor B	Immunity	Secreted
P01025	Complement C3	Immunity	Secreted
P51888	Prolargin	Inhibitor of complement activation	ECM
O11780	Transforming growth factor-beta-induced protein ig-h3	Platelet activation	ECM
P01008	Antithrombin-III	Anticoagulant, antiinflammatory, antiangiogenic	ECM

Table 5: The important proteins identified in JDE protein extract

Uniprot Entry	Protein names	Function	Subcellular location
Q4AC39	MHC class I antigen	Immunity	Membrane
P04231	H-2 class II histocompatibility antigen, E-S beta chain	Immunity	Membrane
P15982	SLA class II histocompatibility antigen, DQ haplotype C beta chain	Immunity	Membrane
Q8HX73	MHC class II antigen	Immunity	Membrane
O15533	Tapasin	Immunity	Endoplasmic reticulum
Q9BXN1	Asporin	Regulatory	ECM
P48819	Vitronectin	Adhesion	Secreted

Table 6: The important proteins identified in UDS protein extract

Uniprot Entry	Protein names	Function	Subcellular location
P29034	Protein S100-A2	Anti-inflammatory	Cytoplasm
P60903	Protein S100-A10	Anti-inflammatory	Membrane
Q2EN75	Protein S100 A6	Pro-inflammatory	Cytoplasm
P32194	Protegrin-1 (PG-1)	Antimicrobial	Secreted
P32196	Protegrin-3 (PG-3)	Antimicrobial	Secreted
P23142	Fibulin-1	Adhesion	ECM
Q9UBX5	Fibulin-5	Adhesion	ECM

3.3.5. Assessment of IgG antibody response

3.3.5.1. Antiserum production

Anti cholecyst ECM scaffold serum was prepared by subcutaneous immunization of Sprague-Dawley rats. The specificity of antiserum was tested by Western-blotting. Fig. 6 shows Western-blot following SDS PAGE separation of CDE protein extract developed with immune serum showed the formation of antibodies reactive to CDE

proteins. Thus immunization was effective with induction of antibody response by scaffold proteins when immunized in rats. As the number of days after immunization passes the number of protein bands increased in the Western blot. But, at 56 days the antibody response was higher than 72 days, as evidenced by the intensity of bands. This shows the decrease in titer of IgG after 56 days of immunization.

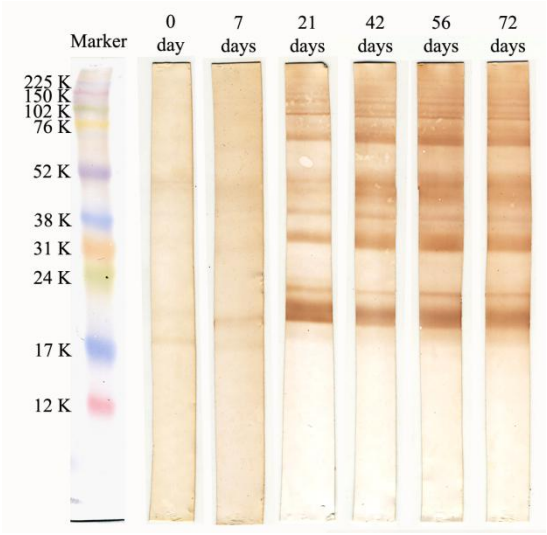

Figure 6: Western-blot following SDS PAGE separation of CDE protein extract developed with immune serum.

3.3.5.2. Quantification of Antibody response

Results of enzyme-linked immunosorbent assay suggested an increase in IgG antibody response with time of implantation of all scaffolds (Fig. 7). All scaffolds elicited IgG antibody response specific to scaffold proteins. The antibody response was baseline up to one week and there was gradual increase thereafter. The response against CDS implant reached highest by 28 days and remained the same up to 90 days of implantation. IgG response against JDS and UDS scaffold reached peak level at 90 days.

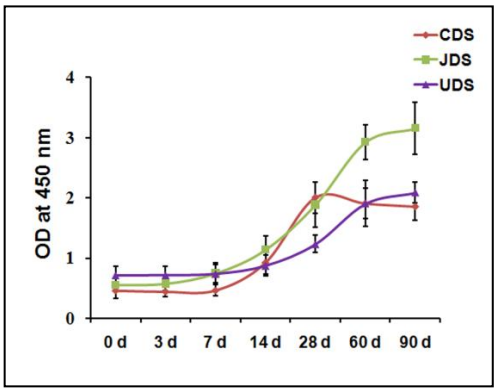

Figure 7: IgG antibody response against scaffolds implanted in subcutaneous tissue of rats. Values represents mean ± SD, n=4.

3.3.6. Identification of Immunogenic proteins in CDE

3.3.6.1. 2D Electrophoresis

The appearance of CDE proteins separated by 2D electrophoresis is shown in Fig. 8.

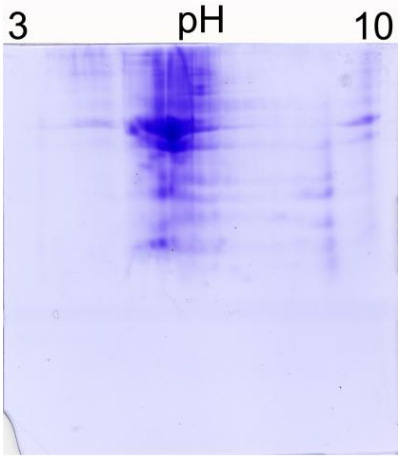

Figure 8: 2D electrophoretogram of proteins extracted from CDE.

3.3.6.2. 2D-Western blot

Figure 9 shows the Western blot developed with immune serum at 56 days and 72 days of immunization. The intensity and number of reactive protein spots were higher with 56

days immune serum than reactive spots obtained with 72 days immune serum, an observation similar to SDS-PAGE followed by Western blotting (Fig. 6). Those selected protein spots that reacted with immune serum were excised from 2D electrophoresis gel and the proteins were identified by mass spectroscopy.

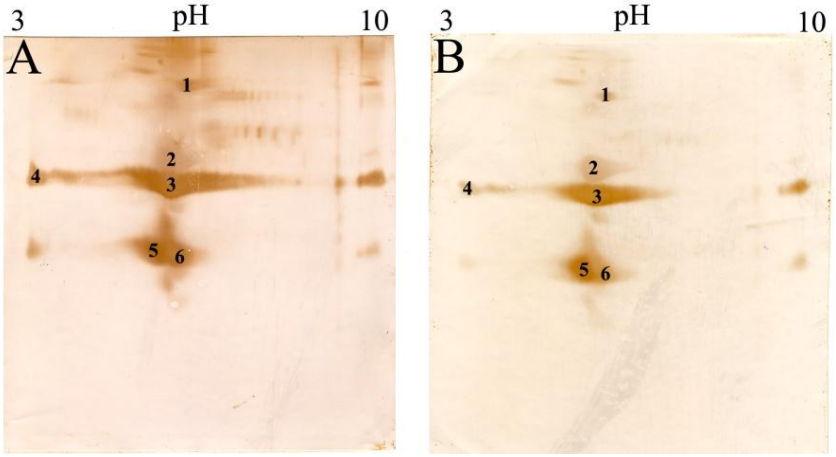

Figure 9: The 2D Western-blot obtained for CDS protein extract developed with 56 day (A) and 72 day (B) immune serum

3.3.6.3. Mass spectroscopy and data base search

A total of 18 proteins that react with immune serum developed by subcutaneous immunization of rats were identified by mass spectroscopy (Table-7). Most of them were cellular in origin that had no reported role in tissue remodeling response following implantation of scaffold *in vivo*. Alpha-2-macroglobulin was the only one secreted protein identified as immunogenic. Annexin-A2, which is a member of the group of non-Gal xenoantigens was also identified as immunogenic protein of CDE.

Table 7: Immunogenic proteins identified by 2D Western-blot followed by mass spectroscopy

Spot number	Protein names	Function	Subcellular location
1	Filamin-A	Cross-linking	Cytoplasm
	Membrane primary amine oxidase	Adhesion	Membrane
	Alpha-actinin-1	Adhesion	Cytoplasm
	Filamin-B	Cross-linking	Cytoplasm
	Alpha-2-macroglobulin	Inhibitor	Secreted
	Vinculin (Metavinculin)	Adhesion	Cytoplasm
2	Actin, aortic smooth muscle	Motility	Cytoplasm
	Actin, cytoplasmic 1 (Beta-actin)	Motility	Cytoplasm
	Desmin	Cross-linking	Cytoplasm
	Vimentin	Structural	Cytoplasm
	ATP synthase subunit beta	Transport	Mitochondria
	DNA repair protein RAD50	Binding	Nucleus
3	Annexin-A2	Binding	Membrane
	L lactate dehydrogenase B chain	Enzymatic	Cytoplasm
	Transducin beta chain 4	Binding	Membrane
4	Actin, gamma-enteric smooth muscle	Motility	Cytoplasm
5	Caveolin-1	Structural	Golgi
6	DJ-1 protein	Binding	Cytoplasm

3.3.7. Test for delayed type hypersensitivity

Guinea pig maximization test was done to study the potential of ECM scaffolds to elicit delayed type hypersensitivity. The result of the study indicated that the physiological saline extract of the CDS, JDS, UDS and physiological saline control treated animals did not show any adverse skin reaction during the induction or challenge period. It was confirmed that the physiological saline extract of the CDS, JDS and UDS were non irritant at the laboratory conditions simulated. Hence, the physiological saline extract of extracellular matrices CDS, JDS and UDS meet the requirements of the test as per ISO 10993-10: 2010 (E).

3.3.8. Evaluation of innate immune response *in vitro*

3.3.8.1. *In vitro* Complement activation

When compared to tissue culture poly styrene surface, all the scaffolds had complement activation potential, as detected by C3a estimation (Fig. 10). The reference material (CSIS) as well as the in-house prepared JDS showed relatively higher complement activation ability than CDS. The UDS induced variable complement activation potential.

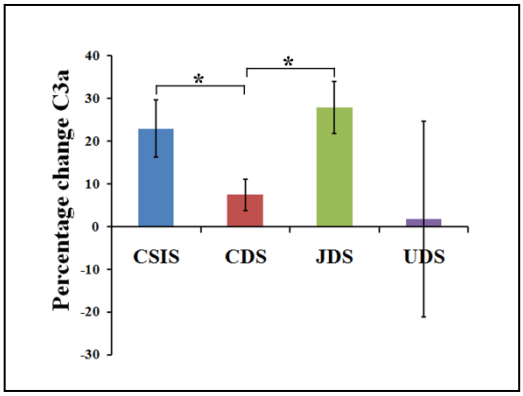

Figure 10: Graph showing the percentage increase in human C3a *in vitro* by enzyme linked immune-sorbent assay (mean±1SD, n=3; * designate significant differences).

3.3.8.2. Estimation of reactive oxygen species

The ROS production by THP-1 macrophage in response to LPS in the presence of scaffolds was tested. Compared to CSIS and JDS scaffolds the CDS and UDS induced significantly less ROS production (Fig. 11). The decreased ROS production potential of CDS probably indicates its relatively less ability to stimulate innate immunity.

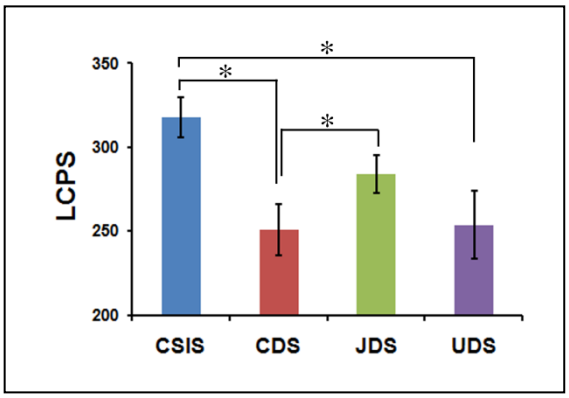

Figure 11: The reactive oxygen species production of THP-1 macrophage in response to LPS in the presence of scaffolds (mean±1SD, n=3; * designate significant differences)

3.3.8.3. Macrophage production of nitric oxide

The RNS production by THP-1 macrophage in response to LPS in the presence of scaffolds was tested. Compared to other scaffolds, CSIS the reference material had the least potential to induce RNS production by THP-1 macrophages. Among the in-house prepared scaffolds CDS induced relatively less RNS production by macrophages (Fig. 12). The decreased RNS production potential of CDS probably indicates its relatively less ability to stimulate innate immunity.

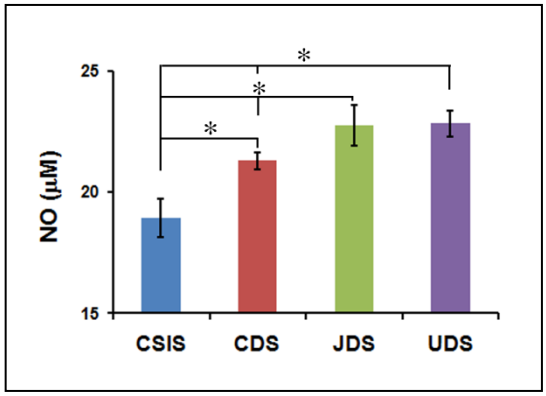

Figure 12: The reactive nitrogen species production of THP-1 macrophage in response to LPS in the presence of scaffolds (mean±1SD, n=3; * designate significant differences)

3.4. DISCUSSION

The aim of this part of the study was to characterize the immunogenic potential of CDS in comparison to JDS, UDS and a reference material. The reference material used was CSIS. It is important to note that the CSIS was a commercial product and the procedure for its preparation was not known but the CDS, JDS or UDS were prepared by an in house non-detergent/enzymatic method (Fig.1) (Anilkumar *et al.*, 2014). The endotoxin load and the number of residual cell nuclei of scaffolds, and extractable proteome of ECM isolates were characterized. The potential of extracellular matrices to raise antibody response, and delayed type hypersensitivity reaction were also studied. Further, the ability of scaffolds to activate innate immunity was characterized by in vitro methods. The results obtained are discussed below.

The presence of endotoxin was evaluated for various reasons. First, endotoxin contamination of biomaterials can stimulate leukocytes to produce inflammatory cytokines and may lead to inadvertent inflammatory reaction (Gorbet and Sefton, 2005). Second, endotoxin contamination of biomaterials alters macrophage function *in vivo* causing delayed giant cell formation and biomaterial degradation (van Putten *et al.*, 2011). Third, according to US FDA, the maximum permissible limit of endotoxin in medical devices is 0.5 EU/mL (US FDA guidelines 1987). Studies on endotoxin contaminated porcine dermal matrix has shown that the current endotoxin limit is well below the levels that induce an adverse acute pro-inflammatory response and associated long-term deleterious effects upon tissue remodeling outcomes (Daly *et al.*, 2012). Considering these clues, the endotoxin content of CDS, JDS, UDS and CSIS were

assessed. In this study the endotoxin content in the scaffolds was estimated by LAL assay. The results suggested that the endotoxin level in all the scaffolds studied was less than 0.5 EU/mL, which is within the safe limit for medical devices (US FDA guidelines 1987). So endotoxin content in the scaffolds prepared by nondetergent/enzymatic method was within safe limit and no adverse reactions were expected.

Immune response to xenogeneic ECM derived biomaterials largely depends on the presence of residual cellular components rather than the ECM proteins that are retained in the graft even after rigorous procedures of chemical decellularization (Gilbert *et al.*, 2006, Badylak and Gilbert, 2008). Therefore, removal of cellular remnants is a major objective of successful decellularization technique (Crapo *et al.*, 2011, Luo *et al.*, 2011, Keane *et al.*, 2012). In the present instance the extent of cell remnants in the scaffolds were evaluated on randomly selected histological sections. The cellular debris, as identified by visible nuclei in histology sections (Fig. 2) were detectable in all samples studied. The number of nuclei in CDS was remarkably low compared to that in the reference material as well as the scaffolds from other sources (Fig. 2&3). Thus the result shows a broad indication that cholecyst derived scaffold may be less immunogenic when compared to scaffold obtained from small intestine and urinary bladder.

The extractable proteins in the extracellular matrices isolates of cholecyst (CDE), jejunum (JDE) and urinary bladder (UDE) were identified by Mass Spectroscopy and data base search as commonly done. About 79% proteins identified in CDE proteins extract were of cellular in origin. In JDE and UDE 90% of proteins identified were

cellular proteins (Table 1). This observation underlines the fact that cellular component are present in the CDS, JDS and UDS. This is not surprising as the preparation of extracellular matrices did not include any rigorous chemical/enzymatic decellularization protocols. In a similar study carried out by Marçal et al (2012) on the proteome of urinary bladder derived biomaterial, which was decellularized through well documented protocol also identified 75 % proteins of cellular origin (Marçal *et al.,* 2012). So it may be assumed that the so called decellularized materials, actually contains cellular components or in other word the decellularization protocols are not making absolutely acellular biomaterials.

When the identified proteins were classified based on their function the largest fraction of proteins in all scaffolds was of enzymatic in function (Table 3). The CDE had lowest percentage of proteins with possible enzymatic activity. All extracellular matrices contained small fraction of proteins that take part in wound healing and immune processes.

Among the in-house prepared extracellular matrices CDE had higher percentage of ECM proteins and lower percentage of cellular proteins (Table 1). About 154 proteins were identified in CDE protein extract with several proteins associated with wound healing response (Table 1 & 4). Proteins like galectin-3 (Cao *et al.*, 2002), alpha-2-HS-glycoprotein (fetuin-A) (Wang *et al.,* 2010), lumican (Saika *et al.,* 2000), decorin (Järveläinen *et al.*, 2006), fibronectin (To and Midwood, 2011), nidogen-1 and Nidogen-2 (Baranowsky *et al.*, 2010, Nischt *et al.,* 2006) are reported to have crucial role in

wound healing. Transforming growth factor-induced protein (TGFBIp)/βig-h3 is an ECM protein that interacts with other ECM molecules including collagen, fibronectin, laminin, and glycosaminoglycan. It has key functions in adhesion, migration, proliferation, and differentiation of various cell types. TGFBIp plays important roles in platelet activation and thrombus formation, which are essential components of wound healing cascade (Kim *et al.*, 2009). Beta-2-glycoprotein 1 (β2GP1 or apolipoprotein H) is a kringle domain-containing plasma glycoprotein and regulates angiogenesis. It binds to endothelial cells through annexin-A2 and functions as an endothelial cell survival factor. The cleavage products of Beta-2-glycoprotein 1 are antiangiogenic like angiostatin protein derived from plasminogen (Sakai *et al.*, 2007). Antithrombin-III is a serine protease inhibitor (serpin) that regulates blood coagulation. It binds to sulfated glycosaminoglycans, heparin or heparan sulfate, to inhibit its target proteases. It has also anti inflammatory and anti-angiogenic activity (Zhang *et al.*, 2005). The proteins in CDE discussed above shows the potential of CDE for fabrication of tissue engineering scaffold.

A small fraction of proteins associated with immune response were present in all extracellular matrices studied. The importance of these proteins in each of the scaffold is discussed below.

CDE contained some proteins of the complement activation pathway like complement proteins C3 and factor B/properdin (Table 4). It has been shown that topical application of complement C3 in a collagen vehicle can increase inflammatory cell recruitment and

thereby enhance wound healing by early fibroblast migration, increased collagen deposition and organization in rats at early time points of 3 days (Sinno *et al.*, 2013). But this may also raise concern about the complement activation potential of CDS. So an *in vitro* complement activation study was carried out to comparatively assess the complement activation potential of CDS. The CDS was the least complement activating biomaterial compared to the biological scaffolds derived from small intestine (Fig. 10). This may be because of the fact that CDS is composed of some other proteins that modify complement activation. In fact, one such protein namely prolargin was identified in the CDE protein extract. Prolargin also known as proline-arginine-rich end leucine-rich repeat protein is a member of small leucin rich proteoglycans secreted in to the ECM. Prolargin anchor basement membrane to the underlying connective tissue by binding collagen type I and type II, heparin and heparan sulphate (Bengtsson *et al.*, 2002). It inhibits all pathways of complement activation by several mechanisms: it dissociates preformed C3-convertases, binds C3 and membrane attack complex proteins, properdin, C3b, C5, C7, C8, and C9. It inhibits membrane attack complex formation at the level of C9 and inhibits C9 Polymerization. It can also locally regulate complement activation by capturing the complement inhibitor C4BP. It also inhibits alternative pathway C3 convertase (Happonen *et al.*, 2012). CDS contains another protein clusterin also known as apolipoprotein J or SP-40 which is a potent inhibitor of complement system. It inhibits formation of membrane attack complex (McDonald and Nelsestuen, 1997).

JDE contained several proteins associated with immune response. This includes histocompatibility antigens like MHC class I antigen, H-2 class II histocompatibility antigen E-S beta chain, SLA (swine leukocyte antigens) class II histocompatibility antigen (DQ haplotype C beta chain) and MHC class II antigen. The porcine histocompatibility antigens also known as SLA are important targets of immune response to xenografts (Murray *et al.*, 1994). SLA antigen present in xenografts are recognized by host T-cells by indirect antigen presentation and contribute to chronic xenograft rejection (Olack *et al.*, 2000). Preformed anti-human leukocyte antigen (HLA) class I antibodies in sensitized patients may cross-react with porcine SLA class I antigen leading to hyperacute xenograft rejection (Naziruddin *et al.*, 1998). So the presence of SLA in JDS may lead to inadvertent graft reactions up on implantation in animal models.

It is remarkable to note that the UDE protein extract did not contain any histocompatibility antigens. However, UDE had complement component C3 and prolargin which is a potent inhibitor of complement system. Few members of S100 family of proteins like S100A2 a tumor suppressor (Feng *et al.*, 2001), S100A-6 a pro-inflammatory protein (Joo *et al.*, 2003) and S100A10 anti-inflammatory protein (Donato, 2003) were present in UDE. Protegrin-1 and Protegrin-3 which are potent antimicrobial peptides (Kosciuczuk *et al.*, 2012) were also detected in UDE protein extract. So, the results suggest that UDS scaffold has a complex protein composition with the presence of pro-inflammatory, anti-inflammatory and antimicrobial proteins.

The discussion above clearly indicated that the scaffolds studied did contain prominent immunogenic proteins. As traditionally performed, the antibody responses elicited by the scaffolds when implanted subcutaneously in rats were quantified by ELSIA. All scaffolds induced an antibody response in rats. The rats were immunized with scaffold proteins for generating anti-scaffold serum which was used as positive control for enzyme-linked immunosorbent assay. Considering the focus of this study on CDS, the efficiency of immunization with CDE proteins was tested by Western blot which also showed that the scaffold contains proteins that can induce an antibody response in rats (Fig. 6). So, the identification of protein antigens in the cholecyst derived scaffold was desired.

In order to identify the immunogenic proteins present in the CDE an immunoproteomic approach reported elsewhere was used (Griffiths *et al.*, 2008). The CDE proteins were first separated by 2D gel electrophoresis (Fig 8) and the corresponding Western blot was probed with hyper-immune serum (Fig 9). The proteins in the reactive spots were the identified by mass spectroscopy. Eighteen CDE proteins were identified as potentially immunogenic (Table 7). Most of these were cellular in origin. This may be due to the fact that ECM proteins are conserved throughout evolution, whereas cellular proteins are not so and hence can be immunogenic to the host (Boot-Handford and Tuckwell, 2003, Hynes, 2012, Hynes and Naba, 2012). All the immunogenic proteins had no known role in tissue remodeling response following implantation of scaffold *in vivo*. Annexin-A2 and alpha-2-macroglobulin were the secreted proteins which was immunogenic. Alpha-2-macroglobulin a highly conserved protein throughout evolution is an abundant plasma

protein that inhibits proteases (Armstrong and Quigley, 1999). There have been no prior reports on the immunogenicity to alpha-2-macroglobulin in the contest of xeno-transplantation. On the other hand annexin-A2 a proven xenoantigen belonging to the group non-Gal epitopes and reported to be associated with the delayed xenograft rejection (Byrne *et al.*, 2008, Byrne *et al.*, 2011). The proteome profiling of porcine urinary bladder submucosa also had shown the presence of annexin-A2 as a component of biological scaffold material (Marçal *et al.*, 2012).

The protein annexin-A2 is a key regulator of fibrinolysis, coagulation, inflammation and apoptosis (Wang and Lin, 2014). Annexins are composed of a family of genes which encode proteins with calcium regulated phospholipid and membrane binding functions. The annexins are mainly intracellular proteins that anchor cytoskeletal elements to the membrane and support membrane to membrane interactions. They are implicated in exocytosis, endocytosis and stabilization of organelle and plasma membrane domains (Bharadwaj *et al.*, 2013). Annexin-A2 is an endothelial surface receptor for plasminogen and tissue plasminogen activator (tPA). Consistent with this reports, annexin-A2 null mice show reduced tPA dependent plasmin generation and exhibit incomplete clearance of arterial thrombi (Cockrell *et al.*, 2008). So extracellular annexin-A2 can promote fibrinolysis and may therefore inhibit graft rejection by limiting the extent of thrombosis. Anti-annexin-A2 antibodies formed upon xenotransplantation may block fibrinolytic function of annexin-A2 and promote thrombosis within the graft leading to graft rejection (McGregor and Byrne, 2013). Additionally, antibody responses to annexin-A2 have been detected in patients with antiphospholipid syndrome and shown

to cause endothelial cell activation and induction of tissue factor which would also contribute to a prothrombotic vasculature (Cesarman-Maus *et al.*, 2006).

The observation that annexin-A2 is a potential xenoantigen present in the cholecyst derived scaffold warrants more studies on the implications of non-Gal epitopes in the immune response to biological scaffold materials. In the present instance, other members of non-Gal antigens, namely tetraspanin 29, membrane cofactor protein, protectin, EC protein C receptor, β 1,4 N-acetylgalactosaminyl transferase 2 were not detected as immunogenic. Only a small repertoire of immunogenic proteins present in the CDE was identified in this study. It may contain several other immunogenic proteins which may require further studies using different protein extraction buffers and protein identification tools. However the study points to the importance of a detailed study to elucidate role of non-Gal epitopes in the immunological consequences of biological scaffold applications *in vivo*.

The potential of physiological saline extracts of in-house prepared ECM scaffolds to induce delayed type hyper sensitivity was studied by guinea pig maximization test as per ISO standards (ISO:10993-6, 2010 (E)). Results indicated that the physiological saline extracts of all scaffolds did not have potential to elicit delayed type hyper sensitivity reaction in guinea pigs.

Some *in vitro* tests were used to evaluate the potential of scaffolds to mount an innate immune response. The innate responses studied *in vitro* were the ability to activate complement pathway, the ability to induce macrophage production of reactive oxygen

species and nitrogen species. The result of *in vitro* complement activation tests shows that all scaffold used in the study could activate complement pathway upon exposure to human whole blood. Complement activation has been prophesized as a cause for initiating inflammatory cell infiltration and acute inflammatory reaction to biomaterials (Nilsson *et al.*, 2007). The CDS induced significantly less complement activation compared to small intestine derived biomaterials, *viz*., CSIS and JDS (Fig 10). This result is in corroboration with the decreased acute inflammatory response and mast cell reaction caused by CDS-grafting (Table 9 and 15). The differences in complement activation potential of scaffolds may be due to their inherent differences in protein composition (Table 4, 5 & 6).

Macrophage production of ROS and RNS are part of innate immune defense mechanism (Bogdan *et al.*, 2000). When studied *in vitro* the CDS scaffold induced less ROS compared to small intestine derived biomaterials, *viz*., CSIS and JDS. RNS production induced by CDS was significantly less than that induced by JDS and UDS. So among the in-house prepared scaffolds CDS induced lowest potential to activate innate immunity.

CHAPTER-4

4. LOCAL TISSUE RESPONSE *IN VIVO* AND BIOCOMPATIBILITY

4.1. INTRODUCTION

This part of the thesis describes the nature of local tissue reaction induced by CDS, JDS and UDS when implanted in rat subcutaneous tissue. The extent of biocompatibility of these scaffolds was studied as per ISO10993, Part-6 standards in comparison with CSIS which is a commercially available scaffold.

4.2. MATERIALS AND METHODS

4.2.1. Subcutaneous implantation of scaffolds in rats

With the approval of Institutional Animal Ethics Committee at the host institution, the materials were implanted subcutaneously into Sprague-Dawley rats as suggested in ISO10993, Part-6 for evaluating local tissue response (ISO:10993-6, 2007). Out bred young adult Sprague-Dawley rats of either sex weighing not less than 200g, were used for the study. Experimental animals were housed in individually ventilated cages at 22°C with 12 h day/night cycle and provided with feed and water *ad libitum*. Forty-eight rats were used for the study under the supervision of a veterinarian: 12 animals each for CSIS, CDS, JDS or UDS subcutaneous implantation. The rats were anaesthetized with intramuscular injection of Ketamin (70mg/Kg) and Xylazin (5mg/Kg). Hair of the supra spinal area was clipped off and swabbed with antiseptic lotion. Four subcutaneous pockets were made through skin incision (1cm), the material (1 cm^2) was folded and implanted in the pockets observing sterile precautions. The incision was then closed by

suturing with 3/0 Mersilk (Ethicon Inc., UK). Animals were allowed to recover. The animals did not receive any antibiotic or analgesic at any stage of the experiment.

After 3 days, 7 days, 14 days, 28 days, 60 days and 90 days two rats from each experimental group were killed in carbon dioxide chamber. The implant tissue was collected from each site. Samples from two sites were used for the study and other two were kept as back-up samples. Each sample was cut into two halves. Then, one half was preserved in NBF for histomorphological evaluation.

4.2.2. Histotechnology

Tissue samples intended for histopathology were fixed and processed by Leica TP1020 automated tissue processor (Leica Biosystems, Germany) and embedded in paraffin wax. Tissue sections of 4 μm micron thickness were cut with Leica RM2255 automated microtome (Leica Biosystems, Germany) and stained with Haematoxylin and eosin as detailed in Section 3.2.3.

4.2.3. Biocompatibility evaluation

Local tissue reaction induced by the CDS was evaluated as per ISO:10993-Part 6, and CSIS was used as the reference biomaterial. In each histology section, the following parameters were studied: number of inflammatory cells (neutrophils, plasma cells, lymphocytes, and macrophages), number of foreign body giant cells (FBGCs), severity of necrosis, extent of neovascularization, extent of fibrosis, and extent of fatty infiltration. All the parameters were quantified by semiquantitative scoring criteria as given in Table-8. Average semiquantitative score was then calculated as [(subtotal-I × 2)

+ subtotal-II], whereas subtotal-I was the sum of scores for neutrophil, lymphocyte, plasma cell, macrophage, giant cell, and severity of necrosis and subtotal-II was the sum of the scores for neovascularization, fibrosis, and fatty infiltration. The difference of the score for the test material from the reference material was designated as the irritancy score for CDS, JDS or UDS.

Table 8: The semiquantitative scoring criteria for assessment of biocompatibility as per ISO:10993-Part 6.

Score	**cells of inflammation***	**Number of giant cells**	**Necrosis**	**Neovascularization**	**Fibrosis**	**Fatty infiltration**
0	0 cells	0 cells	Not present	No capillaries	Absent	Not present
1	1-5 cells	1-2 cells	Minimally present	l–3 capillaries	<5 μm	Minimally present
2	6-15 cells	3-5 cells	Mild degree	4–7 capillaries	6–15 μm	Mild degree
3	Heavy infiltrate	Heavy infiltrate	Moderate degree	Broad blood vessels	16–30 μm	Moderate degree
4	Packed cells	Packed	Severe degree	Extensive vascularization	>30 μm	Severe degree

*****Cells of inflammation include neutrophils (N), lymphocytes (L), plasma cells (P) and macrophages (M).

4.3. RESULTS

4.3.1. Clinical/Gross observations

The general physical and clinical health condition of all experimental animals were normal throughout the experiment. There was no gross evidence of encapsulation infection or necrosis around the implanted materials when retrieved.

4.3.2. Histomorphology for local tissue response

For all materials studied, there was acute inflammatory reaction, predominated by neutrophils at 3 days (Fig. 13A, 14A, 15A, and 16A) but the intensity reaction was less in the CSIS and CDS implanted tissues compared to UDS and JDS.

By 7 days (Fig. 13B, 14B, 15B, and 16B), the acute inflammation appeared to have subsided. Cellular infiltration was seen in the space created between folds of the scaffold materials. There was abundant granulation tissue composed of proliferating fibroblast, mononuclear cell infiltrate in the tissue reaction. The amount of granulation tissue was more in CSIS and CDS implanted tissues while this was less in JDS and UDS implanted tissue. Neovascularization was obvious around all scaffolds. In addition, a few foreign body giant cells (FBGC) were also present in the tissue reaction.

At 14 days (Fig. 13C, 14C, 15C, and 16C), granulation tissue occupied the entire space between the folds of the implanted materials. Additionally, there was multifocal granulomatous inflammation with abundance of FBGCs at the tissue material interface. At that stage of the tissue reaction there was fragmentation of scaffold in to fine pieces

and the staining intensity of all the implanted scaffolds appeared to have decreased probably indicating degradation of the scaffold.

The number of polymorphs were few by 28 days (Fig. 13D, 14D, 15D, and 16D) and granulation tissue appeared to have matured but the extent of mononuclear cell infiltration was more compared to other time points. Moreover, there were plenty of FBGCs present around the implant tissue. The reference material, CSIS appeared to have undergone significant degradation compared to other scaffolds. The UDS followed by the JDS underwent minimal degradation compared to the CSIS or CDS.

Even at 60 days the degradation of the materials was not complete (Fig. 13E, 14E, 15E, and 16E). Mononuclear infiltration was evident as in 28 days. There was progressive fibrous capsule formation at the interface of normal tissue and biomaterial implants. Number of FBGCs was less compared to 28 days. FBGCs were highest in CDS and least in JSD. Compared to other scaffolds JDS induced persistent acute inflammation as evidenced by the presence of neutrophil infiltration.

At 90 days there was no evidence of acute inflammation in CDS implanted tissue (Fig. 13F, 14F, 15F, and 16F). Neutrophil infiltration was relatively less in CDS compared to other scaffolds. In JDS implant there was persistent acute inflammation. Compared to the 4^{th} week samples the number of FBGCs was less in 90 days in all scaffold induced reactions. Mononuclear cell infiltration was less than that of 60 days in all scaffold induced reactions.

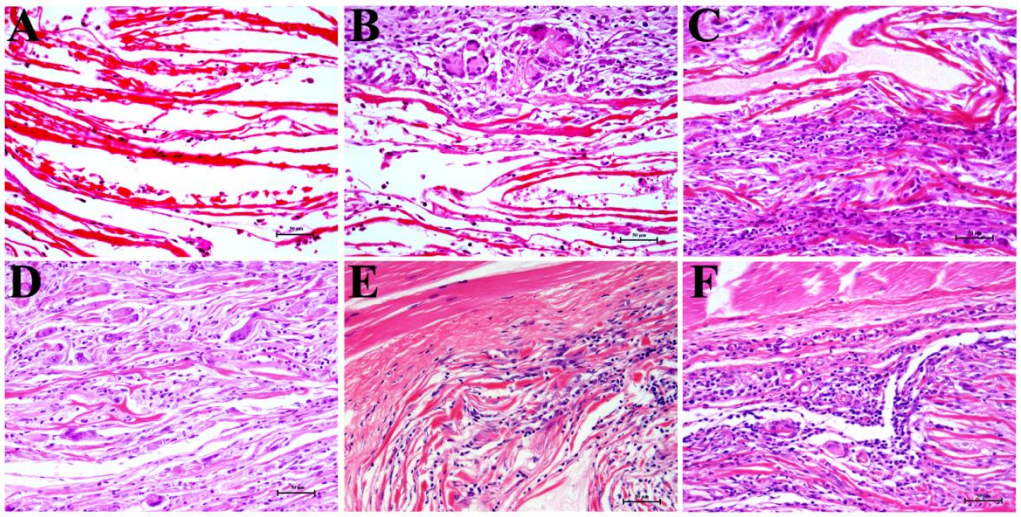

Figure 13: Light micrograph of Haematoxylin and eosin stained tissue sections showing the nature of tissue reaction induced by the CSIS in rat subcutaneous tissue at 3 days (A), 7 days (B), 14 days (C), 28 days (D), 60 days (E) and 90 days (F) respectively (Scale bar indicates 50µm).

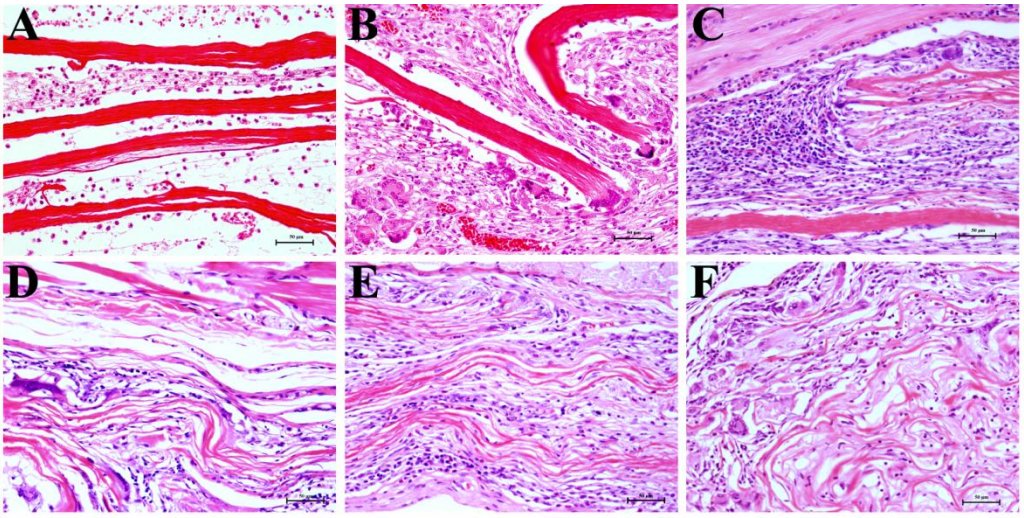

Figure 14: Light micrograph of Haematoxylin and eosin stained tissue sections showing the nature of tissue reaction induced by the CDC in rat subcutaneous tissue at 3 days (A), 7 days (B), 14 days (C), 28 days (D), 60 days (E) and 90 days (F) respectively (Scale bar indicates 50µm).

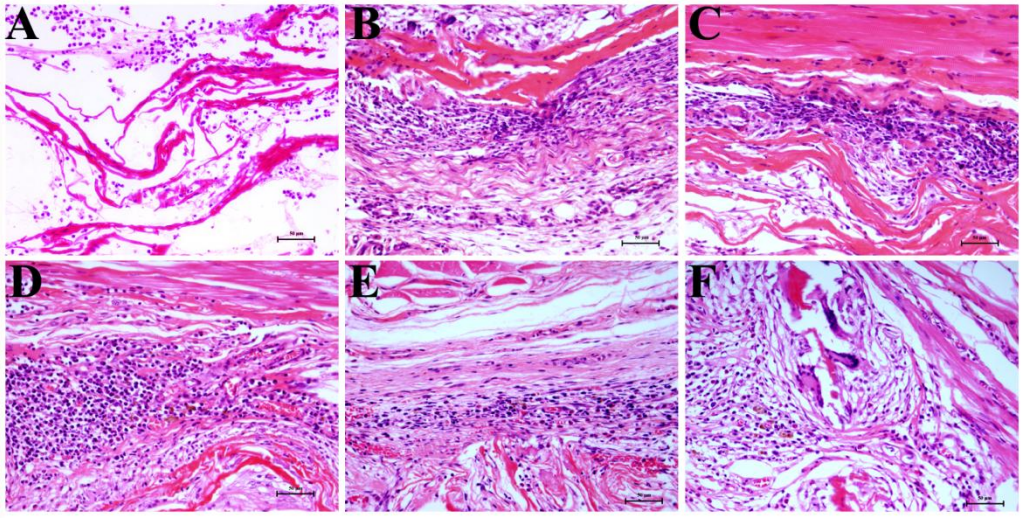

Figure 15: Light micrograph of Haematoxylin and eosin stained tissue sections showing the nature of tissue reaction induced by the JDS in rat subcutaneous tissue at 3 days (A), 7 days (B), 14 days (C), 28 days (D), 60 days (E) and 90 days (F) respectively (Scale bar indicates 50μm).

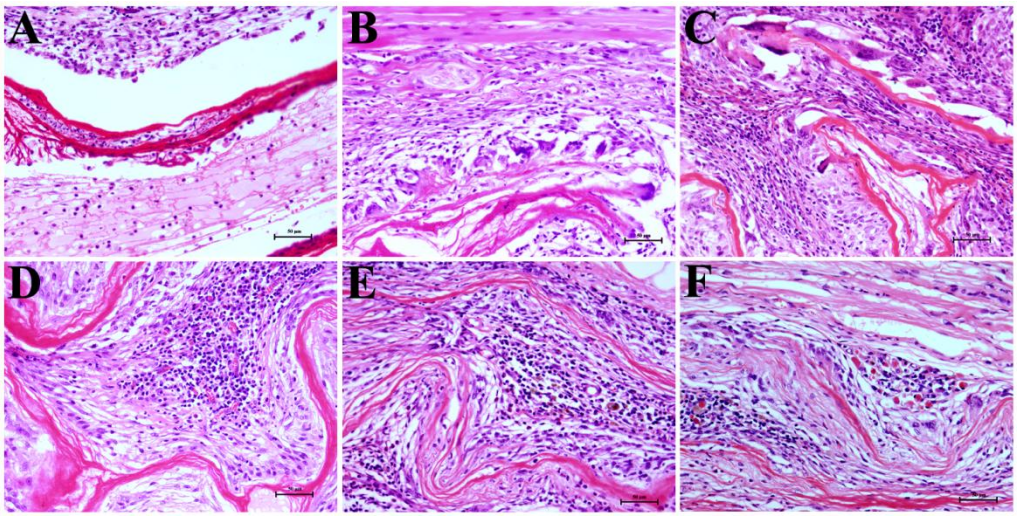

Figure 16: Light micrograph of Haematoxylin and eosin stained tissue sections showing the nature of tissue reaction induced by the UDS in rat subcutaneous tissue at 3 days (A), 7 days (B), 14 days (C), 28 days (D), 60 days (E) and 90 days (F) respectively (Scale bar indicates 50μm).

4.3.3. Biocompatibility evaluation

The semi-quantitative parameters evaluated as per ISO 10993 Part-6 are summarized in Table 9.

Table 9: Semi-quantitative scores obtained from histopathology evaluation

Experimental groups		N	L	P	M	GC	SN	NV	F	FI
3 days	CSIS	3	1	0	2.33	0	0.66	0	0	0
	CDS	3	0.33	0	1.33	0	0.66	0	0	0
	JDS	4	0.33	0	1	0	1.67	0	0	0
	UDS	3.67	0	0	1	0	1.33	0	0	0
7 days	CSIS	2.67	1.33	0.33	2	3	0.67	2	0	0
	CDS	3	0.67	0	2	1.67	1	2	0	0
	JDS	4	0.33	0	2.33	0.33	1.33	2.33	0.33	0
	UDS	3.33	0	0	2.67	1.33	1	2	0	0
14 days	CSIS	0.75	1.25	0.25	2.75	3	0.75	1	0.5	0
	CDS	1.33	1	0	2	2	0.66	2	0	0
	JDS	3	1	0	2.25	2	1	2	0.25	0
	UDS	2.25	1	0	3	2	0.75	2	0.25	0
28 days	CSIS	0	1	0	3	3.5	0	1.75	1	0
	CDS	0.67	1	0	3	2.66	0	2	1	0
	JDS	2	0.75	0	3.75	2	0	2	0.5	0
	UDS	1.75	1	0	3.5	2	0	1.75	0	0
60 days	CSIS	0	1.33	0	2	1.66	0	1	1.33	0
	CDS	1	1	0	2.5	1.25	0	1.25	0.75	0
	JDS	1.25	0.75	0	1.25	2	0.25	2	2	0.25
	UDS	1	1	0	3	2	0	2	1	0
90 days	CSIS	0.67	1.33	0	2	1	0	1	1	0
	CDS	0.25	1	0	2	2.25	0	1.5	1.75	0
	JDS	1.25	1	0	2	1.25	0.5	2.25	2.25	1.25
	UDS	1	1	0	2.25	2	0	1.25	1	0

All values represent mean (n=4) of the semi-quantitative score of local tissue response as per ISO:10993 Part-6, local effects of implantation. (N; polymorphonuclear cells, L; lymphocytes, P; plasma cells, M; macrophage, GC; Giant cells, SN; severity of necrosis, NV; Neovascularisation, F; Fibrosis, FI; Fatty infiltrate)

The irritancy scores for CDS, JDS and UDS were calculated against the CSIS (Table 10). For CDS and UDS the scores were less than 2.9 at all time points of the study. In the case of JDS the score was 2.91 at 60 days and 5.75 at 90 days, which indicated slight irritancy compared to the CSIS.

Table 10: Irritancy score calculated as per ISO:10993 Part-6

Scaffolds	**3 days**	**7 days**	**14 days**	**28 days**	**60 days**	**90 days**
CDS	0	0	0	0	1.16	2.25
JDS	0	0	1.75	1.75	2.91	5.75
UDS	0	0	0	0	2.41	2.75

CSIS was used as control material. Non irritant- 0 to 2.9, slight irritant- 3.0 to 8.9, moderate irritant - 9.0 to 15.0, severe irritant-more than 15

4.4. DISCUSSION

An assessment of biocompatibility based on histomorphological evaluation of local tissue in appropriate site/animal to potential biomaterials is a standard pre-clinical evaluation procedure. Biocompatibility of the scaffolds was assessed as per ISO 10993, Part 6 standards (ISO:10993-6, 2010 (E)). CSIS originally prepared from porcine small intestinal submucosa was used as the biocompatible reference material. Small intestinal submucosa has been used successfully for treatment various human ailments in more than a million human patients worldwide (Badylak, 2007). The semi-quantitative scores obtained for various parameters (Table 9) indicated that the reference scaffold induced moderate acute inflammation and minimal necrosis at 3 days of implantation. At 7 days the reaction was similar to that of 3 days with heavy infiltration of foreign body giant cells and neovascularization. The mononuclear cell infiltration was higher than that of 3 days. However by 14 days the acute inflammation and vascularization was minimal. Further at 28 days the acute inflammation subsided, but mononuclear cell infiltration and FBGC reaction was at its peak level and the scaffold underwent substantial degradation. A fibrous capsule was evident at the tissue material interface. At 60 days the reaction was less severe compared to that of 28 days. At 90 days the degradation of the material was not complete and the FBGC reaction decreased. The mononuclear cell infiltration was still present but less severe than 28 days. The overall reaction was similar to that expected for any biomaterial (Anderson, 2001), except relatively early onset of mononuclear cell infiltration and minimal degree of fibrosis. This type of tissue reaction usually referred to as the constructive tissue remodeling response have been observed

for several biological scaffold materials (Valentin *et al.*, 2006, Badylak and Gilbert, 2008, Badylak *et al.*, 2008).

Compared to CSIS the CDS was biocompatible at all time points of the study as indicated by the biocompatibility scores (Table 9 and 10). The reaction induced by CDS was almost similar to that induced by CSIS with notable difference with respect to scaffold degradation and FBGC reaction at later time points. The degradation of the material was slower than that of CSIS and moderate degree of FBGC reaction continued till 90 days of implantation. This differences in tissue reaction observed here may be due to the differences in processing methods, source organ used for scaffold preparation etc (Valentin *et al.*, 2006).

The biocompatibility score obtained for JDS scaffold at 90 days was 5.75 which indicated that the JDS is slightly irritating to the tissue when compared to CSIS reference material (Table 10). In fact the JDS induced severe acute inflammation relatively higher necrosis at early time points of the study. The rate of scaffold degradation was less than that of CDS. JDS induced persistent acute inflammation, relatively higher fibrosis and fatty infiltration at later time points (Table 9). These adverse tissue reactions may be due to the inherent immunogenic potential of JDS which may be partially attributed to the presence of histocompatibility antigens (MHC class I and II), and cellular debris retained in the scaffold as discussed in chapter 3 (Table 5, Fig. 2 and 3).

The UDS also induced a biocompatible reaction at all time points of implantation (Table

10). However the degree of acute inflammation, severity of necrosis and chronic inflammation were higher than that induced by CDS scaffold. There was persistence of minimal degree of acute inflammation throughout the study period (Table 9). Possible explanation for this adverse reaction may be attributed to the presence of proteins like complement component C3, S100 proteins (Table 6) and higher quantity of cellular residue in UDS when compared to other scaffolds as discussed in chapter 3 (Fig. 2 and 3).

CHPATER-5

5. DISTRIBUTION/FUNCTION OF IMMUNOCOMPETENT CELLS AROUND THE GRAFTS IMPLANTED IN RAT SUBCUTANEOUS TISSUE

5.1. INTRODUCTION

The data on biocompatibility presented in chapter-4 warranted a detailed comparative study on the nature of local immunogenicity of the scaffolds prepared from cholecyst, jejunum and urinary bladder. Therefore, in this chapter the distribution/function of immunocompetent cells in the rat subcutaneous tissue implanted with scaffolds were studied. The distribution of immunocompetent cells like mast cells, M1 and M2 macrophages, helper and cytotoxic T lymphocytes, and B lymphocytes at the graft site were detected and quantified histomorphometrically. The M1/M2 macrophage functional polarization and TH1/TH2 lymphocyte functional polarization induced by the grafts were studied by real-time RT-PCR for at least four marker genes, one for each of the cell types studied.

5.2. MATERIALS AND METHODS

5.2.1. Subcutaneous implantation of scaffolds in rats

The CDS, JDS and UDS materials were implanted subcutaneously into Sprague-Dawley rats as described in Section 4.1. After days 3,7,14, 28, 60 and 90 postimplantation, two rats from each experimental group were killed in carbon dioxide chamber. The implanted tissue was collected from each site. Samples from two sites were used for the study and other two were kept as back-up samples. Each sample was cut into two halves.

Then, one of them was preserved in NBF for histomorphological evaluation. The other half of the tissue sample for gene expression analysis was put in RNA*later* (Sigma) and stored in -20^{0}C freezer.

5.2.2. Histotechnology

The implant tissue was processed in automated tissue processor, embedded in paraffin wax and tissue sections were taken as described in Section 3.2.3.

5.2.3. Number and distribution of various cells in implant tissue

5.2.3.1. Toluidine blue staining for mast cells

The mast cells in the implant tissue were studied by staining with toluidine blue. Mononuclear cells with purple metachromatic granules were identified as mast cells.

5.2.3.2. Immunohistochemistry

Immunohistochemistry was performed on histology sections to detect macrophage and lymphocyte subtypes participating in the local tissue reaction using antibodies raised against CD80, CD163, CD4, CD8 and CD79a (Table 11). Briefly tissue sections were deparaffinized and washed in distilled water and treated with antigen retrieval buffer (Tris/EDTA buffer; 10 mM Tris Base, 1 mM EDTA solution, pH 9.0 for CD4-immunostaining and Citrate buffer; 10mM Sodium citrate pH 6.0 for CD8-, CD80-, CD163-, and CD79a-immunostaining) for 20 minutes at 92°C and allowed to cool for 30 minutes. The endogenous peroxidase activity was inhibited by treating the slides with 5% H_2O_2 for 15 minutes and the non-specific reactivity of secondary antibody was blocked by using 10% goat serum (Santa Cruz Biotechnologies, Inc. USA) for 30

minutes. Later, the sections were washed with 10mM trisodium citrate solution pH 6.0 and treated with primary antibody for one hour at room temperature. The reaction was detected using Supersensitive polymeric-HRP^{TM} detection system (BioGenex Laboratories, USA) according to manufacturer's instructions. Finally, the sections were counter stained with Harris's haematoxylin (Electron Microscopy Sciences, Hatfield, PA).

Table 11: List of monoclonal antibodies used for immunohistochemistry

Target antigen	Cell type identified	Clone	Company
CD4	Helper T cell	OX-38	Abcam
CD8	Cytotoxic T cell	OX-8	Abcam
CD79a	B cell	HM47/A9	Abcam
CD80	M1 macrophage	EP1155Y	Abcam
CD163	M2 macrophage	ED2	Santa Cruz Biotechnologies, Inc.

5.2.3.3. Histomorphometry

Histomorphometry was performed on histology images (original magnification, 400x) captured with a DP71 camera loaded on to a BX51 microscope (Olympus Corporation, Japan) using ImagePro version 3DS6.1 software (Media Cybernetics, Silver Spring, MD). The microscope had an automated stage-movement system. The implant tissue was imaged, frame by frame, through automation to obtain a series of images that covered the entire implant tissue. The number of images varied with the area occupied by the tissue reaction. The number of immunostained cells in the reaction zone with appropriate phenotypic features were counted manually. Macrophages were identified as immunopositive mononuclear cells with large cytoplasm and pear shaped/oval nucleus.

Lymphocytes were identified as immunopositive mononuclear cells with scanty cytoplasm and relatively higher nuclear to cytoplasmic ratio. Mast cells were identified as mononuclear cells with purple metachromatic granules in tissue sections stained with toluidine blue. The area occupied by the implant tissue and associated inflammatory tissue was also estimated. The number of cells per mm^2 was determined and the respective ratio was calculated.

5.2.3.3.1. M1/M2 macrophage polarization

Macrophages in the implant tissue were stained with CD80 M1 macrophage marker and CD163 M2 macrophage marker. The number of immunostained cells was counted as described in Section 5.2.3.3. The M1/M2 macrophage ratio was calculated for determining the M1/M2 macrophage polarization.

5.2.3.3.2. CD4/CD8 ratio

Implant tissue was stained with CD4 and CD8 T cell markers. The number of immunostained cells was counted using Image-Pro software as described in Section 5.2.3.3. The CD4/CD8 T cell ratio was calculated.

5.2.4. Gene expression studies

5.2.4.1. RNA isolation

Total RNA was isolated from tissue samples put in RNA*later* using Trizol reagent (Invitrogen, USA) as per manufacturer's protocol. Briefly, implant tissue (100mg) in 1mL of Trizol reagent was grinded using tissue homogenizer (IKA Germany) and incubated for 5 min. It was then centrifuged at 12000g for 10 min in a refrigerated

centrifuge (Eppendorf, Germany) and incubated. The supernatant was then pipetted out in to another centrifuge tube and in to it added 200µl of chloroform. The tubes were mixed thoroughly by vortexing for 15 seconds and incubated for 2-3 minutes at room temperature. It was centrifuged at 12000g for 15 minutes at 4°C. The upper aqueous layer was pipette out in to another centrifuge tube containing 0.5 mL 75% alcohol, vortexed and incubated at room temperature for 10 min. It was centrifuged at 12000g for 10 min at 4°C and the supernatant was discarded. The pellet was again washed with 75% alcohol and centrifuge at 7500g for 5 minutes. The supernatant was discarded and the RNA pellet obtained was allowed to air dry for 5-10 minutes. In to the RNA pellet 20µl of distilled water was added and allowed to dissolve completely by keeping 55°C water bath for 10min.

The purity and concentration of the RNA was tested using NanoDrop ND-1000 spectrophotometer (NanoDrop, Wilmington, DE, USA). Only RNA with 260/280 nm absorption ratio more than 1.8 was used for cDNA synthesis.

5.2.4.2. cDNA synthesis

cDNA synthesis was carried out in Chromo4 system (Bio-Rad, Hercules, CA, USA) using SuperScript^{TM} III reverse transcriptase, Oligo $(dT)_{20}$ primer, 0.1M DTT, 40IU/mL Rnase out recombinant ribonuclease inhibitor and 5X First-strand buffer (Invitrogen Corporation, USA). 1µg of RNA was used for cDNA synthesis. The reagents were added into 200µl PCR tubes in two steps according to the Table 12. After the step-1 the mixture was heated at 65°C for 5 minutes and incubated on ice for 1 minute. Reagents of

step-2 were added, mixed well and kept at 25°C for 5 minutes. The reverse transcription was carried out at 50°C for 1h followed by stopping the reaction at 75°C for 15 minutes. The cDNA thus synthesized were then stored at -20°C freezer.

Table 12: Reagents added for cDNA synthesis

	Reagent	**Volume**
Step-1	Oligo $(dT)_{20}$ primer	1μL
	10nM dNTP mix	1μL
	RNA	1 μg
	Sterile water	Up to 13 μL
Step-2	RT buffer (5X First-strand buffer)	4μL
	0.1M DTT	1μL
	Rnase out recombinant ribonuclease inhibitor (40IU/mL)	1μL
	Superscript III reverse transcriptase	1μL

5.2.4.3. Real time Polymerase chain reaction

The primer sets for glyceraldehyde 3-phosphate dehydrogenase (GAPDH) housekeeping gene, iNOS, Arginase-I, INFγ, IL4, TNF-α and IL10 were custom designed and obtained from eurogentech Belgium (Table 13). Real time PCR was carried out in Chromo4 system (Bio-Rad, Hercules, CA, USA) using qPCR MasterMix Plus for SYBR® Green I No ROX which is a mixture of dNTPs (including dUTP), HotGoldStar DNA polymerase, $MgCl_2$ (5mM final concentration), Uracil-N-Glycosylase, SYBR® Green I and stabilizers (Eurogentec, Belgium). The reagents were added as per Table 14. The thermocycler was set with the following protocol. An initial HotGoldStar activation step for 10 min at 95°C, followed by 40 cycles of melting (95°C for 30 sec), annealing (60°C for 30 sec) and extension step (72°C for 1 minute). The quality of PCR reaction

was confirmed by analyzing the melting curve of the PCR product from 60°C to 90°C. Gene expression was then analyzed by $2^{-\Delta\Delta Ct}$ method using gene expression of CSIS implanted tissue samples as control. Relative expression of M1/M2 genes ($RE_{(M1/M2)}$) and TH1/TH2 genes ($RE_{(TH1/TH2)}$) were calculated by the following formulae $RE_{(M1/M2)} = 2^{-\Delta Ct}$ (iNOS) / $2^{-\Delta Ct}$ (Arginase I) and $RE_{(TH2/TH1)} = 2^{-\Delta Ct}$ (INF-γ)/ $2^{-\Delta Ct}$ (IL4) respectively (Brown *et al.*, 2009).

Table 13. List of primer sequences used for real time RT-PCR analysis.

Gene	Accession Number	Forward primer	Reverse primer
GAPDH	NM_017008.4	CAAGTTCAACGGCACAGTCAAG	ACATACTCAGCACCAGCATCAC
iNOS	NM_012611.3	AAGAGACGCACAGGCAGAGG	AGCAGGCACACGCAATGATG
Arginase- I	NM_017134.3	GGCAGTGGCGTTGACCTTG	GTTCTGTTCGGTTTGCTGTGATG
INF-γ	NM_138880.2	AACCCACAGATCCAGCACAAAG	TTTCCGCTTCCTTAGGCTAGATTC
IL-4	NM_201270.1	ACAAGGAACACCACGGAGAAC	TTCAAGCACGGAGGTACATCAC
TNF-α	NM_012675	CCGAGATGTGGAACTGGCAGAG	TTCAGTAGACAGAAGAGCGTGGTG
IL10	NM_012854	CATCAACTGCATAGAAGCCTAC	TTGGAGAGAGGTACAAACGAG

Table 14: Reagents added for real-time PCR reaction

Reagent	Volume
qPCR MasterMix Plus for SYBR® Green I No ROX	10 µL
Forward Primers (100 nM)	2.00 µL
Reverse Primers (100 nM)	2.00 µL
cDNA template	2.00 µL
Sterile Water	4.00 µL

5.2.5. Statistical analysis

One-way analysis of variance and Tukey-Kramer multiple comparisons tests were performed using GraphPad InStat software version 3.10 (GraphPad Software, Inc. CA, USA) to determine significant different between groups. Those differences with p value less than 0.05 was considered significant.

5.3. RESULTS

5.3.1. Number and distribution of various immunocompetent cells in implant tissue

5.3.1.1. Mast cells

Toluidine blue stained tissue sections were evaluated for mast cells in the reaction zone. Mast cells were detected by the presence of purple metachromatic granules in cytoplasm of mononuclear cells. Mast cells were present at all time points of the study, in histology sections, around all implanted materials (Fig. 17).

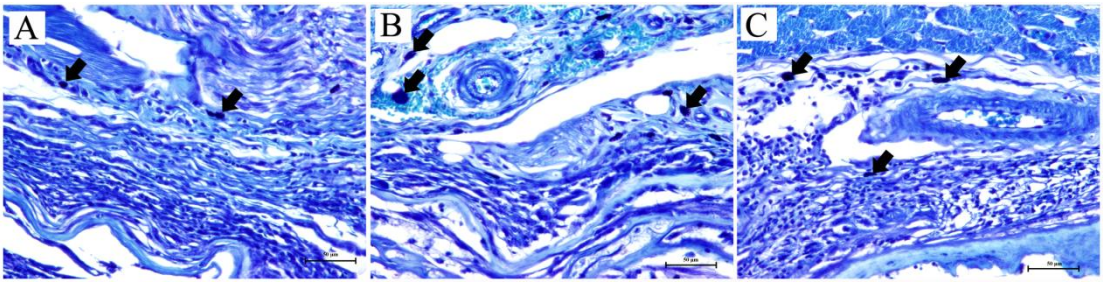

Figure 17: Light micrograph of toluidine blue stained tissue sections showing mast cells (thick arrows) in the tissue reaction induced by CDS (A), JDS (B) and UDS(C) at 14 days (Scale bar indicates 50μm). See Table 15 for quantitative data.

5.3.1.2. Immunohistochemistry

Immunohistochemistry for CD80-positive M1 macrophages, CD163-positive M2 macrophages, CD4-positive helper-T cells, CD8-positive cytotoxic-T cells and CD79a-positive B cells (Fig. 18) indicated significant infiltration of these cell types in to the reaction zone at all time points. Generally, the extent of infiltration of each cell type progressed with time. The quantitative data are presented in quantitative histomorphology section below.

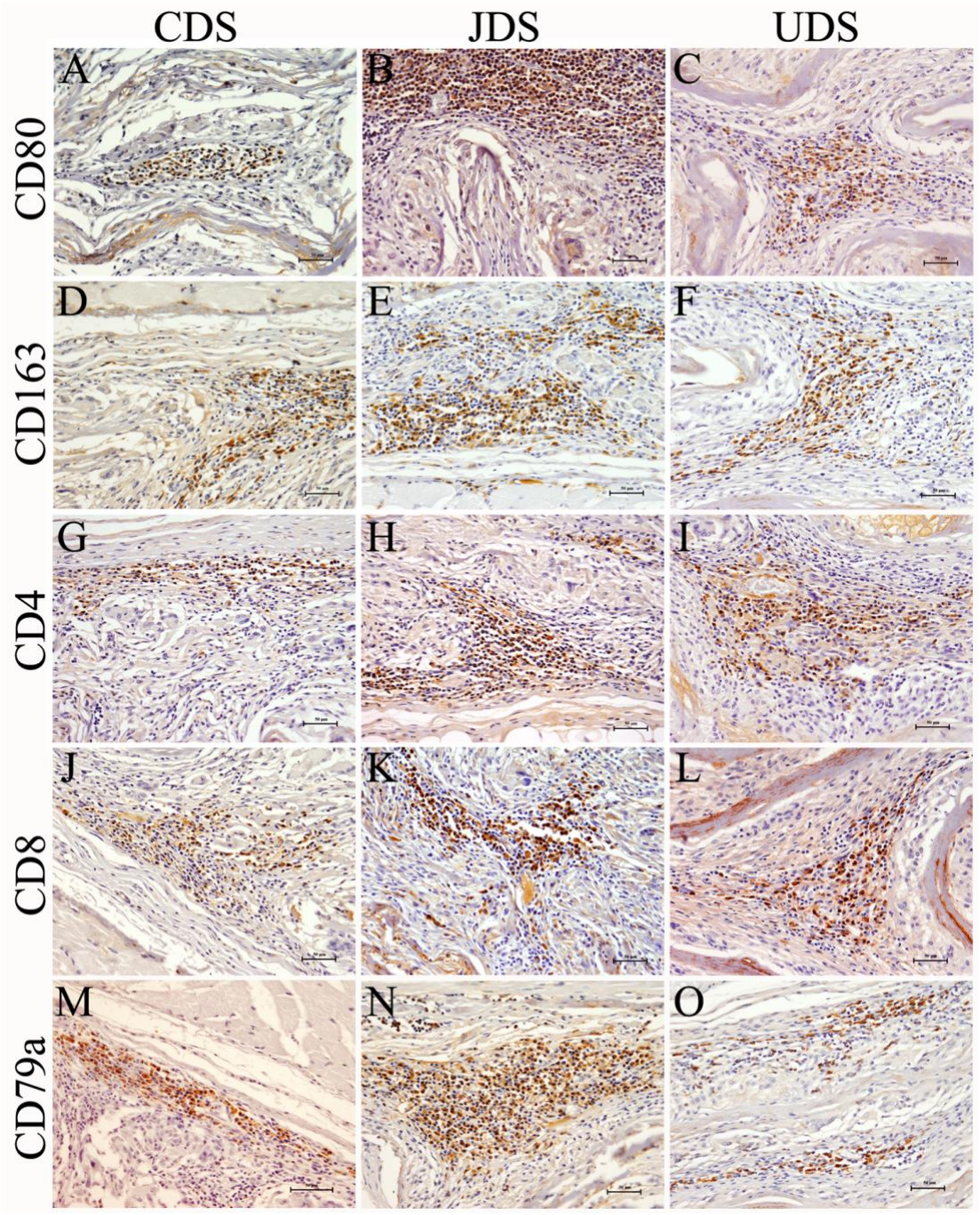

FIGURE 18: Immunohistochemical demonstration of CD80, CD163, CD4, CD8 and CD79a positive mononuclear cells in the tissue reaction at 28 days following implantation of the scaffolds in rat subcutaneous tissue. Brown color represents positive cells. Scale bar indicates 50μm. See Tables 16, 17 and 18 for quantitative data.

5.3.1.3. Quantitative histomorphology

5.3.1.3.1. Mast cell response

The number of mast cell infiltration in to the reaction zone is shown in Table 15. The overall reaction indicated that the mast cell numbers increased over time from 3 days to 14 days. There was reduction in mast cell reaction around CDS and JDS by 28 days. For all scaffolds highest mast cell infiltration was observed at 60 days and 90 days. Compared to JDS the CDS had significantly less mast cell infiltration at 3, 7 and 14 days. There was also significant less mast cell infiltration when compared to UDS at 28 days and 90 days. However, CDS induced higher mast cell infiltration at 60 days.

Table 15: The number and distribution of mast cells in the reaction zone obtained by image analysis.

	CDS	**JDS**	**UDS**
3 days	2.34±0.36 [a]	4.19±0.32	3.42±0.56
7 days	3.45±0.37 [a]	6.44±0.86 [c]	3.10±0.03
14 days	4.90±0.72 [a]	6.68±0.73 [c]	4.75±0.25
28 days	2.03±0.37 [b]	2.04±0.24 [c]	5.77±0.88
60 days	19.3±2.77 [a]	9.1±1.23 [c]	15.8±1.72
90 days	13.72±2.56 [b]	9.75±1.33 [c]	24.94±8.65

Values represent number of mast cells per mm^2 of implant tissue (mean±1SD, n=4).

[a] Significant difference between CDS and JDS
[b] Significant difference between CDS and UDS
[c] Significant difference between JDS and UDS.

5.3.1.3.2. Macrophage response

There was progressive increase in infiltration of both M1 and M2 cells over time (Table 16). All scaffolds showed highest macrophage infiltration at 28 days/60 days. The

macrophage infiltration decreased from 60days to 90days. CDS induced higher M1 and M2 macrophage infiltration compared to JDS at 60days and 90days.

Table 16: The number of CD80 and CD163 positive macrophages in the reaction zone obtained by image analysis.

		CDS	**JDS**	**UDS**
CD80	3 days	1.58±0.11	2.51±0.44	2.41±0.61
	7 days	1.48±0.32[a]	20.55±6.87 [c]	1.96±0.46
	14 days	13.18±2.26	14.93±3.44	14.96±4.66
	28 days	141.48±16.48 [a]	254.20±40.18	200.52±33.59
	60 days	317.19±52.28 [a]	151.13±36.79[c]	281.87±28.34
	90 days	187.85±64	130.31±36	202.3±62.94
CD163	3 days	5.30±3.19	2.96±1.57	1.38±1.22
	7 days	3.66±1.08 [a]	15.28±6.29 [c]	2.62±1.53
	14 days	51.49±33.56	32.83±11.58	21.26±21.48
	28 days	260.94±11.57 [a]	469.59±66.1 [c]	274.07±19.67
	60 days	295.84±71.01 [a]	168.98±45.26[c]	293.29±28.28
	90 days	174.45±79.72 [a]	116.92±22.54[c]	215.88±83.95

Values represent number of mast cells per mm^2 of implant tissue (mean±1SD, n=4)

[a] Significant difference between CDS and JDS
[b] Significant difference between CDS and UDS
[c] Significant difference between JDS and UDS

5.3.1.3.2.1. M1/M2 macrophage polarization

The M1/M2 macrophage ratio (Fig. 19) indicated a predominance of M2 macrophages in CDS up to 28 days of implantation. M2 predominance was also observed at 14 days and 28 days in JDS induced reaction. However, UDS induced M2 reaction 28 days only. Thus induction of M2 macrophage was relatively a late event in JDS and UDS induced

reactions. However, by 60 days all scaffolds induced equal distribution of M1 and M2 macrophages.

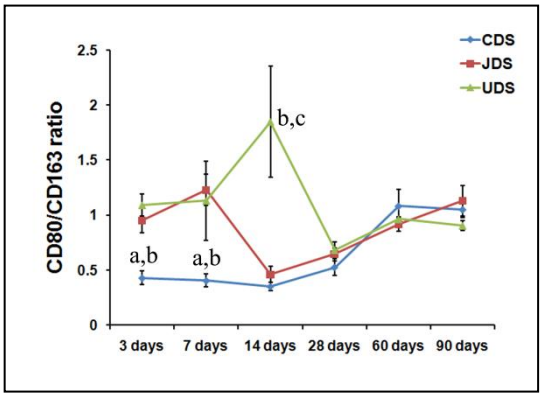

Figure 19: M1/M2 macrophage ratio as obtained by histomorphometry. Values represent mean±1SD, n=4.

[a] Significant difference between CDS and JDS
[b] Significant difference between CDS and UDS
[c] Significant difference between JDS and UDS

5.3.1.3.3. Lymphocyte response

There was progressive increase in the number of both CD4 and CD8 cells over time (Table. 17). At 28 days CDS induced lower CD4 and CD8 T cell infiltration compared to JDS scaffold. For all implants the CD4 and CD8 T cell infiltration decreased after 28 days.

Table 17: The number and distribution of CD4 and CD8 positive lymphocytes in the reaction zone obtained by image analysis.

		CDS	JDS	UDS
CD4	3 days	2.95±1.30	4.42±1.61	3.68±0.32
	7 days	3.54±1.35 [a]	1.73±0.43[c]	2.93±0.16
	14 days	42.35±17.36	22.46±9.28	20.61±4.25
	28 days	234.26±32.14 [a,b]	431.14±98.86	307.75±33.11
	60 days	259.14±17.22 [a]	108.94±32.71[c]	220.73±39.45
	90 days	169.36±53.52 [a]	58.3±11.83 [c]	178.12±50.54
CD8	3 days	2.46±0.46[a,b]	1.69±0.18	1.57±0.37
	7 days	5.94±1.46[b]	7.10±2.31[c]	1.02±0.36
	14 days	42.70±14.55[b]	37.78±15.17[c]	8.75±2.54
	28 days	283.21±31.67[a]	469.03±82.52[c]	296.27±32.58
	60 days	166.44±10.79[a]	89.77±27.21[c]	193.84±34.57
	90 days	118.3±31.86[a]	58.22±14.32[c]	140.55±49.44

Values represent number of mast cells per mm^2 of implant tissue (mean±1SD, n=4).

[a] Significant difference between CDS and JDS
[b] Significant difference between CDS and UDS
[c] Significant difference between JDS and UDS

5.3.1.3.3.1. CD4/CD8 ratio

The CDS consistently showed CD4/CD8 ratio of one at all time points of the study without any predominance for either CD4 or CD8 T-cells (Figure 20). JDS at 7 days induced CD8 T cell predominance as evidenced by CD4/CD8 ratio less than one. At 28 days of implantation, for all implant materials the CD4 to CD8 ratio was approximately equal to one, showing the equal number of CD4 and CD8 in the implant tissue. UDS stimulated higher CD4 T-cell predominance in the tissue reaction at 3, 7 and 14 days of

implantation. At 60 days CDS showed CD4 cell predominance. At 90 days all scaffolds showed CD4/CD8 ratio of one.

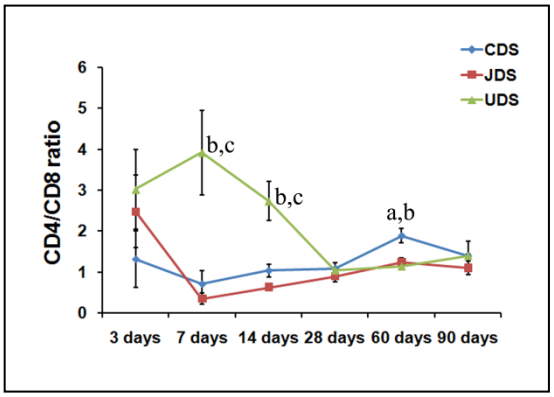

Figure 20: CD4/CD8 T-cell ratio as obtained by histomorphometry. Values represent mean±1SD, n=4.

[a] Significant difference between CDS and JDS
[b] Significant difference between CDS and UDS
[c] Significant difference between JDS and UDS

5.3.1.3.3.2. B cell response

B lymphocytes infiltration (Table 18) increased gradually with time and by 28 days there was significantly higher number of these cells in the tissue. The number of B cells decreased at 60 days and 90 days. The CDS induced lower B cell infiltration than JDS and UDS at 28 days. At 60 days CDS induced higher B cell infiltration than JDS. There was higher B cell infiltration in CDS implanted tissue compared to JDS and UDS implanted tissues at 90 days.

Table 18: The number and distribution of CD79a positive B lymphocytes in the reaction zone obtained by image analysis.

	CDS	JDS	UDS
3 days	1.51±0.43[a]	4.6±1.38	2.66±0.99
7 days	2.7±0.56 [b]	4.2±1.13	6.35±0.95
14 days	40.1±21.8	50.1±11.55	35.12±9.18
28 days	237.4±46.68 [a,b]	463.9±60.62	328.17±41.22
60 days	53.6±12.5 [a]	4.0±0.62 [c]	46.53±12.29
90 days	48.4±15.76 [a,b]	5.5±3.54 [c]	19.06±7.63

Values represent number of B-lymphocytes per mm^2 of implant tissue (mean±1SD, n=4).

[a] Significant difference between CDS and JDS
[b] Significant difference between CDS and UDS
[c] Significant difference between JDS and UDS

5.3.2. Gene expression analysis

5.3.2.1. Inflammatory cytokine (TNF-α) expression

The gene expression of TNF-α was studied as a representative of inflammatory cytokine (Fig. 21). CDS induced highest expression of TNF-α at 3 days and decreased thereafter. JDS and UDS scaffolds constantly showed increased TNF-α expression up to 28 days. Compared to CDS, there was significantly higher inflammatory cytokine expression in JDS and or UDS at 7, 14, 28 and 60 days of implantation

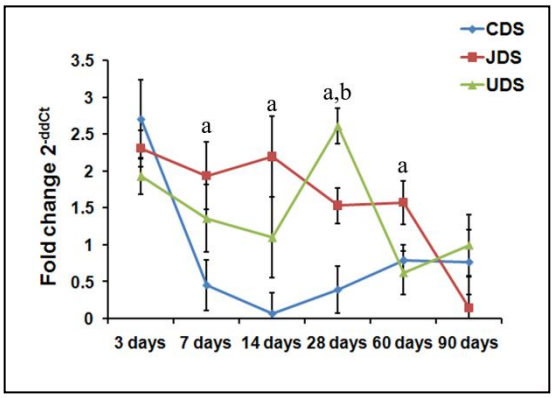

Figure 21: The TNF-α gene expression. Values represent mean±1SD, n=4.

[a] Significant difference between CDS and JDS
[b] Significant difference between CDS and UDS
[c] Significant difference between JDS and UDS

5.3.2.2. Anti-inflammatory cytokine (IL10) expression

The gene expression of IL10 was studied as representative of ant-inflammatory cytokine (Fig. 22). CDS induced highest expression of IL-10 at 28 days. JDS induced lower IL-10 expression at all time points. UDS implanted tissues showed higher IL-10 expression at 60 days and 90 days.

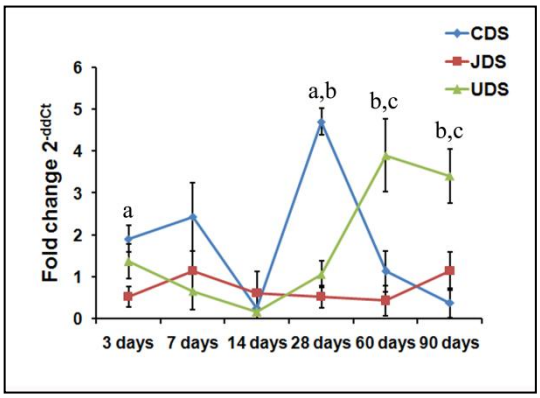

Figure 22: The IL10 gene expression**.** Values represent mean±1SD, n=4.

[a] Significant difference between CDS and JDS
[b] Significant difference between CDS and UDS
[c] Significant difference between JDS and UDS

5.3.2.3. M1/M2 macrophage functional polarization

The M1/M2 macrophage functional polarization was studied by real time RT-PRC. The relative ratio of expression of M1 marker iNOS to that of M2 marker arginase-1 was used to study the M1/M2 macrophage functional polarization (Figure 23). A ratio less than one indicated M2 polarization and ratio more than one indicated M1 polarization. The results showed that the CDS induced M2 macrophage polarization at all time points of the study. The extent of M2 polarization induced by JDS and UDS were less than that induced by CDS. For JDS and UDS, M2 polarization was a relatively late event as indicated by the M2 polarization at 90 days and 60 days respectively in JDS and UDS induced reactions.

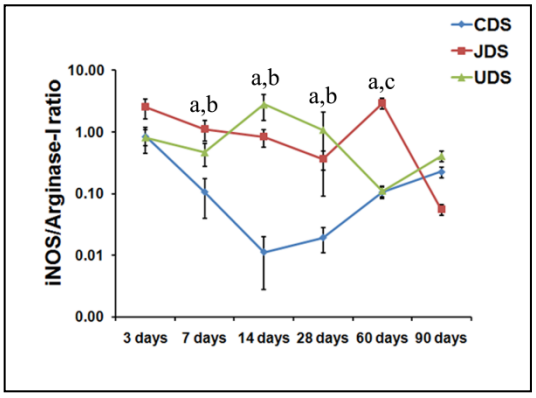

Figure 23: The M1/M2 macrophage functional polarization as obtained by real time RT-PCR. Values represent mean±1SD, n=4.

[a] Significant difference between CDS and JDS
[b] Significant difference between CDS and UDS
[c] Significant difference between JDS and UDS

5.3.2.4. TH1/TH2 lymphocyte functional polarization

The TH1/TH2 lymphocyte functional polarization was studied by real time RT-PRC. The relative ratio of expression of TH1 marker INF-γ to that of TH2 marker IL4 was used to study the TH1/TH2 lymphocyte functional polarization (Fig. 24). A ratio less than one indicated TH2 polarization and ratio more than one indicated TH1 polarization. The results showed that the CDS induced TH2 lymphocyte functional polarization all time points of the study. The extent of TH2 polarization induced by JDS and UDS were less than that induced by CDS or CSIS scaffolds at 28 days, 60 days and 90 days.

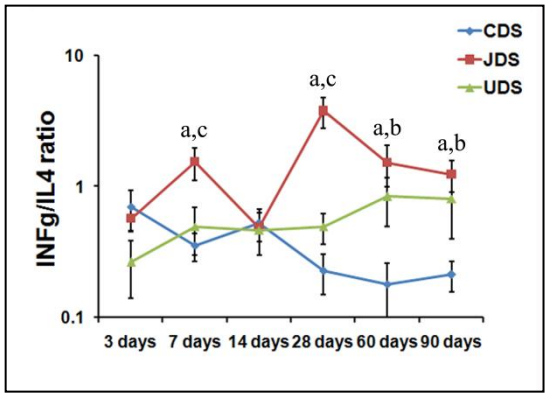

Figure 24: The TH1/TH2 lymphocyte functional polarization as obtained by real time RT-PCR. Values represent mean±1SD, n=4.

[a] Significant difference between CDS and JDS
[b] Significant difference between CDS and UDS
[c] Significant difference between JDS and UDS

5.4. DISCUSSION

In order to assess the actual immunogenic potential of the ECM scaffolds, different functional components of the immune response were evaluated using appropriate markers in a rat subcutaneous implantation model. Subcutaneous implantation of biomaterials in animal models has been suggested for studying the probable nature of tissue reaction as well as the immunogenic potential of biomaterials (Higgins *et al.*, 2009). ECM scaffolds were implanted subcutaneously into Sprague-Dawley rat and the nature of the tissues reaction was evaluated histomorphologically at 3 days, 7 days, 14 days, 28 days, 60 days and 90 days. The different functional segments of the immune reaction studied were mast cell response, macrophage response, T-helper cell response, cytotoxic T-cell response, and B-cell response. The inflammatory cytokine and anti-inflammatory cytokine expression were also studied.

The scaffolds were present in all histology samples at the subcutaneous site beneath the panniculus carnosus muscle (Fig. 14, 15 and 16) even at 90 days. As expected, all implants induced a tissue reaction predominated by neutrophils at 3 days of implantation, that gave way for granulation tissue and mononuclear cell reaction by 7 and 14 days. Chronic granulomatous reaction and giant cell infiltration were the predominant local tissue response at 28 days. At 60 days and 90 days the histomorphology had hallmarks of material induced tissue reaction. In summary, the histomorphological features suggested a healing reaction predominated by foreign-body granuloma at the tissue-material interface (Anderson, 2001).

However, the intensity of graft induced-reaction and the nature of infiltration of various sub-populations of cells participating in immune function varied significantly with different scaffolds. Mast cells are source of histamine and other inflammatory modulators responsible for acute/immediate hypersensitivity reactions (hypersensitivity type I) and they are implicated in biomaterial-induced tissue reaction (Tang *et al.*, 1998). In the present study, the induction of mast cell reaction was found minimal following CDS-grafting/implantation. Soon after the implantation, at early time point (3 days) when compared to all other scaffolds, the CDS attracted significantly fewer numbers of mast cells at the reaction zone (Fig. 17 & Table 15) indicating that it is not likely to induce acute hypersensitivity type I reaction. Early mast cell activation and degranulation may also stimulate fibrotic reaction of the biomaterial (Thevenot *et al.*, 2011). This is consistent with the higher fibrotic response observe in JDS implanted tissue at 60 days and 90 days.

Immunohistochemisty for studying sub-population of cells significant in immune function, especially the macrophages and lymphocytes gave insight into the nature of immune function at the local site of implantation. Macrophage responses are usually classified either M1 or M2 types, which are essentially the simplified extremes of a continuum of phenotypes depending on their contributory role in inflammation. Whereas, the M1 macrophages are pro-inflammatory cells participating in aggressive chronic inflammation, M2 macrophages are anti-inflammatory in nature that promotes constructive remodeling process (Mills *et al.*, 2000). It is also known that, in any immunopathological tissue reaction, both these phenotypes can be expected but the

predominance of either one of these macrophage phenotypes determines the outcome of tissue reaction largely by regulating the cytokine milieu of the microenvironment (Stout *et al.*, 2005). In fact, it has been shown that ECM xenograft-scaffolds when implanted in animal models elicited M2 predominated macrophage response rather than M1 inflammatory cells in instances where constructive remodeling reaction happened at the implant site (Brown *et al.*, 2009). Immunohistochemistry for macrophage subtypes M1 and M2 cells showed infiltration of both of these cells in the implant tissue (Fig. 18 and Table 16). In the present study, the CDS induced a desirable macrophage reaction predominated by the M2 phenotype at time points up to 28 days (Fig. 19). At 60 days and 90 days there was equal number of M1 and M2 macrophage infiltration indicating a balanced equilibrated reaction without any predominance for either M1 or M2 macrophage response. This was again confirmed by real-time RT-PCR gene expression analysis using iNOS and arginase-1 expression, which are the biochemical markers for M1 and M2 functions. The ratio of gene expression of M1 and M2 genes consistently showed M2 macrophage polarization of CDS implanted tissue at all time points of implantation (Fig. 23). The results suggested that CDS induced relatively higher M2 macrophage response compared to JDS and UDS. The CDS implantation probably created a microenvironment that favor M2 macrophage predominance and therefore deemed to induce constructive remodeling of the implant tissue.

The T lymphocyte subpopulations studied were helper T cells and cytotoxic T cells (Fig. 18). The cells increased in number with time from 3 days to 28 days and then decreased at 60 days and 90 days, at the site of tissue healing reaction induced by all the scaffolds

studied (Table 17). It was evident that the materials caused T-lymphocyte infiltration as expected for any tissue-material interaction (Ohtani, 2013, Klinge *et al.*, 2014). However, it is believed that rather than actual numbers, the relative proportion of helper and cytotoxic cells (CD4/CD8 ratio) determines the outcome of the reaction (Amadori *et al.*, 1995, Hautz *et al.*, 2012, Li *et al.*, 2013). The normal value of CD4/CD8 ratio in rats may vary according to the tissue/organ (Jimenez *et al.*, 2001). Whereas equal numbers of CD4 and CD8 or slightly higher numbers of CD4 cells are considered as a desirable feature, predominance of either of these cell types can contribute to pathology associated with transplant rejection (Amadori *et al.*, 1995, Hautz *et al.*, 2010). So, the T cell subtypes were stained immunohistochemically and the ratio was calculated (Fig. 20). Considering that a few non helper T cells (e.g.; monocytes, dendritic cells) also can be CD4-immuno reactive, manual counting ensured identification of immunopositive lymphocytes. For all scaffolds except UDS, the ratio was less than one showing the cytotoxic T-cell predominance at 7 days. At 28 days all scaffolds induced CD4/CD8 ratio one, indicating equal distribution of CD4 and CD8 cells. By 60 days and 90 days CDS showed ratio of 1.88 and 1.4 respectively with CD4 cell predominance. UDS induced significantly higher CD4/CD8 ratio at 7 days and 14 days (Fig. 20). These observations made about UDS cannot be considered a desirable reaction because higher CD4 predominance is also sometimes observed with graft rejection (Hautz *et al.*, 2010). However, it may be inferred that the CDS is not likely to induce an undesirable cytotoxic reaction compared to UDS.

In addition to the study of T-cell sub-population by immunohistochemistry, the

functional status of helper-T cells was also studied. Helper-T cell activity may be TH1 or TH2 polarized (Abbas *et al.*, 1996). It has been shown that TH2 predominance causes acceptance of the graft rather than rejection (Allman *et al.*, 2001). Hence TH2 polarization is desirable after the xenograft implantation. Here, the ratio of expression of TH1 and TH2-cytokines (Fig. 24) suggested higher TH2 polarization in the CDS implanted tissue at 28 days to 90 days. On the other hand, the JDS implanted tissue, at 28 days onwards, showed destructive TH1 polarization. Therefore, compared to JDS and UDS, as evidenced by a desirable TH2 polarization of lymphocytes, the CDS is less immunogenic when used as a xenograft.

An enhanced TH2 reaction has been viewed as a sign of prominent humoral immune response (Abbas *et al.*, 1996). In order to ascertain the ability of the scaffolds to activate humoral immunity, the occurrence of B-cells in the reaction tissue was studied. All scaffolds induced B cell infiltration in to the reaction zone indicating their ability to induce humoral immune response. The number of B-cells steadily increased over time up to 28 days and then decreased significantly (Table 18). The number of B cell infiltration varied highly among the in-house prepared scaffolds. JDS scaffold induced higher B cell infiltration than other scaffolds at 28 days. At 60 days and 90 days JDS induced only a little B cells consistent with TH1 lymphocyte polarization. So the results indicated that the humoral response to biological scaffold depends largely on the tissue of origin.

The ability of scaffolds to induce inflammatory response was evaluated by assessing the

mRNA expression of TNF-α and IL10. TNF-α is a well known inflammatory cytokine. IL-10 is an anti-inflammatory/immunosuppressive cytokine that can induce M2 alternative macrophage activation and inhibit the generation of classically activated M1 macrophages (Katakura *et al.*, 2004). CDS induced relatively less TNF-α expression and higher IL10 expression (Fig. 21 & 22). This observation is in consistent with the M2 macrophage polarization induced by CDS scaffold as discussed above. The overall results suggested that CDS is having relatively less inflammatory potential than other scaffolds.

CHAPTER-6

6. COMPARATIVE STUDY OF LOCAL IMMUNOGENICITY OF CHOLECYST DERIVED SCAFFOLD AND COMMERCIALLY AVAILABLE REFERENCE MATERIAL IMPLANTED IN RAT SUBCUTANEOUS TISSUE

6.1. INTRODUCTION

The observations presented in Chapter-5 largely suggested that cholecyst derived scaffold is relatively less immunogenic compared to scaffolds prepared from small intestine and urinary bladder. This prompted a comparative study on the nature of immunogenic reaction caused by CDS with a commercial product. The Chapter 6 is thus a comparative study of distribution/function of immunocompetent cells around cholecyst derived scaffold and commercially available reference material implanted in rat subcutaneous tissue.

6.2. MATERIALS AND METHODS

6.2.1. Subcutaneous implantation of scaffolds in rats

The CDS and CSIS were implanted subcutaneously into Sprague-Dawley rats as described in Section 4.2.1 After 3 days, 7 days, 14 days, 28 days, 60 days and 90 days two rats from each experimental group were killed in carbon dioxide chamber. The implant tissue was collected from each site. Samples from two sites were used for the study and other two were kept as back-up samples. Each sample was cut into two halves. Then, one of them was preserved in NBF for histomorphological evaluation. The other

half of the tissue sample for gene expression analysis was put in RNA*later* (Sigma) and stored in -20^{0}C freezer.

6.2.2. Histotechnology

The implant tissue was processed in automated tissue processor, embedded in paraffin wax and tissue sections were taken as described in Section 3.2.3.

6.2.3. Number and distribution of various cells in implant tissue

6.2.3.1. Toluidine blue staining for mast cells

The mast cells in the implant tissue were studied by staining with toluidine blue.

6.2.3.2. Immunohistochemistry

Immunohistochemistry was performed on histology sections to detect macrophage and lymphocyte subtypes participating in the local tissue reaction using antibodies raised against CD80, CD163, CD4, CD8 and CD79a (Table 11). Briefly tissue sections were deparaffinized and washed in distilled water and treated with antigen retrieval buffer (Tris/EDTA buffer; 10 mM Tris Base, 1 mM EDTA solution, pH 9.0 for CD4-immunostaining and Citrate buffer; 10mM Sodium citrate pH 6.0 for CD8-, CD80-, CD163-, and CD79a-immunostaining) for 20 minutes at 92°C and allowed to cool for 30 minutes. The endogenous peroxidase activity was inhibited by treating the slides with 5% H_2O_2 for 15 minutes and the non-specific reactivity of secondary antibody was blocked by using 10% goat serum (Santa Cruz Biotechnologies, Inc. USA) for 30 minutes. Later, the sections were washed with 10mM trisodium citrate solution pH 6.0 and treated with primary antibody for one hour at room temperature. The reaction was

then detected using Supersensitive polymeric-HRP^{TM} detection system (BioGenex Laboratories, USA) according to manufacturer's instructions. Finally, the sections were counter stained with Harris's haematoxylin (Electron Microscopy Sciences, Hatfield, PA).

6.2.3.3. Histomorphometry

Histomorphometry was performed on histology images (original magnification, 400x) captured with a DP71 camera loaded on to a BX51 microscope (Olympus Corporation, Japan) using ImagePro version 3DS6.1 software (Media Cybernetics, Silver Spring, MD). The microscope had an automated stage-movement system. The implant tissue was imaged, frame by frame, through automation to obtain a series of images that covered the entire implant tissue. The number of images varied with the area occupied by the tissue reaction. The number of immunostained cells in the reaction zone with appropriate phenotypic features was counted manually. Macrophages were identified as immunopositive mononuclear cells with large cytoplasm and pear shaped/oval nucleus. Lymphocytes were identified as immunopositive mononuclear cells with scanty cytoplasm and relatively higher nuclear to cytoplasmic ratio. Mast cells were identified as mononuclear cells with purple metachromatic granules in tissue sections stained with toluidine blue. The area occupied by the implant tissue and associated inflammatory tissue was also estimated. The number of cells per mm^2 was determined and the respective ratio was calculated.

6.2.3.3.1. M1/M2 macrophage polarization

Macrophages in the implant tissue were stained with CD80 M1 macrophage marker and CD163 M2 macrophage marker. The number of immunostained cells was counted as described in Section 6.2.3.3. The M1/M2 macrophage ratio was calculated for determining the M1/M2 macrophage polarization.

6.2.3.3.2. CD4/CD8 ratio

Implant tissue was stained with CD4 and CD8 T cell markers. The number of immunostained cells was counted using Image-Pro 3DS6.1 software as described in Section 6.2.3.3. The CD4/CD8 T cell ratio was calculated.

6.2.4. Gene expression studies

6.2.4.1. RNA isolation

Total RNA was isolated from tissue samples put in RNAlater using Trizol reagent (Invitrogen, USA) as per manufacturer's protocol. Briefly, implant tissue (100mg) in 1mL of Trizol reagent was grinded using tissue homogenizer (IKA Germany) and incubated for 5 min. It was then centrifuged at 12000g for 10 min in a refrigerated centrifuge (Eppendorf, Germany) and incubated. The supernatant was then pipetted out in to another centrifuge tube and in to it added 200µl of chloroform. The tubes were mixed thoroughly by vortexing for 15 seconds and incubated for 2-3 minutes at room temperature. It was centrifuged at 12000g for 15 minutes at4°C. The upper aqueous layer was pipette out in to another centrifuge tube containing 0.5 mL 75% alcohol, vortexed and incubated at room temperature for 10 min. It was then centrifuged at

12000g for 10 min at 4°C and the supernatant was discarded. The pellet was again washed with 75% alcohol and centrifuge at 7500g for 5 minutes. The supernatant was discarded and the RNA pellet obtained was allowed to air dry for 5-10 minutes. In to the RNA pellet 20µl of distilled water was added and allowed to dissolve completely by keeping 55°C water bath for 10min. The purity and concentration of the RNA was tested using NanoDrop ND-1000 spectrophotometer (NanoDrop, Wilmington, DE, USA). Only RNA with 260/280 nm absorption ratio more than 1.8 was used for cDNA synthesis.

6.2.4.2. cDNA synthesis

cDNA synthesis was carried out in Chromo4 system (Bio-Rad, Hercules, CA, USA) using SuperScript^{TM} III reverse transcriptase, Oligo $(dT)_{20}$ primer, 0.1M DTT, 40IU/mL Rnase out recombinant ribonuclease inhibitor and 5X First-strand buffer (Invitrogen Corporation, USA). 1µg of RNA was used for cDNA synthesis. The reagents were added into 200µl PCR tubes in two steps according to the Table 12. After the step-1 the mixture was heated at 65°C for 5 minutes and incubated on ice for 1 minute. Reagents of step-2 were added, mixed well and kept at 25°C for 5 minutes. The reverse transcription was carried out at 50°C for 1h followed by stopping the reaction at 75°C for 15 minutes. The cDNA thus synthesized were then stored at -20°C freezer.

6.2.4.3. Real time Polymerase chain reaction

The primer sets for glyceraldehyde 3-phosphate dehydrogenase (GAPDH) housekeeping gene, iNOS, Arginase-I, INFγ, IL4, TNF-α and IL10 were custom designed and

obtained from eurogentech Belgium (Table 13). Real time PCR was carried out in Chromo4 system (Bio-Rad, Hercules, CA, USA) using qPCR MasterMix Plus for SYBR® Green I No ROX which is a mixture of dNTPs (including dUTP), HotGoldStar DNA polymerase, $MgCl_2$ (5mM final concentration), Uracil-N-Glycosylase, SYBR® Green I and stabilizers (Eurogentec, Belgium). The reagents were added as per Table 14. The thermocycler was set with the following protocol. An initial HotGoldStar activation step for 10 min at 95°C, followed by 40 cycles of melting (95°C for 30 sec), annealing (60°C for 30 sec) and extension step (72°C for 1 minute). The quality of PCR reaction was confirmed by analyzing the melting curve of the PCR product from 60°C to 90°C. Gene expression was then analyzed by $2^{-\Delta\Delta Ct}$ method. Relative expression of M1/M2 genes ($RE_{(M1/M2)}$) and TH1/TH2 genes ($RE_{(TH1/TH2)}$) were calculated by the following formulae $RE_{(M1/M2)} = 2^{-\Delta Ct}$ (iNOS) / $2^{-\Delta Ct}$ (Arginase I) and $RE_{(TH2/TH1)} = 2^{-\Delta Ct}$ (INF-γ)/ $2^{-\Delta Ct}$ (IL4) respectively (Brown *et al.*, 2009).

6.2.5. Statistical analysis

One-way analysis of variance and Tukey-Kramer multiple comparisons tests were performed using GraphPad InStat software version 3.10 (GraphPad Software, Inc. CA, USA) to determine significant different between groups. Those differences with p value less than 0.05 was considered significant.

6.3. RESULTS

6.3.1. Number and distribution of various cells in implant tissue

6.3.1.1. Mast cells

Toluidine blue stained tissue sections were evaluated for mast cells in the tissue reaction zone. Mast cells were detected as mononuclear cells with metachromatic granules at all time points of the study, in histology sections, around CDS and CSIS reference material (Fig. 25). The quantitative data are presented in quantitative histomorphology Section below.

Figure 25: Light micrograph of toluidine blue stained tissue sections showing mast cells (thick arrows) in the reaction around the CDS (A) and CDSIS (B) at 14 days. Scale bar indicates 50μm. See Table 19 for quantitative data.

6.3.1.2. Immunohistochemistry

Immunohistochemistry for CD80-positive M1 macrophage, CD163-positive M2 macrophages, CD4-positive helper-T cells, CD8-positive cytotoxic-T cells and CD79a-positive B cells (Fig. 26) indicated significant infiltration of these cell types in to the reaction zone at all time points. Generally, the extent of infiltration of each cell type

progressed with time. The quantitative data are presented in quantitative histomorphology Section below.

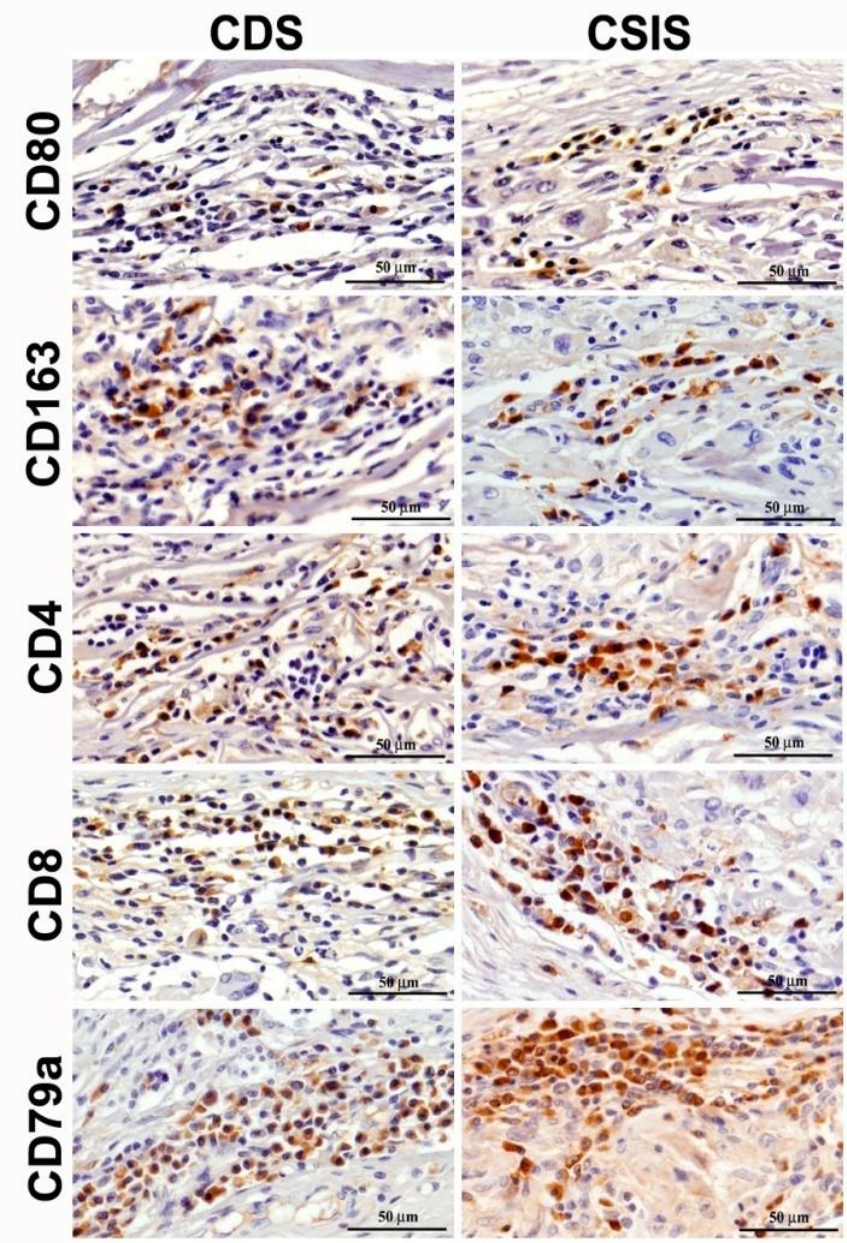

Figure 26: Immunohistochemical demonstration of CD80, CD163, CD4, CD8 and CD79a positive mononuclear cells in the tissue reaction at 28 days following implantation of the scaffolds in rat subcutaneous tissue. Brown color represents positive cells. Scale bar indicates 50µm. See Table 20, 21 and 22 for quantitative data.

6.3.1.3. Mast cell response

The number of mast cell infiltration in to the reaction zone is shown in Table 19. The overall reaction indicated that the mast cell numbers increased over time from 3 days to 90 days. There was reduction in mast cell reaction around CSIS and CDS by 28 days. Highest mast cell infiltration was observed at 60 days and 90 days. CDS induced significantly less mast cell infiltration at 3 days, 28 days and 90 days compared to CSIS reference material.

Table 19: The number and distribution of mast cells in the reaction zone obtained by image analysis

	CDS	CSIS
3 days	2.34±0.36 *	4.16±0.32
7 days	3.45±0.37	4.36±0.72
14 days	4.90±0.72	5.72±0.55
28 days	2.03±0.37 *	2.98±0.42
60 days	19.3±2.77	15.36±3.16
90 days	13.72±2.56 *	19.83±2.35

Values represent number of mast cells per mm^2 of implant tissue (mean±1SD, n=4). * Significant difference between CSIS and CDS

6.3.1.4. Macrophage response

There was progressive increase in infiltration of both M1 and M2 cells over time (Table. 20). Both scaffolds induced highest macrophage infiltration by 28days or 60days. Thereafter, the extent of macrophage infiltration decreased. CDS induced higher M1 and M2 macrophage infiltration compared to CSIS at 28 days.

Table 20: The number of CD80 and CD163 positive macrophages in the reaction zone obtained by image analysis.

		CDS	CSIS
CD80	3 days	1.58±0.11	1.32±0.14
	7 days	1.48±0.32	2.42±0.76
	14 days	13.18±2.26 *	5.06±1.32
	28 days	141.48±16.48 *	99.07±11.23
	60 days	317.19±52.28 *	193.87±30.58
	90 days	187.85±64	123.04±10.68
CD163	3 days	5.30±3.19	2.35±0.24
	7 days	3.66±1.08	7.74±3.11
	14 days	51.49±33.56	12.43±5.71
	28 days	260.94±11.57 *	151.2±27.34
	60 days	295.84±71.01	196.21±45.46
	90 days	174.45±79.72	107.97±18.9

Values represent number of mast cells per mm^2 of implant tissue (mean±1SD, n=4). * Significant difference between CSIS and CDS

6.3.1.4.1. M1/M2 macrophage polarization

The M1/M2 macrophage ratio (Fig. 27) indicated a predominance of M2 macrophages in CDS and CSIS up to 28 days of implantation. However, by 60 days there was equal distribution of M1 and M2 macrophages as indicated by M1/M2 ratio one.

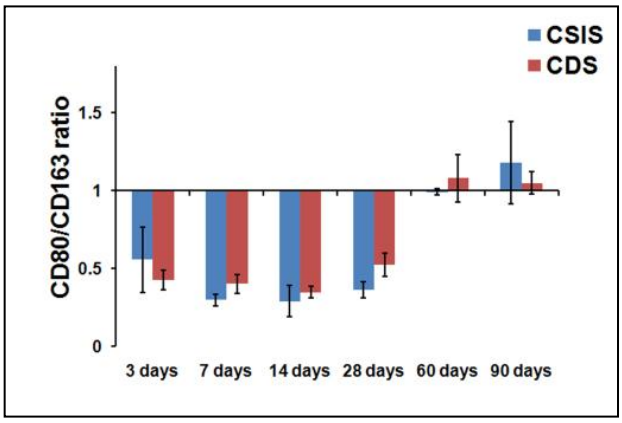

Figure 27: M1/M2 macrophage ratio as obtained by histomorphometry. Values represents mean±SD, n=4.

6.3.1.5. Lymphocyte response

There was progressive increase in the number of both CD4 and CD8 cells from 3 days to 28 days (Table. 21). The number of CD4 and CD8 cell infiltration were higher in CDS implanted tissues compared to CSIS implanted tissues. For both CDS and CSIS implants the CD4 and CD8 T cell infiltration decreased after 28 days. CDS induced higher T cell infiltration compared to CSIS at 60 days.

6.3.1.5.1. CD4/CD8 ratio

CDS induced CD4/CD8 ratio of one up to 28 days and CD4 cell predominance at 60 days and 90 days. CSIS implant induced CD8 cell predominance at 7 days and 14 days and equal distribution of CD4 and CD8 cells at 28 days. At 60 days and 90 days CSIS showed higher CD4 cell predominance compared to CDS (Figure 28).

Table 21: The number and distribution of CD4 and CD8 positive lymphocytes in the reaction zone obtained by image analysis.

		CDS	CSIS
CD4	3 days	2.95±1.30 *	5.77±0.63
	7 days	3.54±1.35	2.65±0.62
	14 days	42.35±17.36 *	11.03±5.11
	28 days	234.26±32.14	226.67±10.74
	60 days	259.14±17.22 *	156.55±23.79
	90 days	169.36±53.52	119.24±32.71
CD8	3 days	2.46±0.46	3.44±0.89
	7 days	5.94±1.46	3.85±0.62
	14 days	42.70±14.55 *	13.99±3.4
	28 days	283.21±31.67	242.36±29.12
	60 days	166.44±10.79 *	38.01±11.35
	90 days	118.3±31.86 *	49.02±7.48

Values represent number of mast cells per mm^2 of implant tissue (mean±1SD, n=4).

* Significant difference between CSIS and CDS

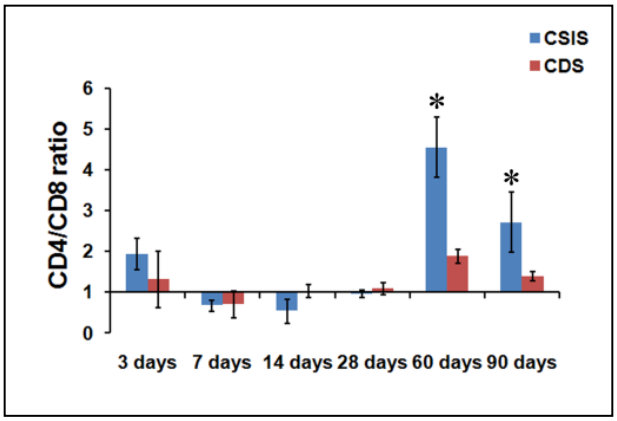

Figure 28: CD4/CD8 T-cell ratio as obtained by histomorphometry. Values represent mean±SD, n=4. * Significant difference between CDS and CSIS.

6.3.1.5.2. B cell response

B lymphocytes infiltration (Table 22) increased gradually with time and by 28 days there was significantly higher number of these cells in the tissue. The CDS induced lower B cell infiltration than CSIS at 60 days and 90 days.

Table 22: The number and distribution of CD79a positive B lymphocytes in the reaction zone obtained by image analysis.

	CDS	CSIS
3 days	1.51±0.43 *	4.37±0.59
7 days	2.7±0.56	2.21±0.94
14 days	40.1±21.8 *	9.4±3.65
28 days	237.4±46.68	246.13±17.5
60 days	53.6±12.5 *	189.1±15.4
90 days	48.4±15.76 *	156.5±22.2

Values represent number of B-lymphocytes per mm^2 of implant tissue (mean±1SD, n=4). * Significant difference between CSIS and CDS

6.3.2. Gene expression analysis

6.3.2.1. Inflammatory cytokine (TNF-α) expression

The gene expression of TNF-α was studied as representative of inflammatory cytokine (Figure 29). CSIS induced highest inflammatory cytokine expression at 28 days. CDS induced highest expression of TNF-α at 3 days and decreased thereafter.

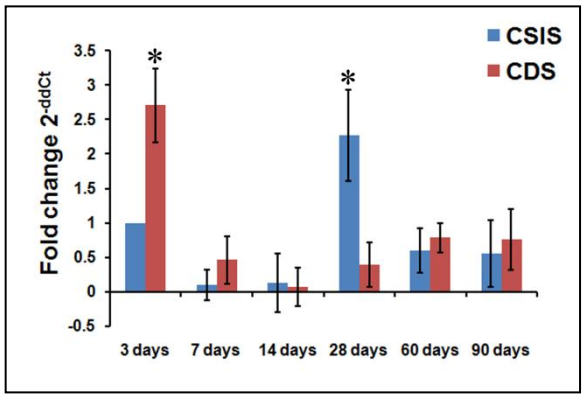

Figure 29: The TNF-α gene expression. Values represents mean±SD, n=4. * Significant difference between CSIS and CDS

6.3.2.2. Anti-inflammatory cytokine (IL10) expression

The gene expression of IL10 was studied as representative of ant-inflammatory cytokine (Fig. 30). CDS induced higher IL10 expression at 3 days and 7days compared to CSIS. Both CSIS and CDS induced highest expression of IL-10 at 28 days.

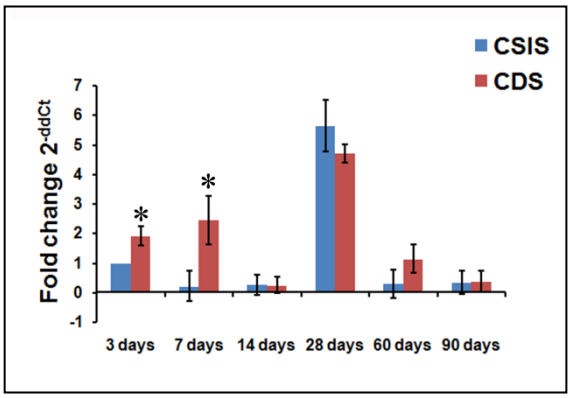

Figure 30: The IL-10 gene expression. Values represents mean±SD, n=4. * Significant difference between CSIS and CDS

6.3.2.3. M1/M2 macrophage functional polarization

The relative ratio of expression of M1 marker iNOS to that of M2 marker arginase-1 was used to study the M1/M2 macrophage functional polarization (Figure 31). A ratio less

than one indicate M2 polarization and ratio more than one indicate M1 polarization. Both the CDS and CSIS scaffolds induced M2 macrophage polarization at all time points of the study (ratio < 1), with higher M2 polarization for CDS than CSIS at 4th and 12th week after implantation. However, the CSIS appeared to have induced more M2 macrophage at the first week of implantation.

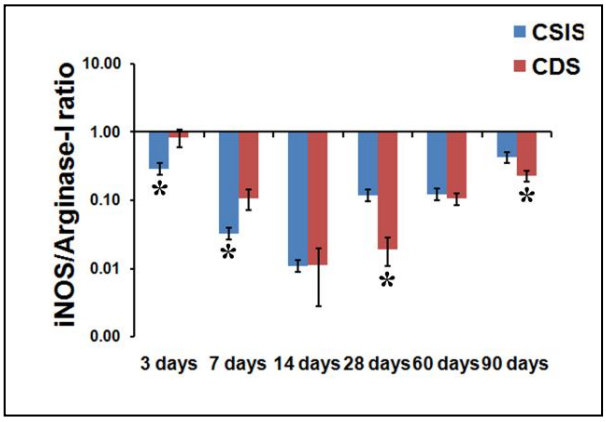

Figure 31: The M1/M2 macrophage functional polarization as obtained by real time RT-PCR. Values represents mean±SD, n=4. * Significant difference between CSIS and CDS.

6.3.2.4. TH1/TH2 lymphocyte functional polarization

The TH1/TH2 lymphocyte functional polarization was studied by real time RT-PRC. The relative ratio of expression of TH1 marker INF-γ to that of TH2 marker IL4 was used to study the TH1/TH2 lymphocyte functional polarization (Fig. 32). A ratio less than one indicate TH2 polarization and ratio more than one indicate TH1 polarization. The results showed that the CDS induced TH2 lymphocyte functional polarization all time points of the study. The reference material CSIS, induced TH2 macrophage polarization from 14 days onward.

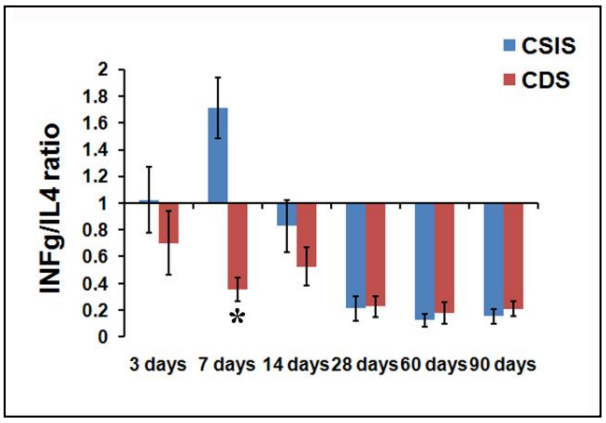

Figure 32: The TH1/TH2 lymphocyte functional polarization as obtained by real time RT-PCR. Values represents mean±SD, n=4. * Significant difference between CSIS and CDS.

6.4. DISCUSSION

The aim of this part of the study was to compare the immunogenic potential of CDS with a commercially available reference material used for regenerative medical applications. The reference material used was CSIS originally derived from porcine small intestinal submucosa. As discussed in Chapter 4, the biocompatibility evaluation as per ISO10993, Part-6 indicated that CDS was similar to the reference material CSIS, as indicated by the irritancy score at different time points (Table 10). However, biocompatibility evaluation as per ISO10993, Part-6 and similar protocols are designed for materials of non-biological origin such as polymers which are not necessarily immunogenic. However, xenogeneic grafts can induce inadvertent immunogenic reaction in man (Badylak and Gilbert, 2008). These, clinical complications of severe pain, inflammation and graft-versus-host disease associated with the use of intestine-derived scaffolds have been attributed to the immunogenicity of the graft material (Ho *et al.*, 2004, Kalota, 2004, Petter-Puchner, 2007, John *et al.*, 2008, Wang *et al.*, 2009). Therefore, it was considered desirable to study the safety of CDS in relation to immunogenic potential in comparison with an appropriate reference material. The reference scaffold selected here was a commercial product from similar source.

The CDS and reference material were implanted subcutaneously into Sprague-Dawley rats and different segments of the immune reaction like mast cell response, macrophage response, T-helper cell response, cytotoxic T-cell response, and B-cell response were studied. The inflammatory cytokine and anti-inflammatory cytokine expression were

also studied using molecular biology tools.

Mast cells are source of histamine and other inflammatory modulators responsible for acute/immediate hypersensitivity reactions (hypersensitivity type I) and they are implicated in biomaterial-induced tissue reaction (Tang *et al.*, 1998). In the present study, the induction of mast cell reaction by CDS was found significantly less than that following CSIS-grafting/implantation at 3 days, 28 days and 90 days (Fig. 25, Table 19). Soon after the implantation, at early time point (3 days) when compared to CSIS, the CDS attracted significantly fewer numbers of mast cells at the reaction zone (Table 19) indicating that it is less likely to induce acute hypersensitivity type I reaction.

Macrophage responses are usually classified either M1 or M2 types, which are essentially the simplified extremes of a continuum of phenotypes depending on their contributory role in inflammation. Whereas the M1 macrophages are pro-inflammatory cells participating in aggressive chronic inflammation, M2 macrophages are anti-inflammatory in nature that promotes constructive remodeling process (Mills *et al.*, 2000). It is also known that, in any immunopathological tissue reaction, both these phenotypes can be expected but the predominance of either one of these macrophage phenotypes determines the outcome of tissue reaction largely by regulating the cytokine milieu of the microenvironment (Stout *et al.*, 2005). It has been shown that ECM xenograft-scaffolds when implanted in animal models elicited M2 predominated macrophage response rather than M1 inflammatory cells in instances where constructive remodeling reaction happened at the implant site (Brown *et al.*, 2009).

Immunohistochemistry for macrophage subtypes M1 and M2 cells showed infiltration of both of these cells in the implant tissue (Fig. 26 and Table 20). Similar to the CSIS reference material the CDS also induced a desirable macrophage reaction predominated by the M2 phenotype at time points up to 28 days (Fig. 27). At 60 days and 90 days there was equal number of M1 and M2 macrophage infiltration indicating that there was no predominance for either M1 or M2 macrophages. This was again confirmed by real-time RT-PCR gene expression analysis using iNOS and arginase-1 expression, which are the biochemical markers for M1 and M2 macrophage functions. The ratio of gene expression of M1 and M2 genes also showed M2 macrophage polarization of CDS and CSIS implanted tissues at all time points of implantation (Fig. 31). So the results suggested that CDS scaffold induced M2 macrophage response similar to the CSIS reference material.

The T lymphocyte subpopulations studied were helper T cells and cytotoxic T cells (Fig. 26). Both of them increased in number with time from 3 days to 28 days and then decreased at 90 days, at the site of tissue healing reaction induced by both CDS and CSIS scaffolds (Table 21). It was evident that the materials caused T-lymphocyte infiltration as expected for any tissue-material interaction (Ohtani, 2013, Klinge *et al.*, 2014). However, it is believed that rather than actual numbers, the relative proportion of helper and cytotoxic cells (CD4/CD8 ratio) determines the outcome of the reaction (Amadori *et al.,* 1995, Hautz *et al.,* 2012, Li *et al.,* 2013). The normal value of CD4/CD8 ratio in rats may vary according to the tissue/organ (Jimenez *et al.*, 2001). Whereas equal numbers of CD4 and CD8 or slightly higher numbers of CD4 cells are

considered as a desirable feature, predominance of either of these cell types can contribute to pathology associated with transplant rejection (Amadori *et al.*, 1995, Hautz *et al.*, 2010). Considering that a few non helper T cells (e.g.; monocytes, dendritic cells) can be CD4-immuno reactive, manual counting of cells with phenotypic features of lymphocytes ensured identification of immunopositive lymphocytes. Both CDS and reference material induced CD4 cell predominance at 3 days. CSIS induced CD8 cell predominance at 7 days and 14 days. By 60 days and 90 days the ratio reached more than 1, indicating CD4 cell predominance and this was significantly higher for CSIS compared to CDS (Fig. 28).This observations made about CSIS cannot be considered a desirable reaction because higher CD4 predominance is also sometimes observed with graft rejection (Hautz *et al.*, 2010). However, it may be inferred that compared to CSIS the CDS is less likely to induce an undesirable cytotoxic reaction.

In addition to the study of T-cell sub-population by immunohistochemistry functional status of helper-T cells were studied by real-time RT-PCR. Helper-T cell activity may be TH1 or TH2 polarized (Abbas *et al.*, 1996). It has been shown that ECM scaffold implantation lead in to TH2 polarization and acceptance of the graft rather than rejection (Allman *et al.*, 2001). Hence TH2 polarization is desirable after the implantation. Here, the ratio of expression of TH1 and TH2-cytokines (Fig. 32) suggested that the CSIS caused a TH1 polarized reaction at 7 days but subsequently harmonized to the desirable TH2 polarized reaction. On the other hand, the CDS implanted tissue consistently had TH2 polarization at all time points indicating its capability to promote graft acceptance rather than rejection. Hence, the results suggested that CDS and CSIS have different

immunologic potential in the rat model.

An enhanced TH2 reaction has been viewed as a sign of prominent humoral immune response (Abbas *et al.*, 1996). In order to compare the ability of the CDS to activate humoral immunity with that of CSIS, the occurrence of B-cells in the reaction tissue was studied. Both materials induced B cell infiltration in to the reaction zone indicating their ability to induce humoral immune response. The number of B-cells steadily increased over time up to 28 days and then decreased significantly (Table 22). The number of B cell infiltration in to the CDS implanted tissue was significantly high at 14 days when compared to that induced by CSIS. At 60 days and 90 days CDS induced significantly less B cells compared to CSIS, indicating its lower potential to induce long term humoral immune response.

The inflammatory response induced by CDS was evaluated in comparison to CSIS reference material by assessing the mRNA expression of TNF-α and IL10 (Fig. 29 & 30). TNF-α is a well known inflammatory cytokine. IL-10 is an anti-inflammatory/immunosuppressive cytokine that can induce M2 alternative macrophage activation and inhibit the generation of classically activated M1 macrophages (Katakura *et al.*, 2004). TNF-α induced by CDS was significantly higher than that induced by CSIS at 3 days and decreased subsequently. AT 28 days CDS induced relatively less TNF-α expression. The CDS induced higher IL10 expression than that of CSIS at early time points and similar expression to that of CSIS thereafter. So the results suggested that CDS is having relatively less inflammatory potential than the reference scaffolds.

CHAPTER-7

7. SUMMARY AND CONCLUSIONS

In this study ECM scaffolds from three different porcine organs with lumen namely cholecyst, jejunum and urinary bladder were prepared by non-detergent/enzymatic method and evaluated their immunogenic potential through several *in vitro* and *in vivo* test procedures. First the scaffolds were characterized extensively for parameters related to immunogenic potential. Compared to the scaffolds derived from jejunum and urinary bladder cholecyst derived scaffold had least quantity of residual cellular components. This observation gave a broad indication that cholecyst derived scaffold may be less immunogenic.

Since the protein profile of biological scaffolds may have significant role in the host response following implantation *in vivo* the extractable proteins were identified by mass spectroscopy. The CDE had higher percentage of ECM proteins and lower percentage of cellular proteins compared to JDE and UDE. In spite of the presence of several proteins that aid wound healing and remodeling response a small fraction of proteins that take part in immune response were also present in all scaffolds. Cholecyst derived scaffold had few complement protein components which may raise concern about its complement activation potential. However, CDS scaffold had lowest complement activation potential when studied *in vitro*. This observation was supported by the identification of prolargin a protein inhibitor of complement pathway in CDE. The urinary bladder scaffold also showed presence of complement protein components and prolargin which is an inhibitor

of complement activation. However, it showed variable complement activation potential. JDE contained both MHC class I and MHC class II histocompatibility antigens which may cause inadvertent graft reactions upon implantation in animal models. The results of extractable protein profiling thus indicated the relatively less immunogenic potential of CDS as compared to JDS and UDS.

The study of IgG antibody response following subcutaneous implantation of scaffolds in rats showed the ability of scaffolds to induce IgG antibodies specific to scaffold proteins. So the identification of immunogenic proteins in CDS desired. Immunoproteomic approach employed identified 18 immunogenic proteins with most of the immunogenic proteins being cellular in origin. Although only a small repertoire of immunogenic proteins could be identified, the detection of non-Gal xenoantigen annexin-A2 as an immunogenic protein indicates the importance of detailed study on the role of non-antigen on the host response to biological scaffold implantation.

When the ability of scaffolds to mount an innate immune response was tested *in vitro*, the cholecyst derived scaffold induced significantly less reactive oxygen species and reactive nitrogen species in THP-1 macrophages *in vitro.* So the CDS had less potential to mount innate immune response.

The local tissue response studied after subcutaneous implantation of CDS in rats induced constructive tissue remodeling response as desired for a biological scaffold. The JDS induced relatively higher adverse tissue reactions like severe acute inflammation, relatively higher necrosis, higher fibrosis and fatty infiltration. The UDS scaffold also

induced persistence of acute inflammation, necrosis and chronic inflammation higher than that induced by CDS scaffold. When the biocompatibility of scaffolds was studied in comparison to a reference material CSIS all the scaffolds studied were found to be biocompatible. However, the JDS scaffolds showed biocompatibility scores indicative of a slightly irritant biomaterial.

The physiological saline extract of all scaffolds did not induce any significant adverse reaction in guinea pigs. The result suggested that all scaffolds studied have no potential to induce delayed type hyper sensitivity reaction in guinea pigs.

The above observations indicated the relatively less immunogenic potential of biological scaffold derived from porcine cholecyst. This prompted a detailed comparative study of the immunogenic potential of scaffold after subcutaneous implantation of CDS, JDS and UDS in rats.

Mast cell response immediately after implantation of scaffolds indicated reduced ability of CDS to induce immediate type-1 hypersensitivity reaction compared to JDS. The CDS induced higher M2 macrophage polarization and TH2 lymphocyte polarization than JDS and UDS scaffolds. The CDS induced a well balanced CD4/CD8 ratio overtime without any undesirable cytotoxic reaction. The gene expression study showed lower inflammatory gene TNF-α and higher anti-inflammatory gene IL10 expression in CDS implanted tissues. The results largely suggested that among the scaffolds prepared by non-detergent/enzymatic method CDS was the least immunogenic biomaterial.

The identification of CDS as a relatively less immunogenic scaffold prompted a comparative study of the immunogenic potential of CDS to that induced by a commercially available reference material CSIS. Early mast cell response after subcutaneous implantation of scaffolds indicated reduced ability of CDS to induce immediate type-1 hypersensitivity reaction compared to CSIS. The CDS induced similar M2 macrophage polarization profile as that of CSIS. However, there was difference in the TH2 lymphocyte polarization profile of CDS and CSIS. Unlike CSIS which showed CD8 cell predominance at early time points and CD4 predominance at later time points the CDS induced a well balanced CD4/CD8 ratio overtime without any undesirable cytotoxic reaction. B cell infiltration into the implant tissue suggested the relatively less potential of CDS to induce long term humoral immune response. The gene expression study showed lower inflammatory gene TNF-α and higher anti-inflammatory gene IL10 expression in CDS implanted tissues. Therefore, the CDS induced a differential immunological responsiveness compared to CSIS reference material.

7.1. Conclusion

The overall conclusion of the study was that, the porcine cholecyst derived scaffold prepared by a non-detergent/enzymatic method is a relatively less immunogenic xenograft when compared to jejunum and urinary bladder derived scaffolds. It may be a preferred scaffold for fabricating clinical products useful for regenerative medical applications.

7.2. Significance of the study

Since the immunogenicity of biological scaffolds can cause undesirable clinical complications up on treatment of human ailments, identification of scaffolds with lower immunogenic potential is important. This study showed that the porcine cholecyst derived scaffold prepared by a non-detergent/enzymatic method was a relatively less immunogenic xenograft when compared to jejunum and urinary bladder derived scaffolds. Hence, cholecyst derived scaffold may be used for regenerative medical applications where minimally immunogenic biomaterial is desired. The study also put forward several immunohistochemical, molecular techniques and proteomic investigations which may be used for evaluation of other biological scaffold materials indented for regenerative medical applications.

The study identified several immunogenic proteins in CDS including annexin-A2 which is a member of non-Gal xenoantigens and reported to be present in other biological scaffolds also. This observation points to the significance of non-Gal antigens in the host response to biological scaffold materials. Therefore removal of such xenoantigens should be tried during the preparation and processing of biological scaffold materials.

7.3. Limitations of the study

The protein composition of extracellular matrices studied was limited to only water soluble proteins extracted with tris-buffer alone. A detailed study using different extraction protocol coupled with protein identification tools may result in identification of more number of proteins in the ECM isolates. In this study local immunogenic

potential of scaffolds were tested after implantation of scaffolds in subcutaneous tissue of rats only. So, before using the CDS as a low immunogenic biomaterial for human applications animal implantation in other species and sites other than subcutis are essential.

7.4. Future perspectives

Future research in this topic includes the study of immunogenicity after long term (>90days) implantation of ECM scaffolds. There is scope for identification of more number of immunogenic proteins in cholecyst derived ECM. The identification of annexin-A2 a non-Gal xenoantigen as an immunogenic protein in cholecyst derived scaffold warrants a detailed study on the role of non-Gal antigens in host response to ECM scaffolds. Regenerative medical applications such as fabrication of hernia repair mesh, dura graft, urethral sling and anal fistula plug using cholecyst derived scaffold which is identified as the relatively less immunogenic biomaterial will also be a focus of future research.

8. REFRENCES

Abbas, AK, Murphy, KM, Sher, A (1996). Functional diversity of helper t lymphocytes. *Nature* 383**:** 787-793.

Agrawal, V, Tottey, S, Johnson, SA, Freund, JM, Siu, BF, Badylak, SF (2011). Recruitment of progenitor cells by an extracellular matrix cryptic peptide in a mouse model of digit amputation. *Tissue Engineering Part A* 17**:** 2435-2443.

Alberts, B, Johnson, A, Lewis, J, Raff, M, Roberts, K, Walter, P 2002. The extracellular matrix of animals. *Molecular biology of the cell.* 4 ed. New York: Garland Scienc.

Allman, AJ, McPherson, TB, Badylak, SF, Merrill, LC, Kallakury, B, Sheehan, C, Raeder, RH, Metzger, DW (2001). Xenogeneic extracellular matrix grafts elicit a th2-restricted immune response. *Transplantation* 71**:** 1631-1640.

Amadori, A, Zamarchi, R, De Silvestro, G, Forza, G, Cavatton, G, Danieli, GA, Clementi, M, Chieco-Bianchi, L (1995). Genetic control of the cd4/cd8 t-cell ratio in humans. *Nat Med* 1**:** 1279-1283.

Anderson, JM (2001). Biological responses to materials. *Annual Review of Materials Research* 31**:** 81-110.

Andree, B, Bar, A, Haverich, A, Hilfiker, A (2013). Small intestinal submucosa segments as matrix for tissue engineering: Review. *Tissue Engineering Part B-Reviews* 19**:** 279-291.

Anilkumar, TV, Vineetha, VP, Revi, D, Muhamed, J, Rajan, A (2014). Biomaterial properties of cholecyst-derived scaffold recovered by a non-detergent/enzymatic method. *J Biomed Mater Res B Appl Biomater* 102B**:** 1506-1516.

Ansaloni, L, Cambrini, P, Catena, F, Di Saverio, S, Gagliardi, S, Gazzotti, F, Hodde, JP, Metzger, DW, D'Alessandro, L, Pinna, AD (2007). Immune response to small intestinal submucosa (surgisis) implant in humans: Preliminary observations. *Journal of Investigative Surgery* 20**:** 237-241.

Armstrong, PB, Quigley, JP (1999). Alpha2-macroglobulin: An evolutionarily conserved arm of the innate immune system. *Dev Comp Immunol* 23**:** 375-390.

Azhim, A, Ono, T, Fukui, Y, Morimoto, Y, Furukawa, K, Ushida, T. Year. Preparation of decellularized meniscal scaffolds using sonication treatment for tissue engineering. *In:* Engineering in Medicine and Biology Society (EMBC), 2013 35th Annual International Conference of the IEEE, 3-7 July 2013. 6953-6956.

Badylak, SE, Gilbert, TW (2008). Immune response to biologic scaffold materials. *Seminars in Immunology* 20**:** 109-116.

Badylak, SF (2007). The extracellular matrix as a biologic scaffold material. *Biomaterials* 28**:** 3587-3593.

Badylak, SF, Freytes, DO, Gilbert, TW (2009). Extracellular matrix as a biological scaffold material: Structure and function. *Acta Biomaterialia* 5**:** 1-13.

Badylak, SF, Hoppo, T, Nieponice, A, Gilbert, TW, Davison, JM, Jobe, BA (2011). Esophageal preservation in five male patients after endoscopic inner-layer

circumferential resection in the setting of superficial cancer: A regenerative medicine approach with a biologic scaffold. *Tissue Engineering Part A* 17**:** 1643-1650.

Badylak, SF, Park, K, Peppas, N, McCabe, G, Yoder, M (2001). Marrow-derived cells populate scaffolds composed of xenogeneic extracellular matrix. *Experimental Hematology* 29**:** 1310-1318.

Badylak, SF, Valentin, JE, Ravindra, AK, McCabe, GP, Stewart-Akers, AM (2008). Macrophage phenotype as a determinant of biologic scaffold remodeling. *Tissue Engineering Part A* 14**:** 1835-1842.

Bancroft, JD, Gamble, M (2008). *Theory and practice of histological techniques,* Philadelphia, PA, Churchill Livingstone/Elsevier.

Baranowsky, A, Mokkapati, S, Bechtel, M, Krügel, J, Miosge, N, Wickenhauser, C, Smyth, N, Nischt, R (2010). Impaired wound healing in mice lacking the basement membrane protein nidogen 1. *Matrix Biology* 29**:** 15-21.

Bastian, F, Stelzmuller, ME, Kratochwill, K, Kasimir, MT, Simon, P, Weigel, G (2008). Igg deposition and activation of the classical complement pathway involvement in the activation of human granulocytes by decellularized porcine heart valve tissue. *Biomaterials* 29**:** 1824-1832.

Bejjani, GK, Zabramski, J (2007). Safety and efficacy of the porcine small intestinal submucosa dural substitute: Results of a prospective multicenter study and literature review. *Journal of Neurosurgery* 106**:** 1028-1033.

Bengtsson, E, Mörgelin, M, Sasaki, T, Timpl, R, Heinegård, D, Aspberg, A (2002). The leucine-rich repeat protein prelp binds perlecan and collagens and may function as a basement membrane anchor. *Journal of Biological Chemistry* 277**:** 15061-15068.

Bharadwaj, A, Bydoun, M, Holloway, R, Waisman, D (2013). Annexin a2 heterotetramer: Structure and function. *Int J Mol Sci* 14**:** 6259-6305.

Bogdan, C, Röllinghoff, M, Diefenbach, A (2000). Reactive oxygen and reactive nitrogen intermediates in innate and specific immunity. *Current Opinion in Immunology* 12**:** 64-76.

Boot-Handford, RP, Tuckwell, DS (2003). Fibrillar collagen: The key to vertebrate evolution? A tale of molecular incest. *Bioessays* 25**:** 142-151.

Brody, S, McMahon, J, Yao, L, O'Brien, M, Dockery, P, Pandit, A (2007). The effect of cholecyst-derived extracellular matrix on the phenotypic behaviour of valvular endothelial and valvular interstitial cells. *Biomaterials* 28**:** 1461-1469.

Brown, BN, Valentin, JE, Stewart-Akers, AM, McCabe, GP, Badylak, SF (2009). Macrophage phenotype and remodeling outcomes in response to biologic scaffolds with and without a cellular component. *Biomaterials* 30**:** 1482-1491.

Burugapalli, K, Chan, JCY, Kelly, JL, Pandit, A (2008). Buttressing staples with cholecyst-derived extracellular matrix (cem) reinforces staple lines in an ex vivo peristaltic inflation model. *Obesity Surgery* 18**:** 1418-1423.

Burugapalli, K, Chan, JCY, Kelly, JL, Pandit, AS (2014). Efficacy of crosslinking on tailoring in vivo biodegradability of fibro-porous decellularized extracellular

matrix and restoration of native tissue structure: A quantitative study using stereology methods. *Macromolecular Bioscience* 14**:** 244-256.

Burugapalli, K, Pandit, A (2007). Characterization of tissue response and in vivo degradation of cholecyst-derived extracellular matrix. *Biomacromolecules* 8**:** 3439-3451.

Burugapalli, K, Thapasimuttu, A, Chan, JCY, Yao, L, Brody, S, Kelly, JL, Pandit, A (2007). Scaffold with a natural mesh-like architecture: Isolation, structural, and in vitro characterization. *Biomacromolecules* 8**:** 928-936.

Byrne, GW, Stalboerger, PG, Davila, E, Heppelmann, CJ, Gazi, MH, McGregor, HC, LaBreche, PT, Davies, WR, Rao, VP, Oi, K, Tazelaar, HD, Logan, JS, McGregor, CG (2008). Proteomic identification of non-gal antibody targets after pig-to-primate cardiac xenotransplantation. *Xenotransplantation* 15**:** 268-276.

Byrne, GW, Stalboerger, PG, Du, Z, Davis, TR, McGregor, CG (2011). Identification of new carbohydrate and membrane protein antigens in cardiac xenotransplantation. *Transplantation* 91**:** 287-292.

Caliari, SR, Ramirez, MA, Harley, BAC (2011). The development of collagen-gag scaffold-membrane composites for tendon tissue engineering. *Biomaterials* 32**:** 8990-8998.

Cao, Z, Said, N, Amin, S, Wu, HK, Bruce, A, Garate, M, Hsu, DK, Kuwabara, I, Liu, F-T, Panjwani, N (2002). Galectins-3 and -7, but not galectin-1, play a role in re-epithelialization of wounds. *Journal of Biological Chemistry* 277**:** 42299-42305.

Catena, F, Ansaloni, L, D'Alessandro, L, Pinna, A (2007). Adverse effects of porcine small intestine submucosa (sis) implants in experimental ventral hernia repair. *Surgical Endoscopy and Other Interventional Techniques* 21**:** 690-690.

Cesarman-Maus, G, Rios-Luna, NP, Deora, AB, Huang, BH, Villa, R, Cravioto, MD, Alarcon-Segovia, D, Sanchez-Guerrero, J, Hajjar, KA (2006). Autoantibodies against the fibrinolytic receptor, annexin 2, in antiphospholipid syndrome. *Blood* 107**:** 4375-4382.

Chan, BP, Leong, KW (2008). Scaffolding in tissue engineering: General approaches and tissue-specific considerations. *European Spine Journal* 17**:** S467-S479.

Chan, JCY, Burugapalli, K, Naik, H, Kelly, JL, Pandit, A (2008). Amine functionalization of cholecyst-derived extracellular matrix with generation 1 pamam dendrimer. *Biomacromolecules* 9**:** 528-536.

Christ, GJ, Saul, JM, Furth, ME, Andersson, K-E (2013). The pharmacology of regenerative medicine. *Pharmacological Reviews* 65**:** 1091-1133.

Cintron, JR, Abcarian, H, Chaudhry, V, Singer, M, Hunt, S, Birnbaum, E, Mutch, MG, Fleshman, J (2013). Treatment of fistula-in-ano using a porcine small intestinal submucosa anal fistula plug. *Techniques in Coloproctology* 17**:** 187-191.

Coburn, JC, Brody, S, Billiar, KL, Pandit, A (2007). Biaxial mechanical evaluation of cholecyst-derived extracellular matrix: A weakly anisotropic potential tissue engineered biomaterial. *Journal of Biomedical Materials Research Part A* 81A**:** 250-256.

Cockrell, E, Espinola, RG, McCrae, KR (2008). Annexin a2: Biology and relevance to the antiphospholipid syndrome. *Lupus* 17**:** 943-951.

Cox, TR, Erler, JT (2011). Remodeling and homeostasis of the extracellular matrix: Implications for fibrotic diseases and cancer. *Dis Model Mech* 4**:** 165-178.

Crapo, PM, Gilbert, TW, Badylak, SF (2011). An overview of tissue and whole organ decellularization processes. *Biomaterials* 32**:** 3233-3243.

Daly, KA, Liu, S, Agrawal, V, Brown, BN, Huber, A, Johnson, SA, Reing, J, Sicari, B, Wolf, M, Zhang, XR, Badylak, SF (2012). The host response to endotoxin-contaminated dermal matrix. *Tissue Engineering Part A* 18**:** 1293-1303.

Daly, KA, Stewart-Akers, AM, Hara, H, Ezzelarab, M, Long, C, Cordero, K, Johnson, SA, Ayares, D, Cooper, DK, Badylak, SF (2009). Effect of the alphagal epitope on the response to small intestinal submucosa extracellular matrix in a nonhuman primate model. *Tissue Eng Part A* 15**:** 3877-3888.

Deeken, CR, White, AK, Bachman, SL, Ramshaw, BJ, Cleveland, DS, Loy, TS, Grant, SA (2011). Method of preparing a decellularized porcine tendon using tributyl phosphate. *Journal of Biomedical Materials Research Part B-Applied Biomaterials* 96B**:** 199-206.

Dhandayuthapani, B, Yoshida, Y, Maekawa, T, Kumar, DS (2011). Polymeric scaffolds in tissue engineering application: A review. *International Journal of Polymer Science*.

Ding, J-X, Chen, X-J, Zhang, X-y, Zhang, Y, Hua, K-Q (2014). Acellular porcine small intestinal submucosa graft for cervicovaginal reconstruction in eight patients with malformation of the uterine cervix. *Human Reproduction* 29**:** 677-682.

Donato, R (2003). Intracellular and extracellular roles of s100 proteins. *Microscopy Research and Technique* 60**:** 540-551.

Feinberg, AW (2012). Engineered tissue grafts: Opportunities and challenges in regenerative medicine. *Wiley Interdisciplinary Reviews: Systems Biology and Medicine* 4**:** 207-220.

Feng, G, Xu, XC, Youssef, EM, Lotan, R (2001). Diminished expression of s100a2, a putative tumor suppressor, at early stage of human lung carcinogenesis. *Cancer Research* 61**:** 7999-8004.

Galili, U (2005). The [alpha]-gal epitope and the anti-gal antibody in xenotransplantation and in cancer immunotherapy. *Immunol Cell Biol* 83**:** 674-686.

Galili, U, Shohet, SB, Kobrin, E, Stults, CL, Macher, BA (1988). Man, apes, and old world monkeys differ from other mammals in the expression of alpha-galactosyl epitopes on nucleated cells. *Journal of Biological Chemistry* 263**:** 17755-17762.

Gemmell, CH, Black, JP, Yeo, EL, Sefton, MV (1996). Material-induced up-regulation of leukocyte cd11b during whole blood contact: Material differences and a role for complement. *J Biomed Mater Res* 32**:** 29-35.

Gilbert, TW, Freund, JM, Badylak, SF (2009). Quantification of DNA in biologic scaffold materials. *Journal of Surgical Research* 152**:** 135-139.

Gilbert, TW, Sellaro, TL, Badylak, SF (2006). Decellularization of tissues and organs. *Biomaterials* 27**:** 3675-3683.

Gilbert, TW, Stewart-Akers, AM, Badylak, SF (2007). A quantitative method for evaluating the degradation of biologic scaffold materials. *Biomaterials* 28**:** 147-150.

Gorbet, MB, Sefton, MV (2005). Endotoxin: The uninvited guest. *Biomaterials* 26**:** 6811-6817.

Gordon, S, Taylor, PR (2005). Monocyte and macrophage heterogeneity. *Nature Reviews Immunology* 5**:** 953-964.

Grayson, WL, Fröhlich, M, Yeager, K, Bhumiratana, S, Chan, ME, Cannizzaro, C, Wan, LQ, Liu, XS, Guo, XE, Vunjak-Novakovic, G (2010). Engineering anatomically shaped human bone grafts. *Proceedings of the National Academy of Sciences* 107**:** 3299-3304.

Greenwood, HL, Thorsteinsdottir, H, Perry, G, Renihan, J, Singer, P, Daar, A (2006). Regenerative medicine: New opportunities for developing countries. *International Journal of Biotechnology* 8**:** 60-77.

Griffiths, LG, Choe, LH, Reardon, KF, Dow, SW, Christopher Orton, E (2008). Immunoproteomic identification of bovine pericardium xenoantigens. *Biomaterials* 29**:** 3514-3520.

Happonen, KE, Fürst, CM, Saxne, T, Heinegård, D, Blom, AM (2012). Prelp protein inhibits the formation of the complement membrane attack complex. *Journal of Biological Chemistry* 287**:** 8092-8100.

Hautz, T, Zelger, B, Brandacher, G, Mueller, H, Grahammer, J, Lee, A, Cavadas, P, Margreiter, R, Pratschke, J, Schneeberger, S (2012). Histopathologic characterization of mild rejection (grade i) in skin biopsies of human hand allografts. *Transpl Int* 25**:** 56-63.

Hautz, T, Zelger, B, Grahammer, J, Krapf, C, Amberger, A, Brandacher, G, Landin, L, Muller, H, Schon, MP, Cavadas, P, Lee, AWP, Pratschke, J, Margreiter, R, Schneeberger, S (2010). Molecular markers and targeted therapy of skin rejection in composite tissue allotransplantation. *American Journal of Transplantation* 10**:** 1200-1209.

Higgins, DM, Basaraba, RJ, Hohnbaum, AC, Lee, EJ, Grainger, DW, Gonzalez-Juarrero, M (2009). Localized immunosuppressive environment in the foreign body response to implanted biomaterials. *Am J Pathol* 175**:** 161-170.

Ho, KLV, Witte, MN, Bird, ET (2004). 8-ply small intestinal submucosa tension-free sling: Spectrum of postoperative inflammation. *Journal of Urology* 171**:** 268-271.

Honma, T, Hamasaki, T (1996). Ultrastructure of multinucleated giant cell apoptosis in foreign-body granuloma. *Virchows Arch* 428**:** 165-76.

Hynes, RO (2012). The evolution of metazoan extracellular matrix. *The Journal of Cell Biology* 196**:** 671-679.

Hynes, RO, Naba, A (2012). Overview of the matrisome—an inventory of extracellular matrix constituents and functions. *Cold Spring Harbor Perspectives in Biology* 4.

Iannotti, JP, Codsi, MJ, Kwon, YW, Derwin, K, Ciccone, J, Brems, JJ (2006). Porcine small intestine submucosa augmentation of surgical repair of chronic two-tendon rotator cuff tears. *The Journal of Bone & Joint Surgery* 88**:** 1238-1244.

ISO:10993-6 (2007). Biological evaluation of medical devices-part 6: Tests for local effects after implantation. *International Organization for Standardization ISO, Geneva, Switzerland*.

ISO:10993-6 (2010 (E)). Biological evaluation of medical devices-part 10: Test for local irritation and skin sensitization, clause 7.5: Guinea pig maximization test (gpmt). *International Organization for standardization, Geneva, Switzerland.*

ISO:10993-10. (2010(E)). Biological evaluation of medical devices part l0: Test for irritation and skin sensitization clause 7.5: Guinea pig maximization tes. *International Organization for standardization, Geneva, Switzerland.*

Järveläinen, H, Puolakkainen, P, Pakkanen, S, Brown, EL, Höök, M, Iozzo, RV, Sage, EH, Wight, TN (2006). A role for decorin in cutaneous wound healing and angiogenesis. *Wound Repair and Regeneration* 14**:** 443-452.

Jimenez, E, Vicente, A, Sacedon, R, Munoz, JJ, Weinmaster, G, Zapata, AG, Varas, A (2001). Distinct mechanisms contribute to generate and change the cd4: Cd8 cell ratio during thymus development: A role for the notch ligand, jagged1. *Journal of Immunology* 166**:** 5898-5908.

John, TT, Aggarwal, N, Singla, AK, Santucci, RA (2008). Intense inflammatory reaction with porcine small intestine submucosa pubovaginal sling or tape for stress urinary incontinence. *Urology* 72**:** 1036-1039.

Joo, JH, Kim, JW, Lee, Y, Yoon, SY, Kim, JH, Paik, S-G, Choe, IS (2003). Involvement of nf-κb in the regulation of s100a6 gene expression in human hepatoblastoma cell line hepg2. *Biochemical and Biophysical Research Communications* 307**:** 274-280.

Kajbafzadeh, A-M, Sabetkish, S, Heidari, R, Ebadi, M (2014). Tissue-engineered cholecyst-derived extracellular matrix: A biomaterial for in vivo autologous bladder muscular wall regeneration. *Pediatric Surgery International* 30**:** 371-380.

Kalota, SJ (2004). Small intestinal submucosa tension-free sling: Postoperative inflammatory reactions and additional data. *Journal of Urology* 172**:** 1349-1350.

Kasimir, MT, Rieder, E, Seebacher, G, Nigisch, A, Dekan, B, Wolner, E, Weigel, G, Simon, P (2006). Decellularization does not eliminate thrombogenicity and inflammatory stimulation in tissue-engineered porcine heart valves. *J Heart Valve Dis* 15**:** 278-86; discussion 286.

Katakura, T, Miyazaki, M, Kobayashi, M, Herndon, DN, Suzuki, F (2004). Ccl17 and il-10 as effectors that enable alternatively activated macrophages to inhibit the generation of classically activated macrophages. *Journal of Immunology* 172**:** 1407-1413.

Keane, TJ, Londono, R, Turner, NJ, Badylak, SF (2012). Consequences of ineffective decellularization of biologic scaffolds on the host response. *Biomaterials* 33**:** 1771-1781.

Kehoe, S, Zhang, XF, Boyd, D (2012). Fda approved guidance conduits and wraps for peripheral nerve injury: A review of materials and efficacy. *Injury* 43**:** 553-572.

Kheir, E, Stapleton, T, Shaw, D, Jin, ZM, Fisher, J, Ingham, E (2011). Development and characterization of an acellular porcine cartilage bone matrix for use in tissue engineering. *Journal of Biomedical Materials Research Part A* 99A**:** 283-294.

Kim, HJ, Kim, PK, Bae, SM, Son, HN, Thoudam, DS, Kim, JE, Lee, BH, Park, RW, Kim, IS (2009). Transforming growth factor-β–induced protein (tgfbip/β ig-h3) activates platelets and promotes thrombogenesis. *Blood* 114**:** 5206-5215.

Klinge, U, Dietz, U, Fet, N, Klosterhalfen, B (2014). Characterisation of the cellular infiltrate in the foreign body granuloma of textile meshes with its impact on collagen deposition. *Hernia* 18**:** 571-578.

Konakci, KZ, Bohle, B, Blumer, R, Hoetzenecker, W, Roth, G, Moser, B, Boltz-Nitulescu, G, Gorlitzer, M, Klepetko, W, Wolner, E, Ankersmit, HJ (2005). Alpha-gal on bioprostheses: Xenograft immune response in cardiac surgery. *European Journal of Clinical Investigation* 35**:** 17-23.

Kosciuczuk, EM, Lisowski, P, Jarczak, J, Strzalkowska, N, Jozwik, A, Horbanczuk, J, Krzyzewski, J, Zwierzchowski, L, Bagnicka, E (2012). Cathelicidins: Family of antimicrobial peptides. A review. *Molecular Biology Reports* 39**:** 10957-10970.

Li, RD, Sun, Z, Dong, JY, Yin, H, Guo, WY, Fu, ZR, Wang, ZX (2013). A quantitative assessment model of t-cell immune function for predicting risks of infection and rejection during the early stage after liver transplantation. *Clinical Transplantation* 27**:** 666-672.

LifeCell (2014). Health care professionals. [online]. *Available: http://www.lifecell.com/health-care-professionals* [Accessed 11 September 2014].

Luo, JC, Chen, W, Chen, XH, Qin, TW, Huang, YC, Xie, HQ, Li, XQ, Qian, ZY, Yang, ZM (2011). A multi-step method for preparation of porcine small intestinal submucosa (sis). *Biomaterials* 32**:** 706-713.

Lynn, AK, Yannas, IV, Bonfield, W (2004). Antigenicity and immunogenicity of collagen. *Journal of Biomedical Materials Research Part B: Applied Biomaterials* 71B**:** 343-354.

Mantovani, A, Sica, A, Sozzani, S, Allavena, P, Vecchi, A, Locati, M (2004). The chemokine system in diverse forms of macrophage activation and polarization. *Trends in Immunology* 25**:** 677-686.

Marçal, H, Ahmed, T, Badylak, SF, Tottey, S, Foster, LJR (2012). A comprehensive protein expression profile of extracellular matrix biomaterial derived from porcine urinary bladder. *Regenerative Medicine* 7**:** 159-166.

McDonald, JF, Nelsestuen, GL (1997). Potent inhibition of terminal complement assembly by clusterin: Characterization of its impact on c9 polymerization†. *Biochemistry* 36**:** 7464-7473.

McGregor, CGA, Byrne, GW (2013). Methods and materials for reducing cardiac xenograft rejection. *US patent: US 2013/0111614 A1*.

McPherson, TB, Liang, H, Record, RD, Badylak, SF (2000). Galalpha(1,3)gal epitope in porcine small intestinal submucosa. *Tissue Eng* 6**:** 233-239.

Mills, CD, Kincaid, K, Alt, JM, Heilman, MJ, Hill, AM (2000). M-1/m-2 macrophages and the th1/th2 paradigm. *Journal of Immunology* 164**:** 6166-6173.

Mostow, EN, Haraway, GD, Dalsing, M, Hodde, JP, King, D (2005). Effectiveness of an extracellular matrix graft (oasis wound matrix) in the treatment of chronic leg ulcers: A randomized clinical trial. *Journal of Vascular Surgery* 41**:** 837-843.

Murray, AG, Khodadoust, MM, Pober, JS, Bothwell, ALM (1994). Porcine aortic endothelial-cells activate human t-cells - direct presentation of mhc antigens and costimulation by ligands for human cd2 and cd28. *Immunity* 1**:** 57-63.

Naziruddin, B, Durriya, S, Phelan, D, Duffy, BF, Olack, B, Smith, D, Howard, T, Mohanakumar, T (1998). Hla antibodies present in the sera of sensitized patients awaiting renal transplant are also reactive to swine leukocyte antigens. *Transplantation* 66**:** 1074-1080.

NCBI (2013). Sus scrofa database [online]. *Available: ftp://ftp.ncbi.nlm.nih.gov/genomes/Sus_scrofa/protein/* [Accessed 12 September 2013].

Nilsson, B, Ekdahl, KN, Mollnes, TE, Lambris, JD (2007). The role of complement in biomaterial-induced inflammation. *Mol Immunol* 44**:** 82-94.

Nischt, R, Schmidt, C, Mirancea, N, Baranowsky, A, Mokkapati, S, Smyth, N, Woenne, EC, Stark, H-J, Boukamp, P, Breitkreutz, D (2006). Lack of nidogen-1 and -2 prevents basement membrane assembly in skin-organotypic coculture. *J Invest Dermatol* 127**:** 545-554.

Nonaka, PN, Campillo, N, Uriarte, JJ, Garreta, E, Melo, E, de Oliveira, LVF, Navajas, D, Farre, R (2014). Effects of freezing/thawing on the mechanical properties of decellularized lungs. *Journal of Biomedical Materials Research Part A* 102**:** 413-419.

O'Brien, FJ (2011). Biomaterials & scaffolds for tissue engineering. *Materials Today* 14**:** 88-95.

Ohtani, H (2013). Granuloma cells in chronic inflammation express cd205 (dec205) antigen and harbor proliferating t lymphocytes: Similarity to antigen-presenting cells. *Pathology International* 63**:** 85-93.

Olack, B, Manna, P, Jaramillo, A, Steward, N, Swanson, C, Kaesberg, D, Poindexter, N, Howard, T, Mohanakumar, T (2000). Indirect recognition of porcine swine leukocyte ag class i molecules expressed on islets by human cd4+ t lymphocytes. *The Journal of Immunology* 165**:** 1294-1299.

Petter-Puchner, A (2007). Adverse effects of porcine small intestine submucosa implants in experimental ventral hernia repair. *Surgical Endoscopy and Other Interventional Techniques* 21**:** 830-831.

Petter-Puchner, A, Fortelny, R (2010). Use of porcine small intestine submucosa as a prosthetic material for laparoscopic hernia repair in infected and potentially contaminated fields: Long-term follow up assessment; surg endosc (2008) 22: 1941–1946. *Surgical Endoscopy* 24**:** 230-231.

Petter-Puchner, AH, Fortelny, RH, Mittermayr, R, Walder, N, Ohlinger, W, Redl, H (2006). Adverse effects of porcine small intestine submucosa implants in experimental ventral hernia repair. *Surgical Endoscopy and Other Interventional Techniques* 20**:** 942-946.

Raeder, RH, Badylak, SF, Sheehan, C, Kallakury, B, Metzger, DW (2002). Natural anti-galactose α1,3 galactose antibodies delay, but do not prevent the acceptance of extracellular matrix xenografts. *Transplant Immunology* 10**:** 15-24.

Reing, JE, Brown, BN, Daly, KA, Freund, JM, Gilbert, TW, Hsiong, SX, Huber, A, Kullas, KE, Tottey, S, Wolf, MT, Badylak, SF (2010). The effects of processing methods upon mechanical and biologic properties of porcine dermal extracellular matrix scaffolds. *Biomaterials* 31**:** 8626-8633.

Revi, D, Vineetha, VP, Muhamed, J, Rajan, A, Anilkumar, TV (2013). Porcine cholecyst–derived scaffold promotes full-thickness wound healing in rabbit. *Journal of Tissue Engineering* 4.

Rho, KS, Jeong, L, Lee, G, Seo, BM, Park, YJ, Hong, SD, Roh, S, Cho, JJ, Park, WH, Min, BM (2006). Electrospinning of collagen nanofibers: Effects on the behavior of normal human keratinocytes and early-stage wound healing. *Biomaterials* 27**:** 1452-61.

Rieder, E, Nigisch, A, Dekan, B, Kasimir, MT, Muhlbacher, F, Wolner, E, Simon, P, Weigel, G (2006). Granulocyte-based immune response against decellularized or glutaraldehyde cross-linked vascular tissue. *Biomaterials* 27**:** 5634-5642.

Saika, S, Shiraishi, A, Saika, S, Liu, C-Y, Funderburgh, JL, Kao, CW-C, Converse, RL, Kao, WW-Y (2000). Role of lumican in the corneal epithelium during wound healing. *Journal of Biological Chemistry* 275**:** 2607-2612.

Sakai, T, Balasubramanian, K, Maiti, S, Halder, JB, Schroit, AJ (2007). Plasmin-cleaved β-2-glycoprotein 1 is an inhibitor of angiogenesis. *The American Journal of Pathology* 171**:** 1659-1669.

Schmidt, CE, Baier, JM (2000). Acellular vascular tissues: Natural biomaterials for tissue repair and tissue engineering. *Biomaterials* 21**:** 2215-2231.

Sinno, H, Malholtra, M, Lutfy, J, Jardin, B, Winocour, S, Brimo, F, Beckman, L, Watters, K, Philip, A, Williams, B, Prakash, S (2013). Topical application of complement c3 in collagen formulation increases early wound healing. *Journal of Dermatological Treatment* 24**:** 141-147.

Siracusano, S, Ciciliato, S, Lampropoulou, N, Cucchi, A, Visalli, F, Talamini, R (2011). Porcine small intestinal submucosa implant in pubovaginal sling procedure on 48 consecutive patients: Long-term results. *European Journal of Obstetrics & Gynecology and Reproductive Biology* 158**:** 350-353.

Song, J, Hornsby, P, Stanley, M, AbdelFattah, KR, Wolf, SE (2014). Porcine urinary bladder extracellular matrix activates skeletal myogenesis in mouse muscle cryoinjury. *journal of Regenerative Medicine and Tissue Engineering* 3.

Stone, KR, Ayala, G, Goldstein, J, Hurst, R, Walgenbach, A, Galili, U (1998). Porcine cartilage transplants in the cynomolgus monkey. Iii. Transplantation of alpha-galactosidase-treated porcine cartilage. *Transplantation* 65**:** 1577-1583.

Stone, KR, Walgenbach, AW, Turek, TJ, Somers, DL, Wicomb, W, Galili, U (2007). Anterior cruciate ligament reconstruction with a porcine xenograft: A serologic, histologic, and biomechanical study in primates. *Arthroscopy: The Journal of Arthroscopic & Related Surgery* 23**:** 411-419.

Stout, RD, Jiang, CC, Matta, B, Tietzel, I, Watkins, SK, Suttles, J (2005). Macrophages sequentially change their functional phenotype in response to changes in microenvironmental influences. *Journal of Immunology* 175**:** 342-349.

Tang, L, Jennings, TA, Eaton, JW (1998). Mast cells mediate acute inflammatory responses to implanted biomaterials. *Proc Natl Acad Sci U S A* 95**:** 8841-8846.

Tate, CC, Shear, DA, Tate, MC, Archer, DR, Stein, DG, LaPlaca, MC (2009). Laminin and fibronectin scaffolds enhance neural stem cell transplantation into the injured brain. *Journal of Tissue Engineering and Regenerative Medicine* 3**:** 208-217.

The-UniProt-Consortium (2014). Activities at the universal protein resource (uniprot). *Nucleic Acids Research* 42**:** D191-D198.

Thevenot, PT, Baker, DW, Weng, H, Sun, MW, Tang, L (2011). The pivotal role of fibrocytes and mast cells in mediating fibrotic reactions to biomaterials. *Biomaterials* 32**:** 8394-8403.

To, W, Midwood, K (2011). Plasma and cellular fibronectin: Distinct and independent functions during tissue repair. *Fibrogenesis & Tissue Repair* 4**:** 21.

US-FDA. (2014). *Maude-manufacturer and user facility device experience* [Online]. Available: http://www.accessdata.fda.gov/scripts/cdrh/cfdocs/cfMAUDE/search.CFM [Accessed 11 September 2014].

Valentin, JE, Badylak, JS, McCabe, GP, Badylak, SF (2006). Extracellular matrix bioscaffolds for orthopaedic applications. *The Journal of Bone & Joint Surgery* 88**:** 2673-2686.

Valentin, JE, Stewart-Akers, AM, Gilbert, TW, Badylak, SF (2009). Macrophage participation in the degradation and remodeling of extracellular matrix scaffolds. *Tissue Engineering Part A* 15**:** 1687-1694.

van Putten, SM, Wubben, M, Plantinga, JA, Hennink, WE, van Luyn, MJA, Harmsen, MC (2011). Endotoxin contamination delays the foreign body reaction. *Journal of Biomedical Materials Research Part A* 98A**:** 527-534.

Wang, CL, Hsu, CS, Long, CY (2009). Graft-versus-host disease following transobturator tape procedure with small intestinal submucosa (surgisis): A case report. *International Urogynecology Journal* 20**:** 1149-1151.

Wang, CY, Lin, CF (2014). Annexin a2: Its molecular regulation and cellular expression in cancer development. *Disease Markers*.

Wang, TW, Spector, M (2009). Development of hyaluronic acid-based scaffolds for brain tissue engineering. *Acta Biomaterialia* 5**:** 2371-2384.

Wang, X-Q, Hung, BS, Kempf, M, Liu, P-Y, Dalley, AJ, Saunders, NA, Kimble, RM (2010). Fetuin-a promotes primary keratinocyte migration: Independent of

epidermal growth factor receptor signalling. *Experimental Dermatology* 19**:** e289-e292.

Wang, XJ, Cui, J, Zhang, BQ, Zhang, HY, Bi, Y, Kang, Q, Wang, N, Bie, P, Yang, ZY, Wang, HZ, Liu, XD, Haydon, RC, Luu, HH, Tang, N, Dong, JH, He, TC (2014). Decellularized liver scaffolds effectively support the proliferation and differentiation of mouse fetal hepatic progenitors. *Journal of Biomedical Materials Research Part A* 102**:** 1017-1025.

Yang, B, Zhou, L, Sun, Z, Yang, R, Chen, Y, Dai, Y (2010). In vitro evaluation of the bioactive factors preserved in porcine small intestinal submucosa through cellular biological approaches. *Journal of Biomedical Materials Research Part A* 93A**:** 1100-1109.

Yang, M, Chen, CZ, Shu, YS, Shi, WP, Cheng, SF, Gu, YJ (2012). Preseeding of human vascular cells in decellularized bovine pericardium scaffold for tissue-engineered heart valve: An in vitro and in vivo feasibility study. *J Biomed Mater Res B Appl Biomater* 100**:** 1654-1661.

Zhang, W, Swanson, R, Izaguirre, G, Xiong, Y, Lau, LF, Olson, ST (2005). The heparin-binding site of antithrombin is crucial for antiangiogenic activity. *Blood* 106**:** 1621-1628.

Zhang, X-Y, Xue, H, Liu, J-M, Chen, D (2012). Chemically extracted acellular muscle: A new potential scaffold for spinal cord injury repair. *Journal of Biomedical Materials Research Part A* 100A**:** 578-587.

Zheng, MH, Chen, J, Kirilak, Y, Willers, C, Xu, J, Wood, D (2005). Porcine small intestine submucosa (sis) is not an acellular collagenous matrix and contains porcine DNA: Possible implications in human implantation. *Journal of Biomedical Materials Research Part B-Applied Biomaterials* 73B**:** 61-67.

Zhou, J, Fritze, O, Schleicher, M, Wendel, H-P, Schenke-Layland, K, Harasztosi, C, Hu, S, Stock, UA (2010). Impact of heart valve decellularization on 3-d ultrastructure, immunogenicity and thrombogenicity. *Biomaterials* 31**:** 2549-2554.

LIST OF PUBLICATIONS

1. Muhamed, J, Revi, D, Rajan, A, Geetha, S, Anilkumar, TV (2014). Biocompatibility and immunophenotypic characterization of a porcine cholecyst–derived scaffold implanted in rats. *Toxicologic Pathology* (DOI: 10.1177/0192623314550722).

2. Muhamed, J, Revi, D, Rajan, A, Anilkumar, TV (2014). Comparative local immunogenic potential of scaffolds prepared from porcine cholecyst, jejunum, and urinary bladder in rat subcutaneous model. *Journal of Biomedical Materials Research Part B: Applied Biomaterials* (DOI: 10.1002/jbm.b.33296).